COMPARATIVE STUDY OF HIGH PRESSURE AND ATMOSPHERIC ACID LEACHING FOR THE EXTRACTION OF NICKEL AND COBALT FROM REFRACTORY NICKEL LATERITE ORES

A THESIS SUBMITTED TO
THE GRADUATE SCHOOL OF NATURAL AND APPLIED SCIENCES
OF
MIDDLE EAST TECHNICAL UNIVERSITY

BY

KIVANÇ KORKMAZ

IN PARTIAL FULFILLMENT OF THE REQUIREMENTS
FOR
THE DEGREE OF MASTER OF SCIENCE
IN
METALLURGICAL AND MATERIALS ENGINEERING

MAY 2014

Approval of the thesis:

COMPARATIVE STUDY OF HIGH PRESSURE AND ATMOSPHERIC ACID LEACHING FOR THE EXTRACTION OF NICKEL AND COBALT FROM REFRACTORY NICKEL LATERITE ORES

submitted by **KIVANÇ KORKMAZ** in partial fulfillment of the requirements for the degree of **Master of Science in Metallurgical and Materials Engineering Department, Middle East Technical University** by,

Prof. Dr. Canan Özgen _____
Dean, Graduate School of **Natural and Applied Sciences**

Prof. Dr. Hakan C. Gür _____
Head of Department, **Metallurgical and Materials Engineering**

Prof. Dr. Yavuz A. Topkaya _____
Supervisor, **Metallurgical and Materials Engineering Dept., METU**

Examining Committee Members:

Prof. Dr. Ahmet Geveci _____
Metallurgical and Materials Engineering Dept., METU

Prof. Dr. Yavuz A. Topkaya _____
Metallurgical and Materials Engineering Dept., METU

Prof. Dr. İshak Karakaya _____
Metallurgical and Materials Engineering Dept., METU

Prof. Dr. Abdullah Öztürk _____
Metallurgical and Materials Engineering Dept., METU

Prof. Dr. M. Ümit Atalay _____
Mining Engineering Dept., METU

Date: 06.05.2014

I hereby declare that all information in this document has been obtained and presented with academic rules and ethical conduct. I also declare that, as required by those rules and conduct, I have fully cited and referenced all material and results that are not original to this work.

Name, Last Name: Kıvanç Korkmaz

Signature:

ABSTRACT

COMPARATIVE STUDY OF HIGH PRESSURE AND ATMOSPHERIC ACID LEACHING FOR THE EXTRACTION OF NICKEL AND COBALT FROM REFRACTORY NICKEL LATERITE ORES

Korkmaz, Kıvanç

M.Sc., Department of Metallurgical and Materials Engineering

Supervisor: Prof. Dr. Yavuz A. Topkaya

May 2014, 147 pages

The purpose of this study was to compare the high pressure acid leaching (HPAL) with agitated atmospheric leaching (AL) to obtain better extraction efficiencies of nickel and cobalt from refractory nickel laterite ores of Gördes. In order to understand the low nickel and cobalt extraction percentages, several parameters like duration, particle size, NaCl addition and temperature were tested in HPAL experiments. Also the atmospheric leaching experiments were conducted and the optimum conditions for three different types of acid were determined by studying different parameters like duration, acid concentration and particle size.

The HPAL experiments done under the optimum conditions with following conditions (100% -850 μm particle size, 1 h duration, 255 ^{o}C temperature, 324 kg acid/ton ore, 0.3 s/l ratio with sample 1 and no extra addition) resulted in 73.2% nickel and 76.8% cobalt extractions, which were very low when compared with similar experiments with different ore samples. These conditions were selected

based on previous studies and by taking economical and technical restrictions into account. Two limonitic ores with different arsenic contents were used during this study.

In order to understand the reason for low extraction efficiencies, two different theories were tested by performing different sets of experiments. The first theory was the arsenic's possible inhibiting effect on the dissolution kinetics of hematite and the second theory was the precipitation of secondary hematite on primary hematite particles in the autoclave environment thus preventing the contact of hematite with pregnant leach solution and retarding the dissolution kinetics.

The first theory was clearly refuted and the second was partially confirmed. In HPAL studies, even with the limiting experimental conditions the nickel and cobalt extraction values couldn't be obtained above 85%. In atmospheric acid leaching experiments although the nickel and cobalt extraction efficiencies were almost 100%, the problems encountered like acid consumption, dirty pregnant leach solution formation, etc. affected its feasibility negatively.

Keywords: Hydrometallurgy, high pressure acid leaching, atmospheric leaching, nickel, arsenic

ÖZ

REFRAKTER LATERİTİK NİKEL CEVHERLERİNDEN NİKEL VE KOBALTIN YÜKSEK BASINÇ VE ATMOSFERİK ASİT LİÇİNİN KARŞILAŞTIRMA ÇALIŞMASI

Korkmaz, Kıvanç

Y. Lisans, Metalurji ve Malzeme Mühendisliği Bölümü

Tez Yöneticisi: Prof. Dr. Yavuz A. Topkaya

Mayıs 2014, 147 sayfa

Bu tez çalışmasının amacı, Gördes refrakter nikel cevherinden nikel ve kobaltın daha iyi verimle kazanabilmek için uygulanan yüksek basınçlı asit liçi ve karıştırmalı atmosferik liç yöntemlerinin karşılaştırılmasıdır. Yüksek basınçlı asit liç deneylerindeki düşük nikel ve kobalt verimlerinin sebebini anlayabilmek için süre, tane boyutu, NaCl ilavesi ve sıcaklık gibi birçok parametre test edilmiştir. Bunun yanı sıra, üç farklı asit kullanılarak yapılan atmosferik liç deneylerinde, süre, asit konsantrasyonu ve tanecik boyutu gibi değişik parametreler araştırılmıştır.

Optimum şartlarda (1 nolu cevher örneği kullanılarak, 100% -850 μm tanecik boyutu, 1 saat süre, 255 ^{o}C sıcaklık, 324 kg asit/ton cevher, 0.3 katı/sıvı oranı ve hiç bir katkı eklenmeden) yapılan yüksek basınçlı asit liç deneyinden %73.2 nikel ve %76.8 kobalt verimleri elde edilmiş olup, benzer tipteki cevherlerle yapılan deneylerin nikel ve kobalt liç verimi değerlerinden çok aşağıda kalmaktadır. Bu

deney şartları önceki benzer çalışmalar ve bu cevher için uygun ekonomik ve teknik sınırlandırmalar göz önüne alınarak seçilmiştir. Deneylerde farklı arsenik kompozisyonlarında iki tip lateritik cevher kullanılmıştır

Düşük nikel ve kobalt ekstraksiyon değerlerini anlayabilmek amacıyla geliştirilen iki farklı teori, değişik deney setleriyle test edilmiştir. İlk teori, arseniğin hematit mineralinin çözünme kinetiğini herhangi bir şekilde engelliyor olması olasılığıdır. İkinci teori ise, ikincil hematitin eşzamanlı olarak birincil hematit çözünürken onun üzerine çökerek, hematitin metal yüklü liç çözeltisiyle olan temasını kesmek suretiyle çözünme kinetiğini yavaşlatarak, nikel veriminin düşmesine neden olmasıdır.

İlk teori yapılan deneyler sonrasında kesinlikle çürütülmüş, ikinci teori ise kısmen doğrulanmıştır. Limit şartlarda yapılan yüksek basınç altındaki liç deneylerinde bile nikel ve kobalt verimleri %85'in üzerine çıkamamıştır. Atmosferik deneylerde bu rakam neredeyse %100 bulmasına karşın, yüksek asit tüketimi ve kirli metallerle yüklü liç çözeltisi oluşumu gibi sorunlar yöntemin fizibilitesini negatif olarak etkilemektedir.

Anahtar kelimeler: Hidrometalurji, yüksek basınçlı asit liçi, atmosferik liç, nikel, arsenik

To my dear family and especially to my lovely mother Dilara,

1283

ACKNOWLEDGEMENTS

I would like to express my sincere appreciation and gratitude to my supervisor and my mentor Prof. Dr. Yavuz A. Topkaya for his limitless and continuous guidance, wisdom, insight and his endless patience and understanding in preparation of this thesis.

META Nikel Kobalt A.Ş. is gratefully acknowledged for providing the original nickel laterite ore samples and doing the chemical analyses of the experimental samples.

I also would like to express my deepest gratitude and thankfulness to my dear parents, Tacettin & Dilara Korkmaz and my beautiful sister Gülenay Korkmaz for their endless support and being there for me, whether I need or not, throughout my entire life. Especially my mother, Dilara Korkmaz, her compassion, love and endless efforts to make me feel loved kept me on track. I also would like to thank my true advisor, a wise and a visionary man, my uncle Tuncer Kırımer, who believed in me unconditionally.

I must express my special thanks to my co-workers and friends Çağrı Arıcı, Onur Saka, Şerif Kaya, Erman Kondu, Recai Önal, Bengi Yağmurlu, Mehmet Dincer and Derya Kapusuz for their help, guidance, suggestions, and valuable friendships along my journey.

TABLE OF CONTENTS

LIST OF FIGURES

FIGURES

LIST OF TABLES

TABLES

CHAPTER 1

INTRODUCTION

In modern world, nickel is one of the most important elements demanded by many industry branches like, ferrous and non-ferrous alloying industries, nickel based catalyst and battery production, petro-chemical works, aerospace applications, coinage and coating particles and military applications. The amount of nickel used in these industries have been getting higher and higher due to its superior properties and became a critical necessity for many new industrial branches with developing technologies (1).

Parallel to economic development, the nickel consumption has increased in the world with an average growth rate of 4.2% per year. According to Macquarie Research, the nickel supply has increased 4.1% to 1845000 metric tons in 2013 and will increase 3.8% to 1915000 metric tons in 2014. The estimation of nickel consumption was 1.77 million tons in 2013 and is 1.86 million tons in 2014 (2). According to these statistics, although it is understandable that the price and the amount of nickel stocks fluctuate within years due to political and economic reasons, the increase in the price and amount of product within upcoming years are inevitable. The latest price of Nickel is 15500 US dollars per ton in April 1, 2014 according to London Metal Exchange (3).

Until fifty years ago, considerable amount of this demand was supplied from sulfide based nickel ore deposits, although the sulfide ore deposits are only 40% of the world nickel reserve whereas the laterites are 60%. With the wide usage of conventional crushing, grinding and flotation methods, the ore would become ready for pyrometallurgical processing by smelting furnaces. But with developing technology and discovery of less time and capital consuming production routes, the production trends shift mainly on laterite based nickel ores.

Within the guidance of all these statistical data and the obvious advantages of using lateritic ores instead of sulfide ores due to economic and environmental reasons, lateritic nickel ore deposits have already become one of the most important nickel sources with accelerating prominence for upcoming decades.

Region, climate zone, altitude and temperature of the location of mine deposits affect the formation of the nickel laterite ore. The formation of the nickel ore in the deposits has a crucial role in the extraction stage of production process. In addition to that, the chemical composition and mineralogical state of the nickel reserve should be kept in mind in order to solve the possible problems in the extraction process. Depending on the laterization history, different kind of lateritic ore descriptions would form and classified mainly as limonitic, nontronitic and saprolitic depending their mineralogical content (4). The proper metallurgical treatment would be chosen depending on the chemical and mineralogical state of the ore deposit. However, there are three major extraction processes existing due to high complexity of nickel ore deposits. These are mainly, pyrometallurgical route, hydrometallurgical route and “Caron process”. In broad terms, the pyrometallurgical method includes a high energy input process to produce ferronickel and smelting of matte to recover the nickel from its ore. On the other hand, the hydrometallurgical method dissolves the nickel, cobalt and

other contents of ore in such a manner that can be selectively taken out of the acidic media with different methods afterwards (5).

In this thesis, two different hydrometallurgical methods namely, high pressure acid leaching (HPAL) and agitated atmospheric acid leaching (AL), will be studied individually and compared with each other in terms of their optimum parameters and the extraction percentages of nickel and cobalt by using two different kinds of limonitic nickel laterite ore supplied from Manisa/Gördes open pit nickel-cobalt mine. The main objective of the study is to obtain the maximum extraction percentages with the use of optimum parameters to be determined and the comparison of two different leaching methods to find out the reasons for the low extraction percentages of nickel and cobalt in high pressure sulfuric acid leaching.

CHAPTER 2

LITERATURE REVIEW

2.1. Nickel and Its Usage

Nickel is a white, silvery metal with an atomic mass of 58.71. Its position is placed after iron and cobalt in the periodic table which is closely related in terms of both chemical and mineralogical manner. It has mainly a face centered cubic crystal lattice, but it also exits with hexagonal crystal structure. Since it is placed near iron, cobalt and copper, it has similar chemical properties. Mostly, it is present in +2 oxidation state, other than that, +3 and +4 oxidation states are also encountered. But it exists in the aqueous solutions in +2 state on the contrary to iron and cobalt (6).

The main significance of nickel can only be understood when it is used as an alloying element. Because, nickel bearing alloys have many superior properties, for example: high corrosion resistance, high strength and toughness, high melting point and ductility, malleability and magnetic properties. Also it has an important role in the development of the modern materials for aerospace, automotive industry and military applications (7). It can be produced in many different forms like; nickel matte, nickel oxide sinters, refined nickel metal, nickel alloys and ferronickel.

2.2. Nickel Ore Deposits

Nickel has the 24th place among the elements that the Earth's crust is abundant with an approximate content of 0.008%. Although nickel has larger total amounts of deposits than most of the commercially important elements like, copper, zinc and lead worldwide, they exist as smaller number of deposit sites with a great economic value to the industry (7). In nature, nickel does not exist in metallic form but found as various types of minerals. Nickel is more likely to be related with iron and magnesium than with silicon and aluminum, when the worldwide ore deposits are examined. Because of close atomic dimensions of divalent cations of iron, magnesium and nickel, they are highly suited for substitutional atomic replacement for each other in host crystal structures without any considerable distortion of the host lattice as seen in Figure 1.

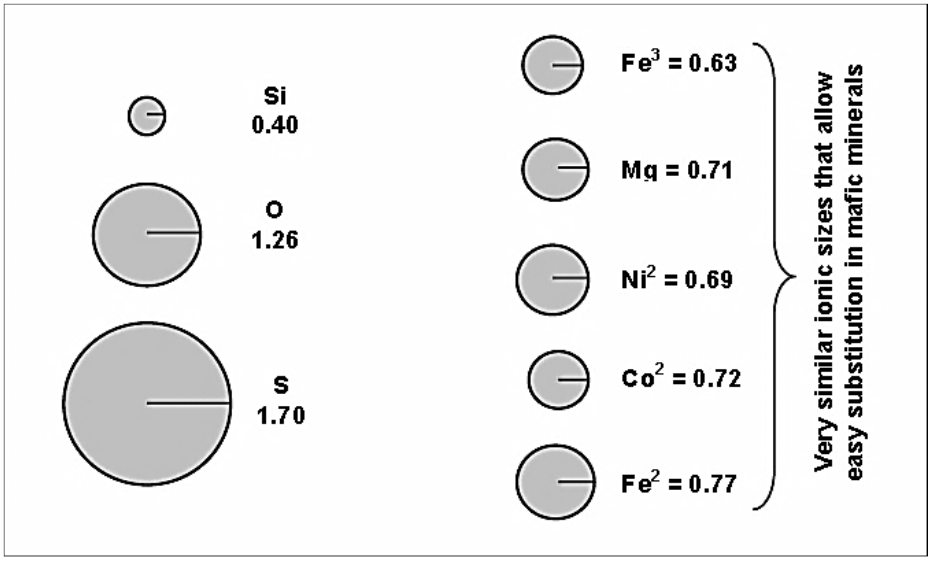

Figure 1: Ionic radii of important elements in the nickel ore mineralogy (8).

Although the technology is insufficient for the complete recycle of the nickel from scrap materials, it is an option with high environmental concerns, thus the

investments are highly focusing on it rather than mining from ore deposits. On the other hand, ore mining depends on the ore grade and the reserve of these ore deposit sites (9). In general, ore deposits of nickel can be divided into two main groups. These are sulfide type deposits and oxide type deposits. In USA, 95000 tons of nickel was recycled and gathered from scrap materials in 2012, which represents 43% of the total USA consumption for the particular year. The world nickel reserves and mine production amounts can be seen in Table 1. Also in Figure 2, the distribution of laterite and sulfide based nickel ores throughout the world can be observed.

Table 1: Worldwide estimates of nickel mine productions and reserves in tons of nickel (10).

Nickel Production			Reserves
	2011	2012	
United States	-	-	7100
Australia	215000	230000	20000000
Botswana	26000	26000	490000
Brazil	109000	140000	7500000
Canada	220000	220000	3300000
China	89.800	91000	3000000
Colombia	76000	80000	1100000
Cuba	71000	72000	5500000
Dominican Republic	21700	24000	970000
Indonesia	290000	320000	3900000
Madagascar	5900	22000	1600000
New Caledonia	131000	140000	12000000
Philippines	270000	330000	1100000
Russia	267000	270000	6100000
South Africa	44000	42000	3700000
Other Countries	103000	120000	4600000
World total(rounded)	1940000	2100000	75000000

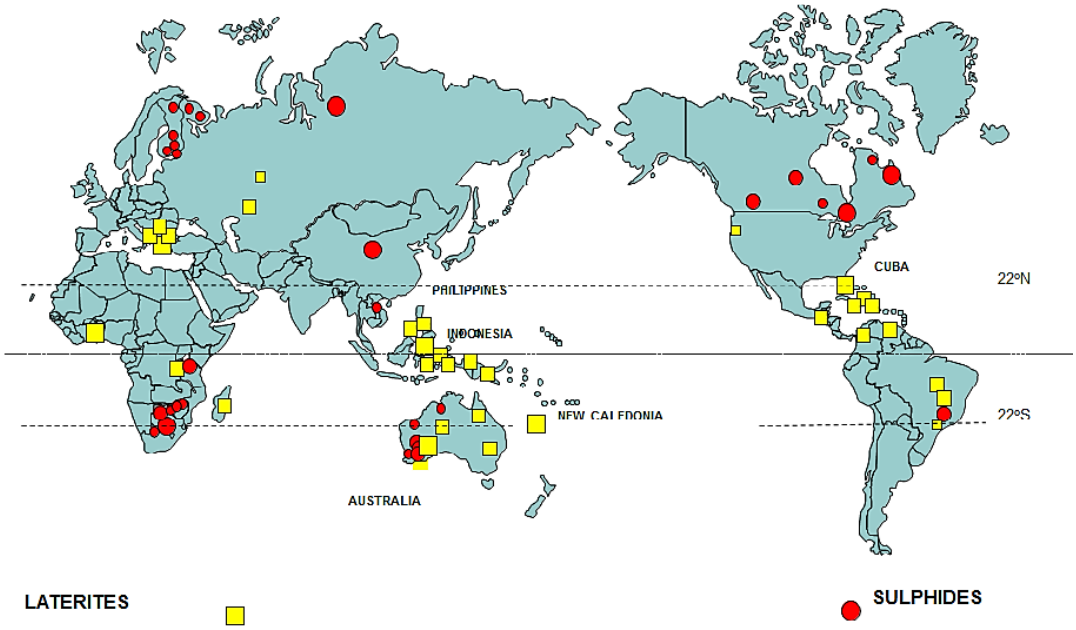

Figure 2: Main reserves of nickel as sulfides and laterites throughout the world (11).

2.2.1. Sulfide Type Nickel Ores

The major used type of nickel resource to produce nickel, is sulfide type of nickel deposits because they are relatively easier and cheaper to mine and process. The nickel percentage of these sulfide ores varies between 0.15 to 8%, but according to the recent studies, 93% of the total sulfide reserves have average 0.2-2% Ni. Different minerals crystalize and remain out of the magma in separate layers due to cooling. An immiscible sulfide liquid forms into which nickel partition selectively as soon as magma becomes saturated. This sulfide immiscibility may results from different processes like, crustal contamination and magma mixing. And the ore grades highly depend on these characteristics, but in general, nickel content varies between 0.2-2 percent (6). The main advantage of sulfide ores is that they can be concentrated by using flotation. Pyrometallurgical extraction is used for most of the nickel production from sulfide ores by using concentrates produced by flotation.

The main nickel bearing sulfide minerals in nickel deposits are; pyrrhotite (Fe_7S_8), and pentlandite $(Ni, Fe)_9S_8$. These sulfide ores generally include 0.4-2.0% nickel, 0.2-2.0% copper, 10-30% iron, and 5-20% sulfur and silica, magnesia, alumina and calcium oxide. Globally, it is known that 60% of the nickel production from sulfide ores are coming from pentlandite $(Ni, Fe)_9S_8$. Most abundant mineral type among the sulfide nickel ores is nickeliferrous pyrrhotite with an average 0.2-0.5% Ni. During the nickel production from sulfide ores, different kinds of byproducts can also be produced by recovering them during the different steps of the production stages. These byproducts are mainly; copper, cobalt, selenium, tellurium, sulfur and iron. In addition to these, some isolated particles of gold, silver, platinum group metals can be found but very rarely, though they are normally present in sulfide minerals as a solid solution (7).

2.2.2. Oxide Type Nickel Ores

Lateritic nickel ores are generally abundant near the surface of Earths' crust and at regions where the climate has some certain characteristics. These certain areas are generally tropical climates and are located around the equator or dry regions of central Australia or parts of Eastern Europe with high humidity. The deposits are formed by the transformation of olivine $(Fe,Mg)_2SiO_4$ rich igneous rocks. The elements inside of a solution move and find a place in new minerals by precipitation after dissolving over time in rain or underground waters. So, it can be said that the climate should be tropical with high humidity and substantial amount of rainfalls. The formation of lateritic ores in a suitable climate follows a chemical concentration process as a consequence of lateritic weathering of peridotite rock. It consists of mainly olivine, a magnesium iron silicate containing up to 0.3% nickel. In order to form soluble magnesium, iron, nickel and colloidal silica, olivine and serpentine are decomposed by underground water with high

content of carbon dioxide. In the presence of air, the soluble iron instantly oxidizes and precipitates as goethite and hematite by hydrolysis. This phenomenon occurs near the surface and stays there at the top of the deposits. It allows the creation of hematitic cap. On the other hand, due to the acidic dissolution of nickel, magnesium and colloidal silica, they are washed deep down to the deposit and remain there until they become neutralized and precipitate as hydrated silicates. Typical cross section of a laterite deposit can be seen in Figure 3 (7).

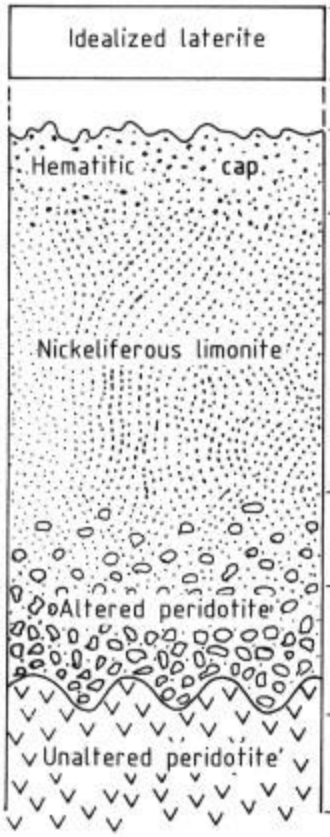

Idealized laterite	Approximate analysis, %					Extractive procedure
	Ni	Co	Fe	Cr_2O_3	MgO	
Hematitic cap	<0.8	<0.1	>50	>1	<0.5	Overburden to stockpile
Nickeliferous limonite	0.8 to 1.5	0.1 to 0.2	40 to 50	2 to 5	0.5 to 5	Hydrometallurgy
Altered peridotite	1.5 to 1.8	0.02 to 0.1	25 to 40	1 to 2	5 to 15	Hydrometallurgy or pyrometallurgy
	1.8 to 3		10 to 25		15 to 35	Pyrometallurgy
Unaltered peridotite	0.25	0.01 to 0.02	5	0.2 to 1	35 to 45	Left in situ

Figure 3: Cross section of a laterite deposit with necessary analysis and extractive procedure (7).

The effect of weathering on the creation of lateritic ores can clearly be seen in Figure 4. The distinct ore types named as limonite, nontronite, saprolite, garnierite, and serpentine with different types of impurity elements like magnesium, iron and silica generally exit in lateritic deposits.

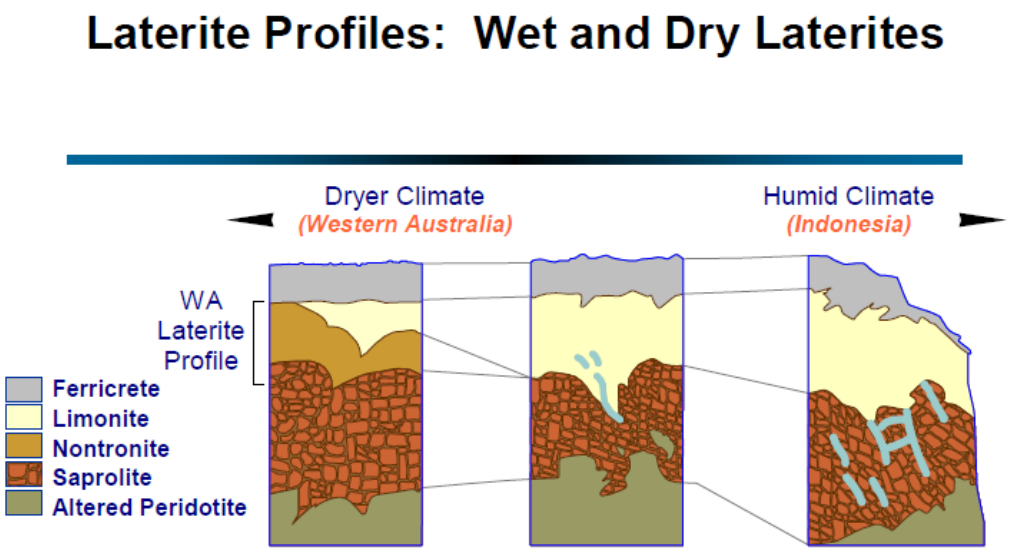

Figure 4: Typical weathering profiles for nickel laterite ores (11).

In some cases nickel may stay in iron rich cap, but the cap remains magnesium and silica depleted. In such cases, the created zone is named as limonitic. This layer mostly consists of ferric oxide minerals. The separation of iron and nickel from silicates are mostly completed in this limonitic zone. The limonitic part of the deposits is present in almost every lateritic ore deposit but the ratios of limonitic part to the whole deposit differ regionally. On the other hand, the lateritic ores are also rich in chromium and cobalt.

One can also see the extractive techniques each layer of the deposit should be treated with in Figure 3. Pyrometallurgical methods should be applied to the parts of the deposit which have chemical and mineralogical heterogeneity, which are silicates in this case. Since the limonitic part of the nickel ore deposit is relatively

homogeneous, both in mineralogical and chemical aspects, it is more suited for hydrometallurgical treatment (7).

The mineral types of different lateritic zones with the most suitable processing technology are listed below with the average contents of nickel and cobalt:

• Limonite: (1 to 1.7% Ni, 0.1 to 0.2 % Co) these are suitable for pressure acid leach and Caron process
• Nontronite: (1 to 5% Ni, 0.05 to 0. 1% Co) these are suitable for pressure acid leach and smelting
• Serpentine: (1.5 to 10% Ni, 0.05 to 0.1 % Co) Typical composition is in the range 1-2% Ni and 0.05 to 0.07% Co. These ores are suitable for pyrometallurgical processes (ferronickel and matte smelting)
• Garnierite: (10 to 20% Ni, 0.05 to 0.1 % Co) Typical composition is in the range of 2-3% Ni and 0.05% to 0.1% Co. These are suitable for pyrometallurgical processes (ferronickel and matte smelting, but especially high carbon ferronickel) (11).

To understand the detailed description of limonitic zone, the division of two main groups should be studied. The first one with reddish color, called red limonite, is dominated with hematite (Fe_2O_3) and with some goethite (FeOOH), which has less than 0.8% Ni, 0.1% Co and greater than 50% of Fe. The second main group is with a lighter color, called yellow limonite, has a Ni content of about 1.5%, 0.2% Co and 45% Fe. So, in total the limonite zone has an average composition of >1.0% Ni, >40% Fe and about 0.15% Co with lower silica and magnesium due to the reasons that was explained earlier. The nickel is associated with iron oxide minerals like goethite (FeOOH), hematite (α-Fe_2O_3), maghemite (γ- Fe_2O_3) and magnetite (Fe_3O_4). The reason for that can be explained by the substitution of Ni^{2+} and Co^{3+} into the goethite as a replacement of Fe^{3+}, since the ionic radii's of them

are very close (0.69 Å, 0.525 Å and 0.645 Å, Ni^{2+}, Co^{3+} and Fe^{3+}, respectively). And the similarity of ionic radii can be also seen in Figure 1 (5, 12).

Under this limonitic layer, another zone with high silica content as magnesium and aluminum silicates starts. The transition zone between the iron oxide and hydrated iron is called nontronite zone or the clay zone and it is created by soft smectite materials. Since the solvent media (acidic water in this case) is not present in large quantities in that zone, the movement of elements is also limited. It takes its name from the most abundant mineral in that zone, which is nontronite ($Na_{0.3}Fe_2(Si,Al)_4O_{10}(OH)_2 \bullet n(H_2O)$). It contains about 2% Ni with the presence of some amount of goethite and manganese oxyhydroxide. Serpentine zone is placed under the nontronite zone. It is also called saprolitic zone. Its mineralogy varies depending on the type of host rock and level of water drainage. The regular saprolitic zone has about 2.4% Ni, 0.05% Co and <15% Fe with high amount of silica and magnesia. The major mineral present is serpentine ($Mg_3Si_2O_5(OH)_4$). But in some cases, the nickel can change place with magnesium in its lattice, in these cases the minerals is called garnierite. Other than major serpentine minerals, there are also goethite, magnetite, maghemite, chromite ($FeCr_2O_4$) minerals existing in the boundaries of this zone (13).

In Turkey, the lateritic nickel ore deposits are mainly locate in the western part of the country. The major deposit sites are within the territories of Manisa/Çaldağ, Manisa/Gördes, Uşak/Banaz and Eskişehir/Yunusemre. The limonitic type of ore that was supplied from Gördes lateritic nickel mine was use in the experimental stage in this thesis study.

2.3. Nickel Production Methods from Lateritic Ores

2.3.1. Pyrometallurgical Routes

2.3.1.1. Roasting, Smelting and Converting

For the production of nickel bearing mattes, 90% of the world's sulfide ore deposits are processed with pyrometallurgical methods. There are three main steps in the pyrometallurgical processing of nickel concentrates; roasting, smelting and converting. Sulfur is removed from concentrate by oxidation and some part of the iron also gets oxidized in the roasting process. The oxidation process follows Rx. 2.1, as the transformation of pyrrhotite to magnetite occurs;

$$3Fe_7S_8 + 38O_2 \rightarrow 7Fe_3O_4 + 24SO_2 \qquad \text{Rx. 2.1}$$

There is no need for an external heat source because this reaction is highly exothermic and produced heat is enough for the roasting itself. Multiple-hearth (Herreshoff furnace) or fluidized-bed roasters can be used for this purpose in industry. In the multiple-hearth roasters, the feed of wet concentrate is charged from the top and it travels with time to the next heart at below via drop holes. During that time, the mix of preheated air and natural gas is fed to the system at the bottom of the furnace to provide necessary oxygen and heat to burn the concentrate. By adjusting the ratio of air to gas, the inner temperature can be controlled. Since the contact area of concentrate and the mixture of gas is limited, the roasting process needs long durations. Also, the production of off-gas with low concentration of sulfur dioxide is not sufficient for sulfuric acid production and it can be counted as a disadvantage of multiple-hearth roaster usage (7).

The use of fluidized bed furnaces is a relative modern approach to the roasting process due to the effective use of gas-concentrate contact and plain structure. It is

a vertical chamber of circular cross section with oxygen blown in the middle of it. The sulfide nickel concentrate is fed from the top and it suspended in blown air, thus the contact surface becomes maximized. All particles are oxidized homogenously and at a fast pace. Then, the product is taken out from below and the off-gas containing a high amount of concentrated sulfur dioxide is highly suitable for sulfuric acid production.

The main objective of the smelting process is to eliminate all the gangue minerals and iron sulfide from the concentrate and obtain a high grade nickel copper matte with a chemical composition of 0.5 - 3.0% Fe and 6 - 22% S. Although one can obtain copper by oxidation of sulfide at smelting temperatures, but the nickel is not possible to obtain with this process at these temperatures (up to 1400 ^{o}C). There are two different phases of smelting nickel sulfide ores; the primary smelting and converting. For the process to be efficient and economically desirable, the removal of iron by oxidation and slagging is very important. In the first step, about 50% of the total iron is oxidized and only 5% of nickel and copper are oxidized. So, a small portion of nickel is lost to the slag and overall due to that small loss, a low grade but high iron matte is created. The loss of nickel and copper takes place by Rx. 2.2 and 2.3:

$$9NiO + 7FeS \rightarrow 3Ni_3S_2 + 7FeO + SO_2 \qquad \text{Rx. 2.2}$$

$$Cu_2O + FeS \rightarrow Cu_2S + FeO \qquad \text{Rx. 2.3}$$

When it comes to the second step, the continuation of iron oxidation and slagging occurs. This is called converting. The slag created in that stage has high nickel and copper content and they can be recovered by returning it to the first step. In the end, two-step smelting process produces a high-grade nickel matte with low

iron and a slag of low-grade and high iron content. It takes place by Rx. 2.4 and 2.5 (7):

$$3Fe_3O_4 + FeS \rightarrow 10FeO + SO_2 \qquad \text{Rx. 2.4}$$

$$2FeO + SiO_2 \rightarrow 2FeO.SiO_2 \qquad \text{Rx. 2.5}$$

2.3.2. Caron Process

The Caron process is named and patented after M.H.Caron in 1924. It is a hybrid processing route for nickel ores. Basically, it starts with roasting and followed by ammonia leaching with the precipitation of nickel as nickel carbonate. It can be used for limonitic and/or mixture of saprolitic and limonitic ore deposits. There are five major plants built in the world and four of them are still in use.

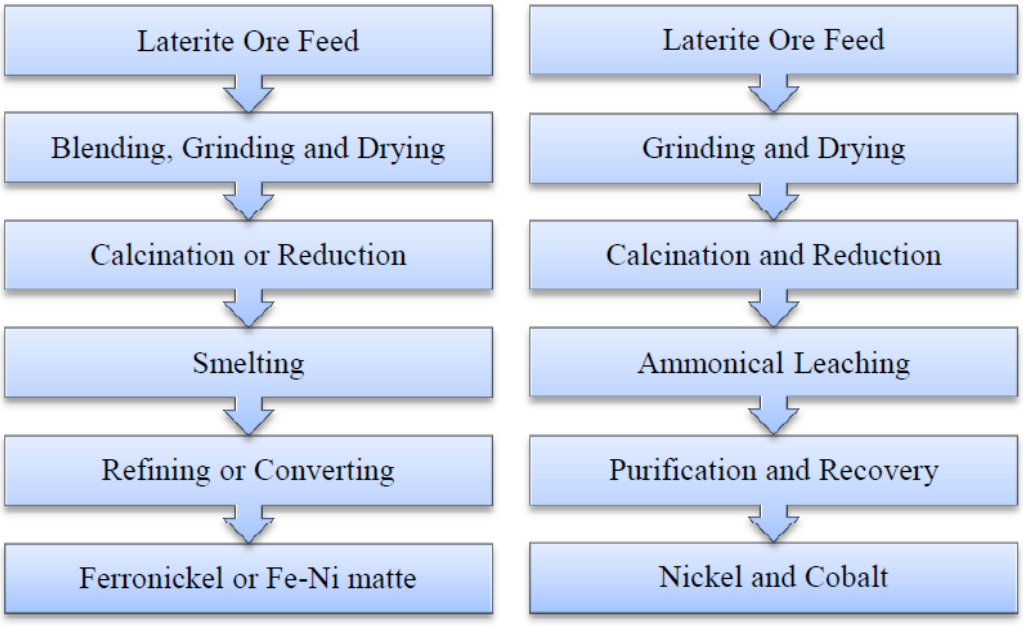

Figure 5: Pyrometallurgical (left) and Caron (right) process flowsheets for lateritic nickel deposits (13).

Firstly, the nickel ore is dried and reduced at 700 ^{o}C in a multiple-hearth furnace. Then, the reduced calcine is cooled for some time so its temperature is reduced down to non-oxidizing conditions. The process continues with the leaching of reduced concentrate in ammoniacal ammonium carbonate solution to selectively extract nickel and cobalt. In order to separate ammonia and carbon dioxide from each other, the pregnant leach solution is heated up to its boiling point. This results in precipitation of nickel and cobalt. From this precipitate mixture nickel and cobalt can be recovered (7). The differences of pyrometallurgical and Caron processes can be seen in Figure 5 step by step.

2.3.3. Hydrometallurgical Routes

In order to replace the old-fashioned, time and energy consuming methods, which were mentioned previously, the first high pressure acid leaching facility was started in Mao Bay, Cuba. The classic methods of extracting metals from ores became not suitable for low grade nickel laterites with high moisture content. From this urgent need for developing new methods, acid centered flowsheets have started to appear to increase the extraction percentages of low nickel bearing ores to obtain higher yields. The maximum temperature for these processes is 270 ^{o}C, which is very low when it is compared with pyrometallurgical methods. These methods are beneficial both economically and environmentally. Decreasing the heat energy input is favored and the releasing of toxic gases to atmosphere like SO_2 in different stages of the old methods is also prevented. Moreover, new branches of elements like scandium and other precious metals are also unlocked to extract with these innovative methods. In this section agitated atmospheric leaching (AL) and high pressure acid leaching (HPAL) will be summarized.

2.3.3.1. Atmospheric Leaching

2.3.3.1.1. Heap and Agitated Atmospheric Leaching

Atmospheric leaching is the process of dissolving an ore with acid and collecting the valuable metallic content into aqueous solution at relatively low temperatures and at open atmosphere conditions. It is much clean and simple with less energy input needs and low initial costs. Known atmospheric leaching methods are heap, column, in-situ, dump and agitated leaching. After giving brief information about heap leaching, the agitated atmospheric leaching will be focused on in this study.

The discovery of nickel heap leaching method goes back to early 1990's. It was patented by a Greek Professor Lina Agatzini-Leonardou at Athens University and named as HELLAS after the initials of HEap Leach LAteriteS. HELLAS was conducted with Greek nickel lateritic ore which was quiet similar to Turkish laterites (14, 15). There is also a heap leaching pilot plant in Çaldağ/ Turkey which is used for the nearby lateritic nickel ore. The heap leaching process is started by piling up the lateritic ore in the shape of heaps on specially made geomembranes to prevent any leakage of acidic media into the environment which could damage the soil and also it means the loss of valuable dissolved metals. After the preparation stage is completed, the acid is fed over the heap via drip irrigation in a continuous manner. With the help of gravity, the acid penetrates through holes of the particles and dissolves the nickel containing minerals. With time, the created pregnant leach solution (PLS) infiltrates to the bottom of heap on the liner system where it's collected from there into ponds and sent to post processing units. The schematic sketch of heap leaching system is given in Figure 6. The chemical base of process is the same with agitated atmospheric leaching, which only shows difference from high pressure acid leaching by regeneration of acid via precipitation of iron and aluminum during the process under high

temperature and pressure conditions. The absence of regeneration of acid in atmospheric leaching is a huge economic burden in terms of investments. However, these are not the only downsides of this process. On the average, the heap leaching takes 1 or 1.5 years and the extraction percentages could seldom go beyond 85% so the extraction efficiency of whole process is low.

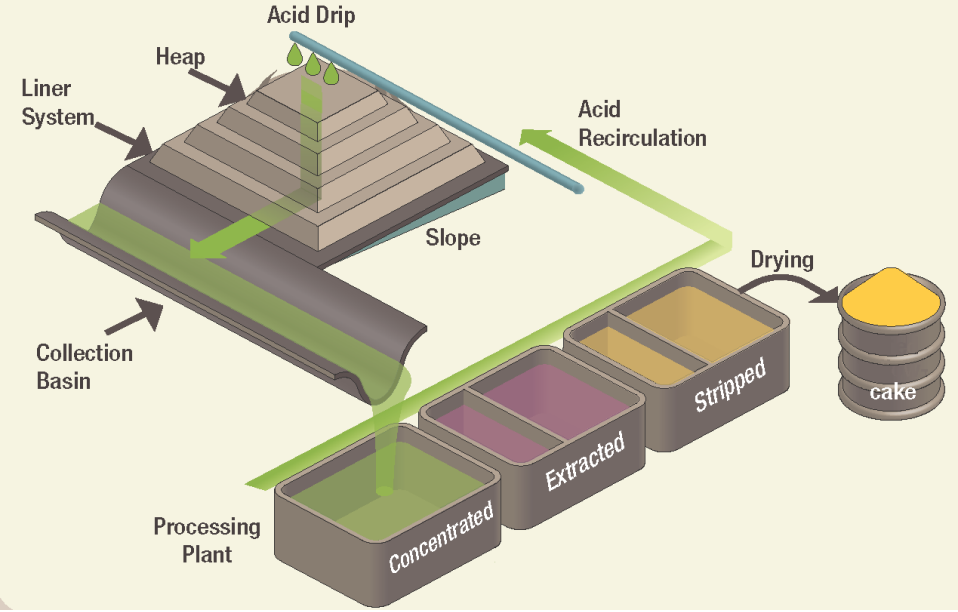

Figure 6: Sketch of a heap leaching system (16).

Agitated atmospheric leaching is very similar to heap leaching but in this case, the duration of the process is reduced by mechanically or pneumatically stirring the system to increase the ore-acid contact area continuously. Since the contact area is important for kinetics of the process, the particle size is relatively fine in this application compared to heap leaching. Temperature requirements for the process is around 95-105 ^{o}C, so it is extremely low when it is compared with pyrometallurgical (up to 1400 ^{o}C) or even with high pressure acid leaching (250-270 ^{o}C) processes. After the comminution stage, the prepared ore is leached in titanium or stainless steel vessels with the addition of necessary amount of acid

and fresh water. During the leaching process, a stirrer constantly stirs the contents of the vessel to increase the ore-acid interaction surface and kinetics. Also heating is provided to fasten the kinetics of reactions. The size of the feed generally is between 0.5 to 1 mm and solids concentration between 25 to 30% to obtain at least 80% nickel and cobalt extraction percentages (17, 18).

Although it has some advantageous points like, less initial and maintenance cost and higher extraction percentages within lower time durations, there are also some negative aspects. High acid consumption and more complex content of pregnant leach solution due to prevented precipitation of iron cause problems in terms of economic feasibility and complications during downstream processes.

Many types of acids can be used for leaching. In literature, it is stated that the strength of acidic media from the weakest to the strongest is ordered as; perchloric, nitric, sulfuric, hydrochloric, hydrofluoric and oxalic acid. Also in the same study it is stated that the nickel dissolution depends on iron dissolution and the strength of acidic media's presence (19).

One of the recent developing methods is chloride leaching. In this atmospheric leaching set-up, the extraction of nickel and cobalt into the pregnant leach solution is possible without any important iron and magnesium dissolution into PLS by using a mixed chloride lixiviant. In the downstream stage, nickel and cobalt are gathered by regular nickel and cobalt hydroxide product from PLS (20). Another method is biohydrometallurgical or bacterial metal extraction of nickel and cobalt from laterites. This is a sort of heap leaching with the help of bacteria. In its regular metabolic cycle, the bacteria produce acids which dissolve the lateritic ore in a similar mechanism as heap leaching. The bacterial content is

either placed on top of laterite ore heaps or sprayed all over it to cover the entire surface (21).

One of the recent studies on atmospheric sulfuric acid leaching was conducted by Apostolidis et al. by following the method of reduction roasting with H_2 due to high magnesium content of ore which was followed by sulfuric acid leaching. The mentioned study was done at 70 ^oC which achieved 80% nickel extraction (22). Additionally, in another study 90% nickel extraction was reported with a relatively higher acid consumption of 1000 kg/ton ore from local laterites. The extraction percentage of nickel was found to be dependent on the specific types of minerals existing in the ore, especially those having nickel in it and temperature of leaching process with the concentration of used acid (23).

The recovery of nickel and cobalt from a roasted copper converter slag by leaching it using ammonium sulfate and sulfuric acid was conducted by Sukla et al. and the extraction results were reported as 81% nickel and 85% cobalt (24). In the studies of Greek nickel laterite ore via agitated atmospheric leaching, Panagiotopolos et al reported 75-80% of nickel and cobalt extractions. The reported extraction values depended on the temperature and pulp density. By using 3 N sulfuric acid concentration and 15% pulp density, the leaching was conducted at 95 ^oC for 4 h. The extractions of nickel and cobalt, as mentioned above, were 75% and 80%, whereas iron and magnesium extraction percentages were 55% and 80%, respectively. The acid consumption was 1600 kg/ton ore (25). Later, the same author studied a similar source of lateritic nickel ore by using three stage counter current leaching set-up. Three different stages were used for 1.5 h per each in order to simulate a whole atmospheric leaching set-up. Although the extraction percentages were very similar, the acid consumption was reduced to 850 kg/ton ore (26).

Similar atmospheric leaching studies have been conducted all over the world. Curlook used a New Caledonia laterite ore with highly serpentinized saprolite fractions and reported 85% nickel extraction value with sulfuric acid atmospheric leaching at between 80 to 100 ^{o}C, within 1 h duration. But most importantly, it was claimed that the agitated atmospheric leaching was feasible at regions where the sulfuric acid was relatively affordable (27).

From the summarized results, it is apparent that the generous usage of acid in atmospheric leaching always results in higher nickel and cobalt extraction percentages. However, the regeneration of acid is not possible and acid itself costs too much alongside with the high cost of neutralization agents. After the researchers realized this, the course of studies shifted to decreasing of the acid consumption and any process which was not expensive to maintain. To help this purpose, a multi-step leaching was developed. In this multi-step leaching process, first of all, goethite was leached as nickel bearing mineral. After that, saprolite type of mineral introduced to the current media. The results were reported as 91-100% nickel and 83-90% cobalt extractions within 10 h of duration at 95 ^{o}C (28).

For the thermodynamics and chemical aspects of atmospheric leaching, the most important point is to unlock the nickel bearing minerals and since it was stated that the acidic media concentration is important in terms of dissolution kinetics and rate changes. The dissolution reactions of nickel containing goethite and asbolane and neutralization of slurry are given in the following Rx's. 2.6 and 2.7;

Ni-containing goethite: $2(Fe,Ni)O.OH + 5H_2SO_4 \rightarrow 2NiSO_4 + Fe_2(SO_4)_3 + 6H_2O$

Rx. 2.6

Asbolane: $(Mn,Co)O_2 + SO_2 + H_2SO_4 \rightarrow MnSO_4 + CoSO_4 + H_2O$ Rx. 2.7

The neutralization of leach slurry and precipitation of iron as goethite:

$Fe_2(SO_4)_3 + 3CaCO_3 + H_2O \rightarrow 2FeO(OH) + 3CaSO_4 + 3CO_2$ Rx. 2.8

The atmospheric leaching processes were done with both limonitic and saprolitic ores under boiling temperature. Fresh and sea water were used to pulp the ore and reacted with sulfuric acid in the first stage (Rx. 2.6). By mild reaction with sulfur dioxide, cobalt was able to be leached from saprolitic ore (Rx. 2.7). And after the leaching processes were completed, in order to neutralize the residual acid and precipitate iron as goethite, calcium carbonate was added to the slurry (Rx. 2.8) (28).

In Turkey, both heap leaching and atmospheric leaching were also studied. To show the contrast of the two methods, Büyükakıncı (29) and Köse's (30) studies were very useful. According to Köse's studies, 83% nickel extraction was obtained from the nontronitic type laterite ore from Gördes with column leaching method and Büyükakıncı reported 96% nickel extraction value with the same ore but with agitated leaching method. Köse's work took 3 months and Büyükakıncı's experiment was 24 h long. This showed the effectiveness of agitated atmospheric leaching over heap leaching in terms of duration and extraction values.

Although for many years both heap and agitated leaching have been studied and they have attractive features like low initial and maintenance cost and fairly acceptable levels of extraction values, the constraints like, high acid consumption,

long leaching durations and low extraction percentages of nickel and cobalt are the repelling features of this method. Because, when it is compared with high pressure acid leaching, the PLS has very complex content, since iron and aluminum ions don't precipitate. That is why this method has rare usage around the world. In this study, the agitated atmospheric studies will only be done to obtain valuable data for the comparison with high pressure acid leaching experiments' data. Also, if an innovative development occurs to access to necessary acidic media easily and generously, the agitated atmospheric leaching will be much more feasible.

2.3.3.1.2. Direct Nickel Process (DNi)

There are also some other developing methods like "direct nickel process" (DNi). Direct nickel process is an atmospheric, hydrometallurgical method which leaches the whole lateritic nickel ore as a single type ore (limonitic to saprolitic). It is the only known process which can treat the lateritic nickel ores in such a unique way. The process uses nitric acid and conducts leaching operations at open atmosphere conditions for 5 h and at temperatures just above 100 ^{o}C. The extraction percentages of Ni, Co, Mn and Mg reach above 90% easily and the leaching of iron, aluminum and chromium depends largely on ore deposit's mineralogical state (31).

The characteristic feature of this process is the ability to regenerate the used reagents over 95%. This is extremely important since it reduces down the operation costs while having great extraction values at the same time. Nitric acid has also an advantage over sulfuric and hydrochloric acid, which is the high solubility of its metal salts compare to others. But this situation might result

negatively, since some elements like calcium, nitrate forms are soluble but the sulfate forms some compounds like gypsum, which create scales on reaction container and increase maintenance costs (31). After the leaching stage, mixed hydroxide precipitation (MHP) method is preferred for intermediate product. Besides acid regeneration, MgO can also be recycled in powder form. But most importantly, the general acid consumption is reduced to 20-40 kg/ton ore and all the initial investments are not expensive when it is compared to HPAL process.

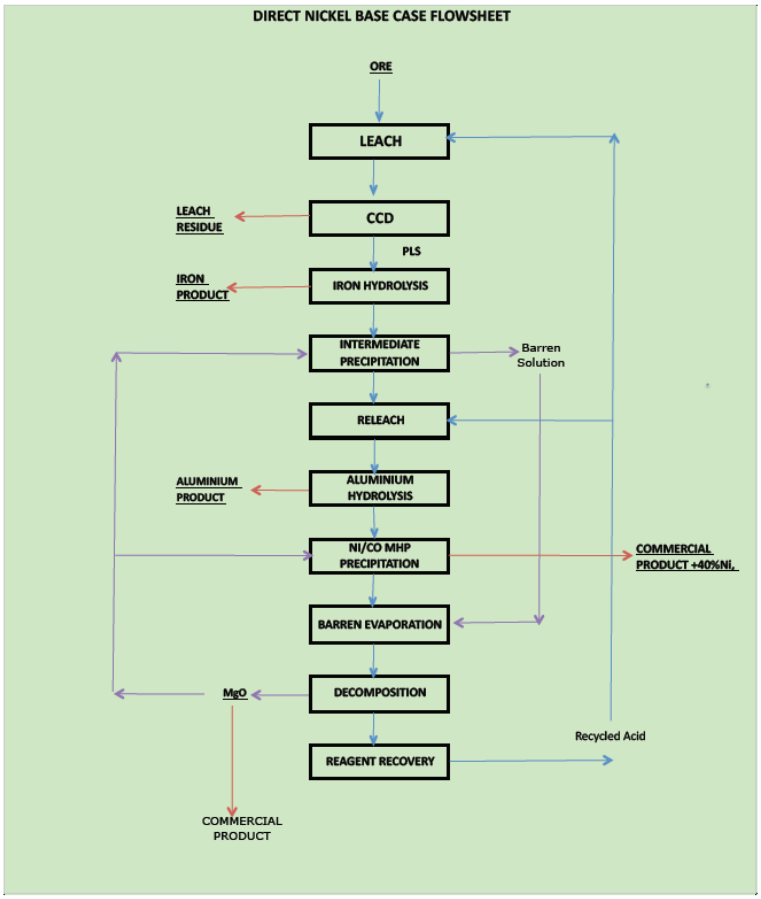

Figure 7: The direct nickel process flowsheet (31).

2.3.3.2 High Pressure Acid Leaching

With developing technology over mechanics and processes, the need to improve the treatment of lateritic ores also increased. In order to survive in the competitive markets, facilities had urge to improve the processes by increasing nickel and cobalt extraction efficiencies and by decreasing expenses like heat input. As one of the advantageous methods of hydrometallurgical processing over pyrometallurgical methods, pressure acid leaching was proposed to fasten the kinetics more than regular atmospheric leaching and to obtain more selective leaching. The first commercial high pressure acid leaching (HPAL or PAL) plant was built in Cuba, Moa Bay in 1959 by U.S. Freeport Minerals Company. But the general curiosity for HPAL plants was lost due to lack of qualified engineering materials and catastrophic engineering problems during operations. But again with increasing technological developments in building titanium autoclaves with strong structural integrity and high corrosive resistance for longer durations of leaching, in late 1990's three new plant were initiated in Western Australia. Unfortunately, Cawse and Bulong plants had to close up due to operational and technical problems and only Murrin Murrin was able to survive (18).

After gaining experience and knowledge on the previous projects, the third generation HPAL plants were started to be built such as Goro in New Caledonia and Rio Tuba in Philippines in 2004. With these new generation HPAL plants, it was understood that processing lateritic nickel ores with this new plant designs and technology is most feasible among all previous methods of processing. These facilities were followed by other plants like Ravensthorpe, Coral Bay, Taganito, Mindora, Ramu, and Ambatovy in Australia, Philippines, New Caledonia, Indonesia, Papua New Guinea, and Madagascar (5, 32). There is also an HPAL plant under construction with capacity of 10000 tons/year Ni which is equivalent to about 33000 tons/year MHP (mixed hydroxide precipitate) in Gördes/Manisa in

Turkey. META Nikel Kobalt A.Ş. is constructing a HPAL plant with all the side processing and supporting units. In this thesis, the limonitic type of ore that will be fed to the HPAL process in Gördes facility will be studied in detail. A simplified flowsheet of HPAL process is given Figure 8.

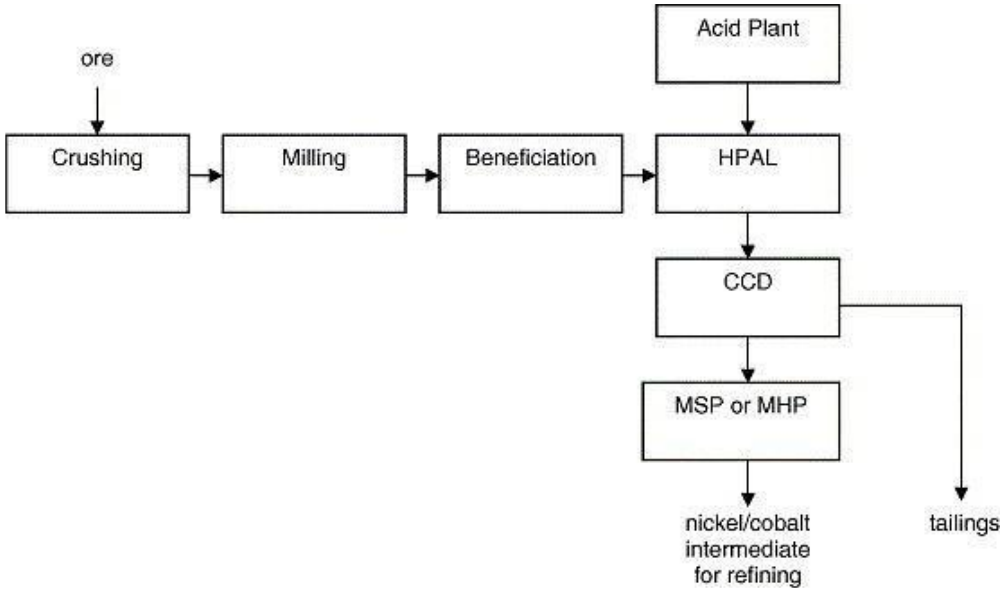

Figure 8: Simplified high pressure acid leaching process flowsheet (13).

By definition, high pressure acid leaching (HPAL) means operation of a reactor under high pressures (35 to 55 atm) and high temperatures (240 - 270 ^{o}C) for 0.5 to 1.5 h in order to leach a specific kind of ore (33). Depending on the mineralogical state of deposit, different kinds of ores can be mixed and fed to the autoclave. Gördes HPAL plant is planning to use limonitic and nontronitic ore mixture to upgrade the resultant nickel and cobalt extraction percentages and to lower the specific amount of acid usage per ton of ore. There is a simplified sketch in Figure 8, but the upstream process which involves all the processing steps like mixed hydroxide precipitation (MHP) and mixed sulfide precipitation (MSP) are not shown in detail. The general expectations on the extraction of nickel and cobalt percentages are at least 95%, but under some extreme conditions this value can be reduced to 90%. There is also a particle size range for the feed

ore as 250 to 500 μm but this value is not a strict restriction. Since the original grain size of goethite is fine, which is the main nickel containing mineral, a coarse size gangue mineral elimination can be practical by mechanical concentration of ore such as scrubbing. After that, the obtained slurry is thickened. The rheology of the slurry, which depends on the ore mineralogy, determines the degree of thickening. The solid concentrations below 25% to 30% are restricted by hydrophilic minerals (1). The possible water resources are either fresh or saline seawater, whichever the facility can provide. These factors directly affect the HPAL process. It is understandable that greater the solid density is, the less operation is conducted for the same amount of finished product. However, it is stated that slurries with higher than 42% solid will increase the viscosity beyond the pumping systems can handle properly through autoclave, CCD tanks and any kind of pipeline between stations (34). The slurry is fed to the autoclave simultaneously with acid injection from another tuyere. One of the most common problems encountered due to characteristics of water is the scale formation and changes in the leach residue character in HPAL.

As the construction material of modern autoclaves, titanium alloys are mostly used due to several reasons. The presence of chloride from sea water usage would be devastatingly corrosive. Titanium alloyed autoclaves have both resistance to corrosion of chloride and sulfuric acid and has structural strength to endure the high pressures without any deformation thanks to their special designs. For that purpose, the design of the modern autoclave had substantially changed. The early model used in Mao Bay had four different and vertical divisions that were lined with acid bricks. But in the latest model, they have been manufactured horizontally, lined with titanium plates and covered with carbon steel shells with seven different separate compartments which have their independent acid injection units. Each compartment is equipped with titanium blade agitators as seen in Figure 9 (17).

After charging the slurry into the first compartment, the prepared quantity of sulfuric acid (98.5% w/w) is injected with high pressure steam at temperatures between 245 - 275 °C. The injected sulfuric acid's amount is related directly with the ore mineralogy and the mixture of the ore feed. A regular limonitic ore demands 200 kg to 400 kg per ton of dry ore acid load while a regular atmospheric acid leaching process needs 1000 kg acid per ton of dry ore on average (17). So the relatively low acid need of HPAL process is acceptable when we consider some of that acid remains in the solution as free acid, at concentrations of 30 - 50 g/L. It is important to prevent any dissolved metals (magnesium, aluminum and iron) from precipitating. The importance of it will be discussed in upcoming sections.

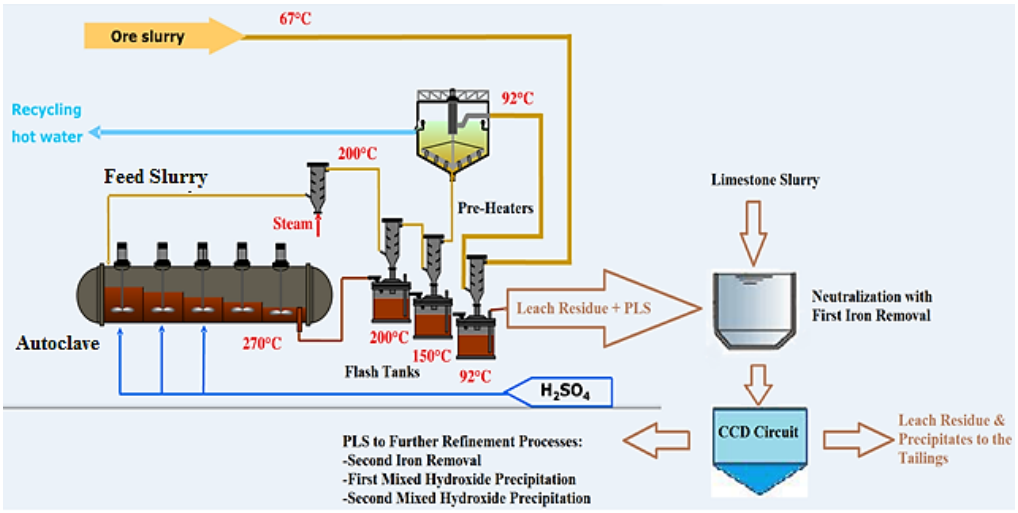

Figure 9: Schematic view of high pressure acid leaching flowsheet followed by mixed hydroxide precipitation process.

Following the acid leaching, for settling purposes of heterogeneous mixture of PLS and leach residue, the mixture is forwarded to counter-current-decantation (CCD) tanks. The neutralization is completed with limestone slurry addition to the mixture before flushing it to the CCD tanks. The dissolved nickel and cobalt are

among with all other dissolved metals in the slurry and they need to be separated from leach residue.

In conclusion, high pressure acid leaching has become more popular due to several logical reasons in the processing technology of nickel laterites deposits. It has some real advantageous points and some drawbacks on its own when it is compared with agitated atmospheric leaching. A detailed comparison is available in Table 2. In this study, both of the processing techniques will be studied with different types of limonitic ore under different experimental parameters.

Table 2: Comparison of HPAL with AL from different aspects (13, 18, and 35).

Issue	High Pressure Acid Leaching	Atmospheric Leaching
Capital Cost	High	Low
Maintenance	High	Low
Acid Consumption	High	Low
Acid Regeneration	Exist	Not Exist
Process Duration	Short	Moderate to Long
Extraction Efficiencies	High (>90%)	Variable (75% - 90%)
Energy Requirement	Moderate	Low
Settling Characteristics	Less challenging	More challenging
Solid Disposal Risk	Low	High

2.4. Chemistry of High Pressure Acid Leaching

2.4.1. Sulfuric Acid Chemistry

The role of sulfuric acid during leaching is one of the foundations of this process. As a polyprotic acid, sulfuric acid ionizes in aqueous solutions at ambient temperatures by Rx. 2.9 and 2.10:

$$H_2SO_4 + H_2O \rightarrow H_3O^+ + HSO_4^- \qquad \text{Rx. 2.9}$$

$$HSO_4^- + H_2O \rightarrow H_3O^+ + SO_4^{2-} \qquad \text{Rx. 2.10}$$

When we think of the autoclave environment, at temperatures exceeding 150 ^oC, the reaction 2.10's rate critically decreases and sulfuric acid becomes the only proton supplier to the media (36). However, some free acid content is also needed in the aqueous solution for the dissolved minerals that is why a specific hydrogen ion activity should be preserved in the solution. This was also defined by Krause et al. with a simple mass balance as the following reaction:

$$[SO_4^{2-}]_{free} \rightarrow [SO_4^{2-}]_{total} - [SO_4^{2-}]_{bound} \qquad \text{Rx. 2.11}$$

The free acid concentration is represented by the first term and the others show the total sulfate amount and sulfate bounded by metallic ions, respectively (36). The need for the free acid increases with the amplifying amounts of metal sulfates in the solution. The reason for that is the reduction of ionic activity due to behavior of metal sulfates in the PLS as proton sinks. However, one should understand the difference of free acid concept between autoclave environment at

high temperatures and after completion of process at room temperatures in the pregnant leach solution. Some research on this subject were conducted by Baghalha and Papangelakis and Rubisov et al. , hoping to explain the reasons for that phenomenon by studying the ternary system including sulfates of iron, aluminum and magnesium (37, 38).

2.4.2. Iron Chemistry

The limonitic layers of laterite ores consist of mainly iron minerals, which are fairly low acid consuming minerals. This is the main reason why limonitic ore deposits are more suitable for high pressure acid leaching. Goethite and hematite are the two main minerals existing in limonitic ore deposits. It is also reported that magnetite and maghemite are found among Chinese laterites (12). Since the majority of iron minerals are goethite and hematite, and since they are the most nickel and cobalt bearing minerals among others, the dissolution of them in HPAL process should be investigated.

The form of iron in goethite and hematite is trivalent; the dissolution reaction of the minerals increases the trivalent (ferric) iron concentration in PLS. Later, the dissolved ferric iron precipitates as hematite in the autoclave environment. Goethite (FeOOH) dissolves and precipitates by the following Rx. 2.12:

$$2FeOOH \rightarrow Fe_2O_3 + H_2O \qquad \text{Rx. 2.12}$$

The transformation of goethite into hematite is promoted by acid's presence at temperatures above 150 ^{o}C, where goethite is unstable (free energy of transformation reaction is negative). Unfortunately, the transformation of goethite

into hematite with a single simple reaction is not entirely accurate. There are two different mechanisms proposed in the literature. In the first proposal, goethite dissolution leads to ferric iron formation which is followed by rapid precipitation of that ferric iron as hematite. This is occurring according to Rx. 2.13 and 2.14;

$$2FeOOH + 3H_2SO_4 \rightarrow 2Fe^{3+} + 3SO_4^{2-} + 4H_2O \qquad \text{Rx. 2.13}$$

$$2Fe^{3+} + 3SO_4^{2-} + 3H_2O \rightarrow Fe_2O_3 + 3H_2SO_4 \qquad \text{Rx. 2.14}$$

And the overall reaction is this:

$$2FeOOH \rightarrow Fe_2O_3 + H_2O \qquad \text{Rx. 2.12}$$

Georgiou and Papangelakis stated that there was no evidence of ferrous phase but there was hematite's presence observed from the results of TEM and XRD inside the leach residue. This meant hematite formation from goethite could be condition dependent (39, 40).

The second proposed mechanism offers a mid-product during the dissolution and precipitation mechanisms. As one can see from Rx. 2.15 and 2.16, basic ferric sulfate forms with the dissolution of goethite during leaching and after that hematite formation occurs with the precipitation.

$$2Fe^{3+} + 2SO_4^{2-} + 2H_2O \rightarrow 2FeOHSO_4(s) + 2H^+ \qquad \text{Rx. 2.15}$$

$$2FeOHSO_4 + H_2O \rightarrow Fe_2O_3\,(s) + 2SO_4^{2-} + 4H^+ \qquad \text{Rx. 2.16}$$

It is noticeable that the net acid consumption in both proposals is zero if only hematite is the one and only final product, which means no acid addition into the solution since it regenerates itself. But, according to reaction 2.16; 2 moles of H^+ are created per 2 moles of goethite dissolution. In reaction 2.13, 2 moles dissolution of goethite consume 3 moles of acid. In total, 1 mole of acid is consumed during the reactions. This is explained by a sudden drop in the acid concentration which increases its level with increasing recovery rate in time. The regeneration reduces the overall demand for acid to leach nickel and cobalt in HPAL process and lowers its economic burden.

Papangelakis et al. proposed that at the very beginning of acid attack, the iron concentration is increased to very high levels instantly and precipitation (with homogeneous nucleation) is started as soon as the iron starts to dissolve in solution. With this supersaturated iron concentration and simultaneously precipitation of hematite process, nickel and cobalt are released from goethite and hematite lattice. After a while, with increasing temperature, the dissolution and precipitation rates come to a balance and iron's concentration in the solution reaches its equilibrium value. Papangelakis and their colleagues reached on a consensus that the iron solubility increases with high acidity and low temperatures. This is finalized with more hematite precipitation, but with the supporting effect of temperature on dissolution rates of goethite and nickel coming to a contradicting balance (41).

In another study conducted in 2008, the ferrous iron concentration in PLS of HPAL was studied extensively, and iron was found to be in divalent condition. The initial results showed very high concentration of iron like 11000 ppm after the first analysis of PLS. The reason for this situation was stated as the need of high temperature for iron to precipitate as hematite. Otherwise, it would stay in

the solution as $FeSO_4$ causing acid consumption (42). The transformation of $FeSO_4$ into hematite is given in the next reaction:

$$4FeSO_4 + O_2 + 4H_2O \rightarrow 2Fe_2O_3 + 4H_2SO_4 \qquad \text{Rx. 2.17}$$

Although the nontronite type lateritic nickel ore is not going to be used in this study, understanding its dissolution kinetics might be important. The nontronite type of lateritic nickel ore can be found in the layers of limonitic ore. The dissolution of nontronite follows Rx 2.18:

$$Fe_2Si_4O_{10}(OH)_2 + 3H_2SO_4 \rightarrow Fe_2(SO_4)_3 + 4SiO_2 + 4H_2O \qquad \text{Rx. 2.18}$$

Sometimes the sodium salts coming from limonitic ore or saline water usage affects the dissolution and precipitation reactions to form natrojarosite as mid-product. Actually jarosites is iron containing member of a larger group of mineral branch with a general formula of $AB_3(SO_4)_2(OH)_6$ where A= H_3O^+, Na^+, K^+, NH_4^+; B= Al, Cu, Fe. Natrojarosite is the one with Na+ ions inserted into the formula. The formation reaction of natrojarosite is given in Rx. 2.19:

$$3Fe_2(SO_4)_3 + 12H_2O + Na_2SO_4 \rightarrow 2NaFe_3(SO_4)_2(OH)_6 + 6H_2SO_4 \qquad \text{Rx. 2.19}$$

Unfortunately, the occurrence of jarosite has some drawbacks when it is compared with hematite. The most important thing is the loss of acid. In jarosite precipitation, acid does not regenerate itself in the same amount with the hematite precipitation. Also hematite has much more stable structure and has potential to

be put on the market as iron based product. Moreover, jarosite precipitation occurs in a scale form on the walls of pressured container. It takes much more effort and cost to scrape it off.

2.4.3. Aluminum Chemistry

Aluminum is one of the important elements that is critical for the both downstream process and for the acid regeneration. In lateritic nickel ores, aluminum has 3 different forms. Gibbsite ($Al(OH)_3$) and Boehmite (AlOOH) are the ones with their own crystal structure. For the third one, aluminum is associated with goethite and chromite as substitution element (43). The gibbsite transforms into boehmite in autoclave at temperatures above 135 ^oC according the following Rx. 2.20:

$$Al(OH)_3 \rightarrow AlOOH + H_2O \qquad \text{Rx. 2.20}$$

After the injection of acid into the autoclave environment, the boehmite dissolves with the following Rx. 2.21:

$$AlOOH + 3H^+ \rightarrow Al^{3+} + 2H_2O \qquad \text{Rx. 2.21}$$

With increasing leaching durations, the concentration of dissolved aluminum in the pregnant leach solution will also increase. In parallel to precipitation of iron, aluminum also precipitates as alunite or other stable phases and regenerates acid into the solution. This regeneration also helps to lower the acid consumption in HPAL operations. The state of the stable phases of aluminum shows difference according to the temperature of the leaching conditions and concentration of acid.

The formation of alunite for the temperatures below 250 ^{o}C occurs by the following Rx. 2.22:

$$6Al^{3+} + 4SO_4^{2-} + 14H_2O \rightarrow 2H_3O.Al_3(SO_4)_2(OH)_6 + 10H^+ \qquad \text{Rx. 2.22}$$

However, for the temperatures above 280 ^{o}C, the thermodynamically stable phase is basic aluminum sulfate formation. This formation also regenerates acid just like the alunite formation. The basic aluminum sulfate formation occurs according to Rx. 2.23:

$$Al^{3+} + SO_4^{2-} + H_20 \rightarrow Al(OH)SO_4 + H^+ \qquad \text{Rx. 2.23}$$

As it was mentioned before, the acid concentration is also important in which stable phase of aluminum precipitates. If acidity is high (higher than 50 g/L), the formation of $Al(OH)SO_4$ is favored for the temperatures above 280 ^{o}C. If the acidity level is between 20 g/L and 50 g/L, the stable phase becomes alunite as precipitate (39, 44).

Also the precipitation of alunite may lead to loss of nickel and cobalt within its crystal structure, since the atomic radii of the nickel and cobalt atoms are suitable for substitutional replacement in aluminum's host crystal structure (45).

2.4.4. Magnesium Chemistry

In HPAL operations the iron and aluminum can safely be removed from pregnant leach solutions with precipitation at great quantities. Removal of these elements helps to lower the overall acid consumption by regenerating the acid. However in magnesium case, there is no such thing. Moreover, the chemistry of it should be well understood in order to maintain the necessary acid concentration. The residual acid concentration is important to prevent nickel and cobalt formation as monohydrate sulfate salts of their own (46).

The general occurrence of magnesium in lateritic type nickel ores is around 1.5% or less which corresponds to 0.2 to 0.4 kg/kg. But in most of the cases saprolitic type ores are blended with limonitic ores in order to increase the extraction percentage of nickel and cobalt in HPAL operations for economic reasons. This mixing process increases the magnesium content overall from 0.9 to 2.7% and also increases the acid consumption from 0.22 to 0.33 kg/kg (47). The reflection of this increase on acid consumption is 50% of total acid demand. The dissolution reaction of simplified saprolitic ore is:

$$Mg_3Si_2O_5(OH)_4 + 3H_2SO_4 \rightarrow 3MgSO_{4\,(aq)} + 2Si(OH)_4 + H_2O \qquad \text{Rx. 2.24}$$

After magnesium dissolution in the pregnant leach solution, it exits as cations. The solubility of magnesium is temperature dependent. That's why the difference in the acid concentrations is dependent to solution's temperature at that moment, whether it is at high temperature or at room temperature. Magnesium sulfate complexes' solubility increase when the solution's temperature drops under 80 ^{o}C, which means the representation of current solubility is not accurate with solubility of magnesium at the high temperatures. To fulfill the free acid requirements even

at high temperatures, the free acid concentration should be raised to 50 g/L from 30 g/L, in other words, to undermine the effects of magnesium's solubility at high temperatures (37, 38).

Although the extraction percentages show differences from variable ore deposits, it is reported that 50 to 60% of magnesium dissolves in HPAL operations. The dissolution of magnesium totally is not studied entirely. Other than increasing the acid consumption incredibly, it allows to formation of soluble silica after leaching according to Rx. 2.25:

$$Mg_3Si_2O_5(OH)_4 + 3H_2SO_4 \rightarrow 3MgSO_4 + 2SiO_2 + 5H_2O \qquad \text{Rx. 2.25}$$

2.4.5. Manganese, Nickel, Cobalt Chemistry

Nickel and cobalt are the sole reason for this kind of studies to happen. In order to increase these valuable metals extractions into the solution from related ores, one must understand the chemistry of the host minerals which they substitute into. Since manganese minerals are one of them, it has great significance to understand the chemistry and its leaching behaviors. The oxyhydroxide minerals of manganese in lateritic nickel-cobalt ores can be listed as following; asbolane $(Co,Ni)_{1-y}(MnO_2)_{2-x}(OH)_{2-2y+2x}\cdot n(H_2O)$, lithiophorite $(Al,Li)MnO_2(OH)_2$ and birnessite $Na_4Mn_{14}O_{27}$ (48, 49).

The cobalt is related with manganese minerals in large quantities so they have similar dissolution kinetics but manganese has slower pace of dissolution compared to cobalt. Goethite is another host mineral that can contain cobalt. But

since cobalt exists in goethite in replacement of iron atoms without creating a substantial structural deformation, the goethite particles are not capable of hosting cobalt as manganese minerals do. Another reason for the amount of cobalt's difference between manganese minerals and goethite can host, is the behavior of them according to weathering conditions during formation of ore deposit. Manceau et al. stated that the cobalt and manganese behave in the same manner to accumulate and create a solid solution in ore deposit (48).

The mentioned manganese minerals are hard to leach and some sort of reducing agents are needed for complete leaching. This causes low nickel and cobalt extraction values. However, some of the clay like minerals may have a reducing agent role by supplying ions to the leaching environment. For example, with the existence of Fe(II) from clays helps to reduce the Mn (IV) in lithiophorite in nontronite type of ores and increases the nickel and cobalt extraction percentages. On the other hand some of the reducing agents may cause problems in terms of Fe^{+2} ions. The major problem is to prevent the reduction of Fe^{+3} into Fe^{+2} from goethite mineral and this may lower the amount of precipitated hematite. The lack of hematite precipitations affect acid regeneration negatively and cause an increase in acid consumption and affect the settling characteristics negatively. Also, large amounts of Fe^{+2} existences in the solution disturb the downstream process mechanisms in a negative manner (50).

It is generally assumed that nickel, cobalt and manganese have simple oxides and the dissolution reactions are conducted according to them as following Rx. 2.26 to 2.30:

$$3MnO_2 + 2H_2O + 2Cr^{3+} \rightarrow 3Mn^{2+} + 2H_2CrO_4 \quad \text{Rx. 2.26}$$

$$2Fe^{2+} + MnO_2 + 4H^+ \rightarrow 2Fe^{3+} + Mn^{2+} + H_2O \quad \text{Rx. 2.27}$$

$$Co_2O_3 + 6H^+ + 2Fe^{2+} \rightarrow 2Co^{2+} + 3H_2O + 2Fe^{3+} \quad \text{Rx. 2.28}$$

$$NiO + 2H^+ \rightarrow Ni^{2+} + H_2O \quad \text{Rx. 2.29}$$

Also many studies stated the importance of free acid in the PLS. According to Da Silva et al., if necessary amount of residual acid is not present in the solution, the nickel and cobalt might precipitate as their respective monohydrate salts $NiSO_4.H_2O$ or $CoSO_4.H_2O$ (46).

2.5. Scandium Recovery as by-Product

The general usages of rare earth elements are becoming more common with developing technologies. Scandium, as one of them can be found in colored televisions, fluorescent lamps, aluminum-scandium alloys in aerospace industry, fuel cells and other high-tech products that depend on high performance materials. That is why the extraction of scandium from related deposits is gaining importance. Scandium has a broad range of existence in different types of ores and in different types of mineral structures. But it does not have a specific type of affinity to a specific mineral, so it prefers to be present as solid solution with more than 100 types of minerals.

The main production lines of scandium are located at China, Kazakhstan, Russia and Ukraine. However, the technical data on ore deposit profiles and extraction flowsheets are not available. In ferromagnesian ore deposits like pyroxene and biotite, scandium exists in 5 to 100 ppm as a trace amount. This is the main reason why scandium is a by-product among other elements. High pressure acid

leaching is one of the methods that scandium can be recovered while processing the lateritic nickel ores. Ion exchange and solvent extraction are possible recovery methods after the pregnant leach solution obtained from HPAL (32). A new method called Neomet was proposed to market by Neomet Technologies Inc., which suggest an atmospheric hydrochloric acid leaching process. The most critical stage in the flowsheet is the addition of a new step where the Sc recovery can be possible following the CCD separation and before aluminum, iron and chromium removal stages as seen in Figure 10 (17).

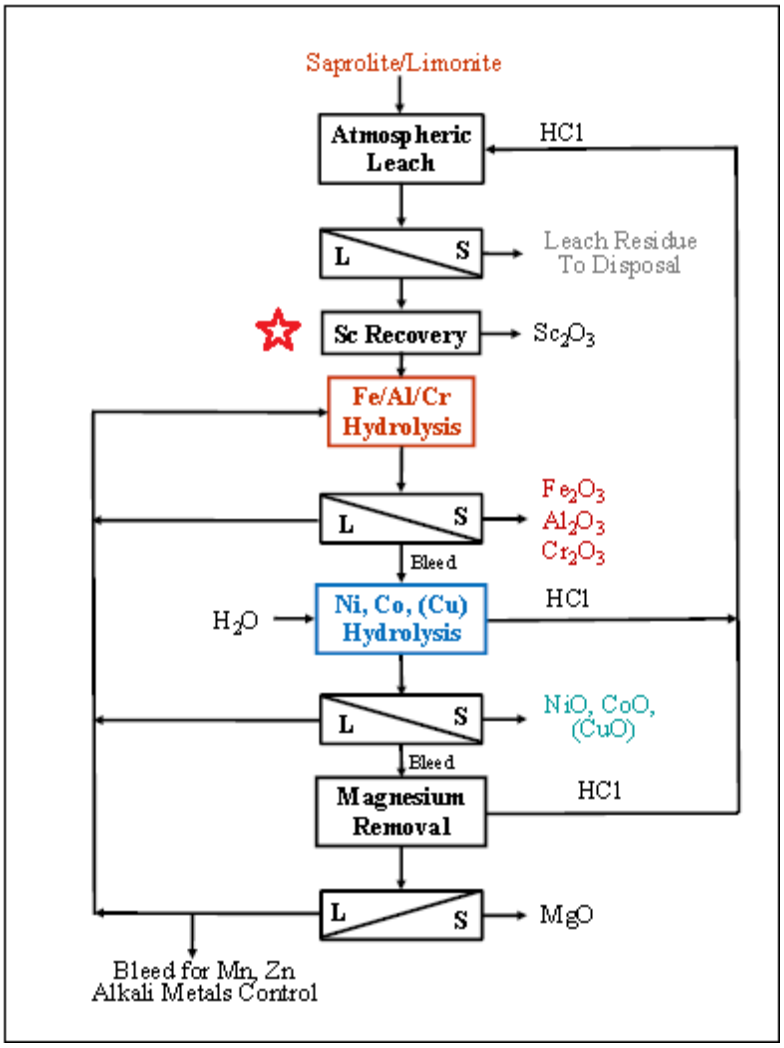

Figure 10: Neomet atmospheric chloride leaching process with addition of scandium recovery step (51).

In conclusion, scandium is one of the critical elements for many high-tech industry and most of the production lines are in very few number of countries' grasp. It can be found in lateritic type nickel ores and can be processed with some additions of extra side facilities to the HPAL flowsheet. In Turkey, both Çaldağ and Gördes have feasible amounts of scandium existing in their nickel ores and extraction of them is being considered in the near future after the additional facilities constructions are completed. For the market value of scandium, USGS reports scandium prices depending on purity level, whether it is in compound form or in elemental form. The base price of scandium oxide with 99% purity was announced as 900 US dollars/kg and the price rises up to 3260 US dollars as the purity increases to 99.9995% (52).

CHAPTER 3

SAMPLE CHARACTERIZATION, EXPERIMENTAL SET-UP AND PROCEDURE

3.1. Sample Description

In this master thesis, two different kinds of limonitic nickel laterite ore were obtained from Manisa/Gördes open pit mine owned by 'META Nikel Kobalt A.Ş.'. The ore samples were subjected mainly to high pressure acid leaching and atmospheric agitated acid leaching tests. Characterization of these ores has been described in the following sections.

3.2. Sample Preparation and Physical Characterization of Ore Samples

Both of the representative limonitic type nickel laterite ore samples numbered as 1 and 2 (coded as KK01001 and KK02002) from Gördes were 200 kg and 20 kg, respectively with as-received sizes of minus 20 mm and minus 74 μm. The first sample which was low in arsenic had dark brown color and the second sample which was high in arsenic had light yellowish brown like color. Bulk and solid density measurements were done for both samples and the results are given in Table 3. The as-received ore samples were used for the bulk density

measurements which were determined according to the ore weight to ore volume ratios. The solid densities of the dried and ground samples were measured with helium pycnometer.

Table 3: Bulk and solid densities of limonitic ore samples (g/cm^3).

Representative Sample	Sample 1 - KK01001 (Limonitic ore)	Sample 2 - KK02002 (Limonitic ore)
Bulk Density, As-received Ore	1.04 g/cm^3	1.09 g/cm^3
Solid Density, (-38 μm)	3.27 g/cm^3	3.57 g/cm^3

The moisture content determinations were carried out after the density measurements. For this purpose, the particle size of sample 1 needed to be reduced to carry out the moisture determination as well as for the high pressure and atmospheric leaching experiments. So, at the beginning total amount of the first ore was reduced to minus 850 μm step by step crushing with jaw and roll crushers. After all of the ore was reduced to minus 850 μm, then it was mixed on a flat surface by forming of a cone with flattened top using a shovel's tip following the conining and quartering method rules and was divided into four quadrants by using a cross. This procedure was repeated until a smaller amount of representative ore was obtained, which was 25 kg for the first ore. The second limonitic ore was already fine and 20 kg in weight. They were both weighted and dried at 105 ^oC overnight in a drying oven until reaching a constant weight. The dry weights were determined after the drying process and the results obtained are given in Table 4. According to these results, since the moisture contents of both of these ores were high, the use of a pyrometallurgical process would most probably be more expensive due to the high cost of removal of physically held water.

Table 4: Moisture contents of the representative limonitic ore samples.

Representative Sample	Moisture Content (%)
Sample 1 - KK01001 (Limonitic ore)	28
Sample 2 - KK02002 (Limonitic ore)	34

In order to prepare the samples for chemical analysis, XRD and SEM and to use in the experimental stage, further particle size reductions were necessary. For that purpose, both ores were sampled with Johns Riffle sampling device. Necessary amounts of them were ground to minus 38 μm by using a disc type laboratory grinder. The ground ore samples were used for chemical and mineralogical characterization purposes and for the experimental studies. Also, in order to find out the particle size distribution, the first ore was subjected to wet screen analysis. For the analysis, a nest of screens made up of 9 different sieves in series was used. They were placed in an order of decreasing sieve aperture sizes by the square root of two, starting from 600 μm and finishing with 38 μm. After doing the wet screen analysis, the solids accumulated on each sieve were collected and dried overnight in a drying oven at 105 ^{o}C. Finally, their weights were determined. The results obtained for the first sample are summarized in Table 5. No wet screen analysis was carried out on the second sample because it was already below 74 μm.

All the experiments related to the effect of particle size on leach extractions were conducted with the first sample and the optimum conditions determined were applied to the second limonitic ore sample.

Table 5: Wet screen analysis of the first limonitic ore ground to -850 μm.

Size (μm)	Weight (%)	Cumulative wt. (%) Oversize	Cumulative wt. (%) Undersize
600	7.80	7.80	92.20
425	5.30	13.10	86.90
300	5.40	18.50	81.50
212	5.25	23.75	76.25
150	4.95	28.70	71.30
106	4.75	33.45	66.55
75	5.05	38.50	61.50
53	5.10	43.60	56.40
38	5.65	49.25	50.75
-38	50.75	-	-
Total	100.00	-	-

3.3. Chemical Characterization of Ore Samples

Numerous elements can be present in nickel laterite ore deposits. Chemical characterization of these limonitic ores is important from many perspectives; first of all the understanding of the chemical structure of these ores will help us to find the causes of lower leach extraction values due to the possible chemical reactions and kinetic phenomena during the leaching processes. Secondly, the data that is gathered from the leach residues and original ores will indicate us how successful we are in terms of the objectives of a specific experiment. Moreover, the chemical analysis of ore will indicate how much acid should be used in the experimental stage. The chemistry of important elements related to this thesis is already summarized in the literature review part. Inductively Coupled Plasma (ICP) method was used for the complete chemical analysis of the limonitic ore samples.

Initially, both samples were ground to minus 38 μm before the chemical analysis. Then, the samples were sent to the ALS Analytical Chemistry and Test Services in Canada. The results are given in Table 6.

Table 6: Complete chemical analysis of limonitic ore samples 1 and 2.

Element	Sample 1 wt. (%)	Sample 2 wt. (%)
Ni	1.08	0.98
Co	0.069	0.038
Fe	29.90	23.30
As	0.85	2.17
Al	3.80	3.70
Mn	0.38	0.12
Si	12.64	16.15
Mg	0.74	0.51
Cr	1.09	1.05
Ca	0.51	1.49
Sc	73 ppm	34 ppm
Loss of Ignition	11.85	10.76

From Table 6, it can be clearly seen that the arsenic contents of the two limonitic samples were substantially different from each other. As it can be noticed from the XRD results in the mineralogical analysis section, arsenic in the ores did not exist in a separate mineral form but was present as a substitutional element similar to nickel and cobalt in the iron oxide crystal structures, namely hematite and goethite.

Also the current wet screen analysis results showed that 50.75% of the first sample was below the particle size of 38 μm. A similar result was reported by Büyükakıncı that 40-49% of the sample he studied was under the particle size of 38 μm. (29) Also Kaya stated that 47.77% of limonitic and 48.91% of nontronitic similar ore samples from Gördes were under the size of 45 μm. (53) Both studies also concluded that the finer fractions of the ore samples had more nickel and cobalt with respect to coarser particles.

3.4. Mineralogical Characterization of Ore Samples

3.4.1. XRD Examinations

For the mineralogical examination of two limonitic ores, Rigaku D/MAX2200/PC model X-ray Diffractometer (XRD) with a Cu-Kα X-ray tube working under 40 kV and 40 mA was used. Initially 200 g of each dry sample was reduced below 38 μm and prepared for the analysis. The XRD patterns of the ores studied are given in Figures 11 and 12.

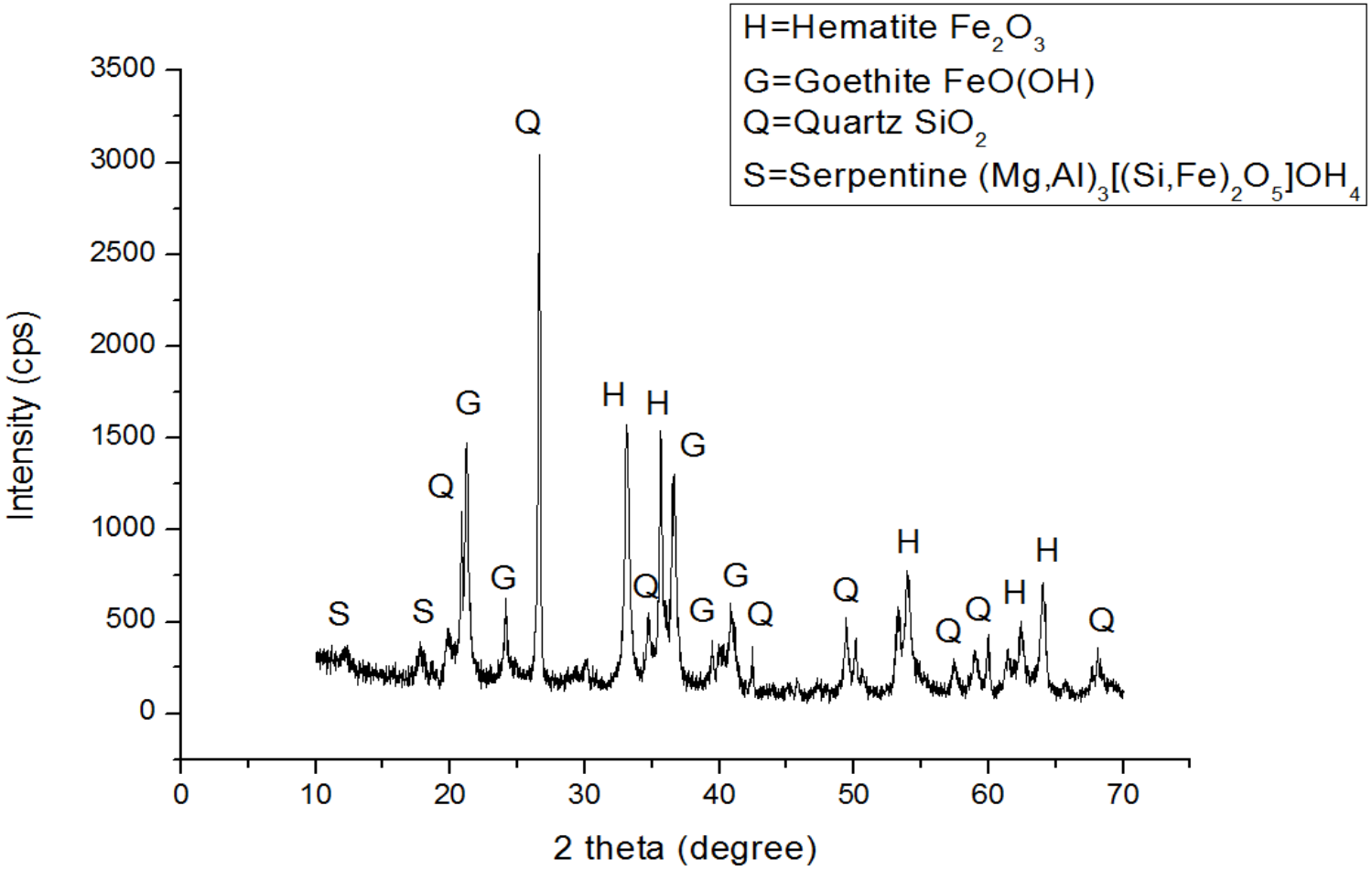

Figure 11: XRD pattern of limonitic ore sample 1.

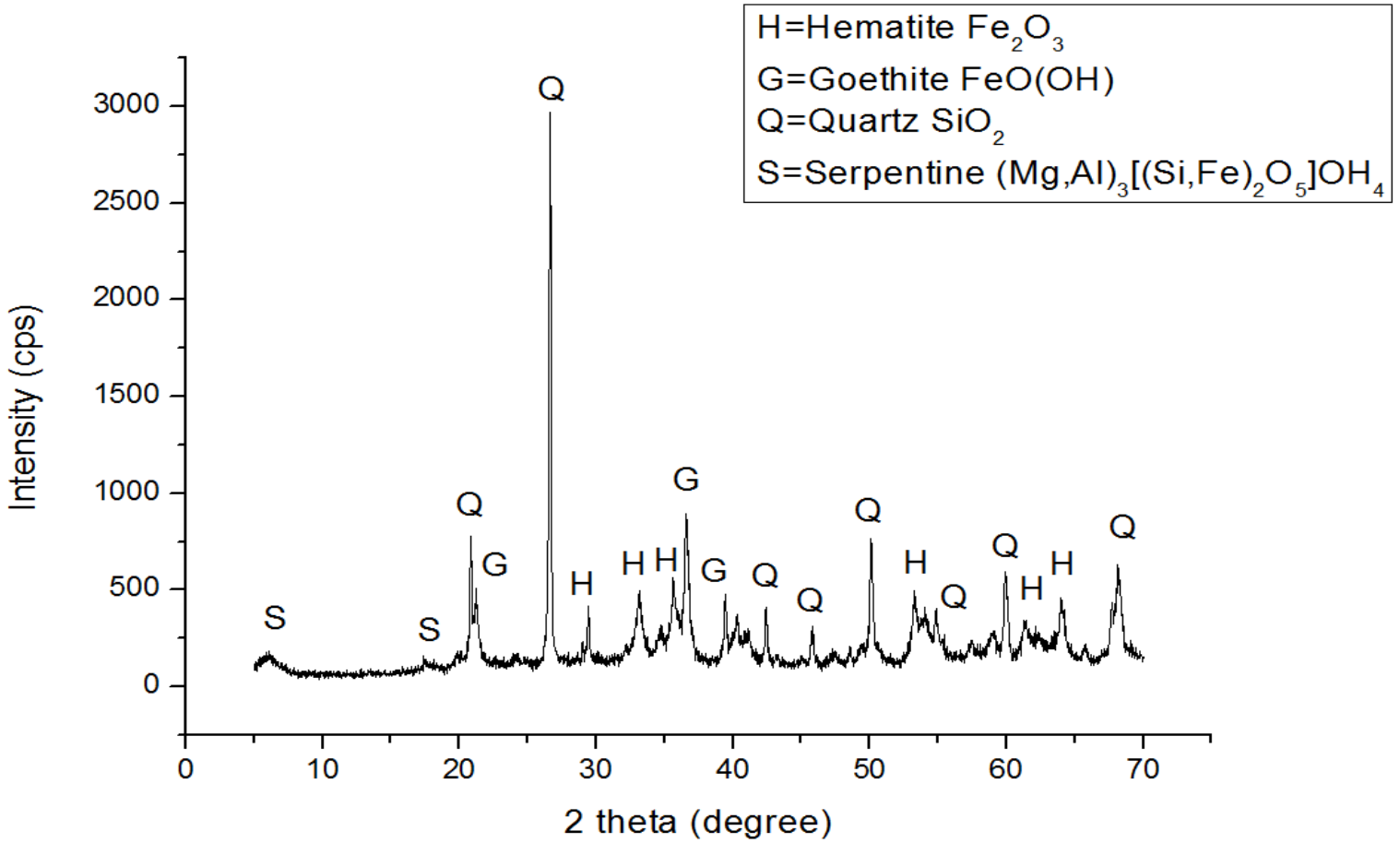

Figure 12: XRD pattern of limonitic ore sample 2.

From the XRD patterns, it was noticed that the major peaks belonged to hematite (Fe_2O_3), goethite (FeOOH) and quartz (SiO_2). Other than the major minerals, some minor minerals were also detected. Serpentine ($(Mg,Al)_3[(Si,Fe)_2O_5]OH_4$) was the main minor mineral detected in the ore samples 1 and 2. There were not many differences between two limonitic ore samples other than the amounts of major minerals. From the mentioned figures, it can be seen that the second limonitic ore had relatively smaller peaks of iron oxide minerals, whereas the first ore had much higher peaks when we compare them in terms of intensity while the main quartz peaks being almost similar. This is understandable when we refer to the chemical characterization part and notice that iron tenor was lower in the second limonitic ore compared to the first limonitic ore. In addition to that, the elemental differences between the samples could not be distinguished, since most of them did not have their own lattice structure, but existed as substitutional or interstitial atoms, such as Ni, Co, As, Mn and Sc in other minerals. To verify this point, scanning electron microscope was used and nickel was found mostly in the lattices of goethite (FeOOH), hematite (Fe_2O_3), smectite and serpentine.

3.4.2. DTA-TGA Studies

For the purpose of validation of identified minerals within each ore sample, the thermal analysis was done. These are named Differential Thermal Analysis (DTA) and Thermo Gravimetric Analysis (TGA), which were conducted at the central laboratory in Middle East Technical University. Ores were ground to 100% -38 μm and sent to analyses which were performed with 10 ^oC/minute heating rate within the temperature range of 35 - 1000 ^oC in air atmosphere in an alumina crucible. The resultant graphical data can be seen in Figures 13 and 14.

Only the initial sections of the graphical data was mainly interpreted. Dehydration is the loss of physically held water with increasing temperature whereas dehydroxylation is the loss of chemically bonded water with increasing temperature. The limonitic nickel ores hold water physically which is removed at 100 ^{o}C which is represented by an endothermic peak in both DTA curves and by a decline in TGA curves linked with a loss of weight. This was observable in both cases.

Normally, goethite gives an endothermic peak between 358 and 405 ^{o}C depending on its purity. For higher temperature intervals (500 - 1000 ^{o}C), it does not show any peaks. Hematite, if it is pure, gives a small endothermic peak around 675 to 680 ^{o}C. This temperature also corresponds to the Curie point of hematite. However, none of the minerals exist as pure substances in ore deposits and the mixed characteristics of them affect the regular peaks and shift the temperature to lower levels with increasing amount of hematite. Moreover, the presence of impurity elements like Ni, Co, Mn, Al and Cr in hematite and goethite also affects the dehydroxylation temperature.

The transformation of one mineral to another is also a common phenomenon during DTA/TGA experiments. These types of behavior have been also mentioned by Lopez et al. ; the transformation of goethite into hematite under oxidative environment happens by goethite losing its chemically held water with the following reaction around 300 ^{o}C (54).

$$2\ \alpha\text{-}FeO(OH) \rightarrow \alpha\text{-}Fe_2O_3 + H_2O \qquad \text{Rx. 3.1}$$

Also Landers et al., stated that this transformation starts from the surface structure of goethite and progresses into the inner sections through holes and cavities, finishing with a clear decrease in the total volume, since the hematite has smaller unit volume than goethite (55).

As one can see from the mentioned figures that the continuing mass loss in TGA curves with increasing temperatures from 320-800 ºC has resulted in very small peaks but in both figures there is an endothermic decrease around 690-700 ºC, which may be the indication of allotropic transformation of quartz from α-quartz to hexagonal β-quartz which occurs at 573 °C ± 40 °C (56).

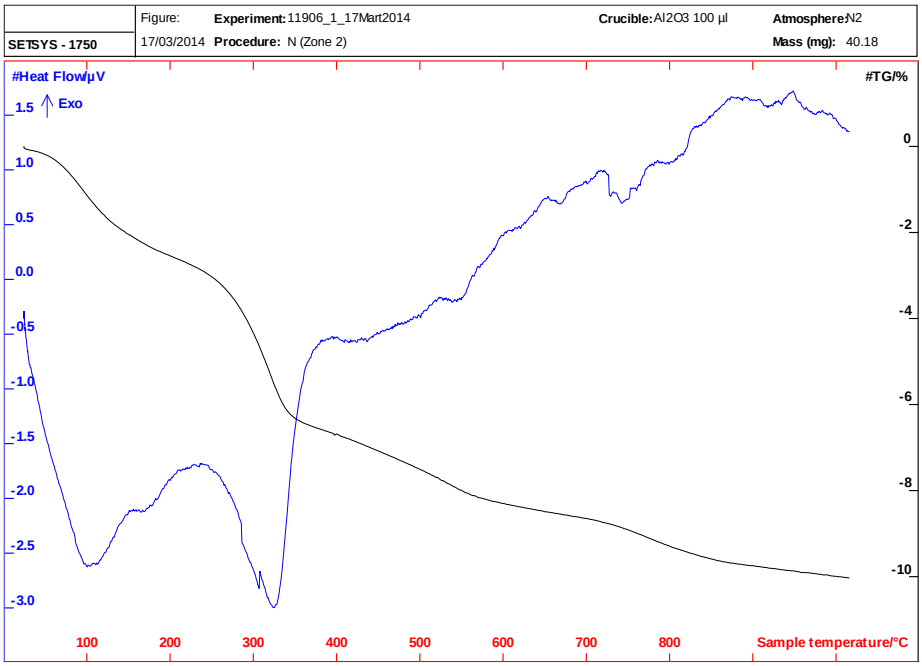

Figure 13: DTA-TGA results for limonitic ore sample 1.

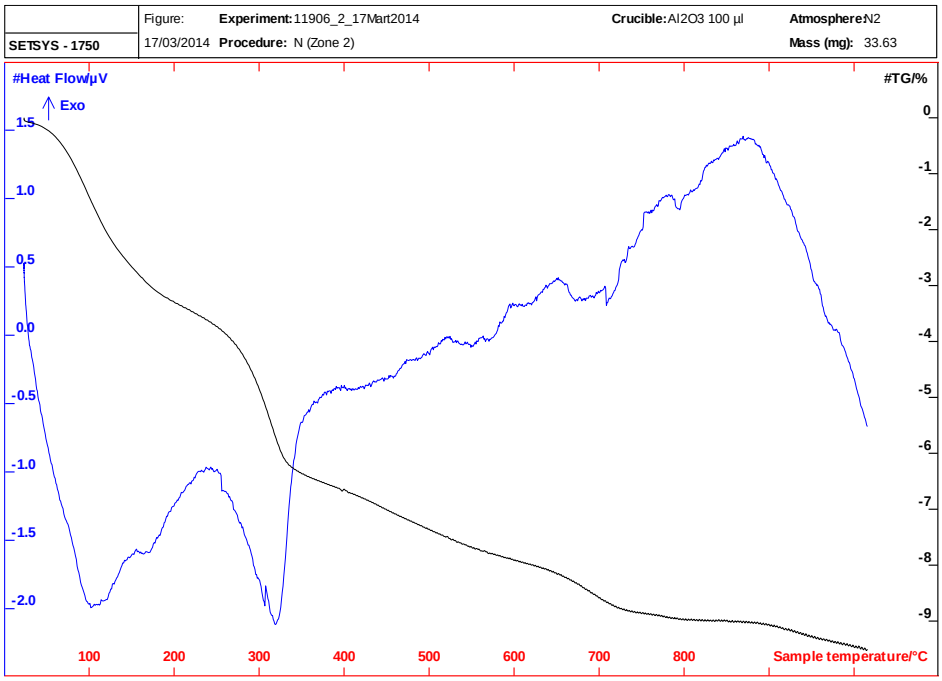

Figure 14: DTA-TGA results for limonitic ore sample 2.

3.4.3. SEM Studies

For the verification of mineralogical characterization done by the XRD, Scanning Electron Microscope (SEM) was used. Both initial ore samples were studied with Nova Nanosem 430 in the Department of Metallurgy and Materials Engineering. Due the insufficient data obtained from both XRD results and thermal analyses, scanning electron microscope usage for the examination of the initial samples is extremely important for several reasons. Firstly, the determination and confirmation of high acid consuming elements like Mg and Al may generate valuable data about the expected acid consumption of experiments. It is very important because of the industrial applications' critical dependence on acid consumption, which was already mentioned in the literature review. Secondly, it may provide information for the extraction process of valuable metals from the host minerals, which means setting free important elements from the lattice of relevant minerals. The information may offer an answer for the low extraction

values in terms of surface and solution kinetics of both atmospheric and high pressure acid leaching experiments. The visual confirmation of existing main minerals like goethite, hematite and quartz was possible with SEM imaging of the ore samples and after the experiments the leach residues. Also further information could be obtained with the use of energy-dispersive X-ray spectroscopy (EDS) unit option. Performing the chemical analysis of the images would support the possible theories and might explain why low valuable metal extraction values were obtained at the experimental stage. The first theory is that the precipitating hematite (secondary) from dissolved goethite and hematite (primary) in an acid environment may inhibit the continuing leaching process of the primary hematite by precipitating on the contact surface of this mineral which is offering a nucleation site during the HPAL process. The second theory suggests that the presence of impurity element like arsenic in lateritic ores, may affect the leaching process which may lead to the loss of valuable metal ions into the leach residue. These theories may only be proven in the light of clea-r evidence and data obtained from SEM analyses.

In the preparation of SEM samples, two methods were followed for different ore samples; the first method was to sieve the ore and collect the relatively large ore pieces with different visual appearances by tweezers. Wash them to clean the surface of the unknown pieces from mud and dust and place them on to carbon tape on a sample holder. This method was only applied to the sample 1. In the second method, very small amount of minus 38 μm ore was mixed with acetone and put into ultrasonic agitator to prevent agglomeration on the carbon tape. After 10 minutes agitation, with the help of a pipette, a couple of drops of the prepared sample were put on the carbon tape on a sample holder. After drying of alcohol, the samples were coated with carbon or platinum to prevent electron clouds on the sample during examination. The general appearances of ore samples 1 and 2 are given in Figures 15 and 16.

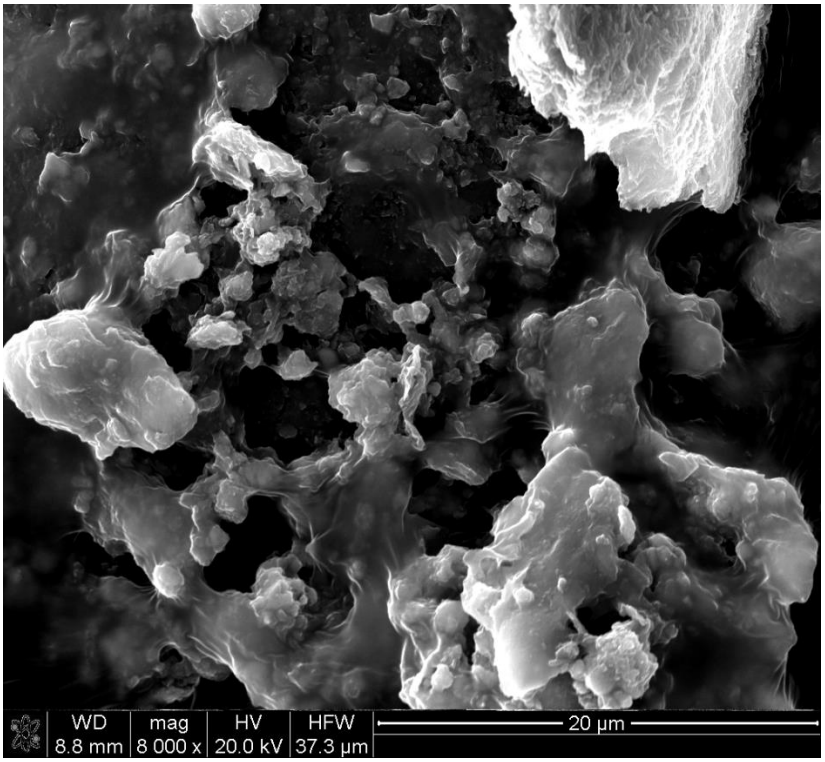

Figure 15: General appearance of ore sample 1.

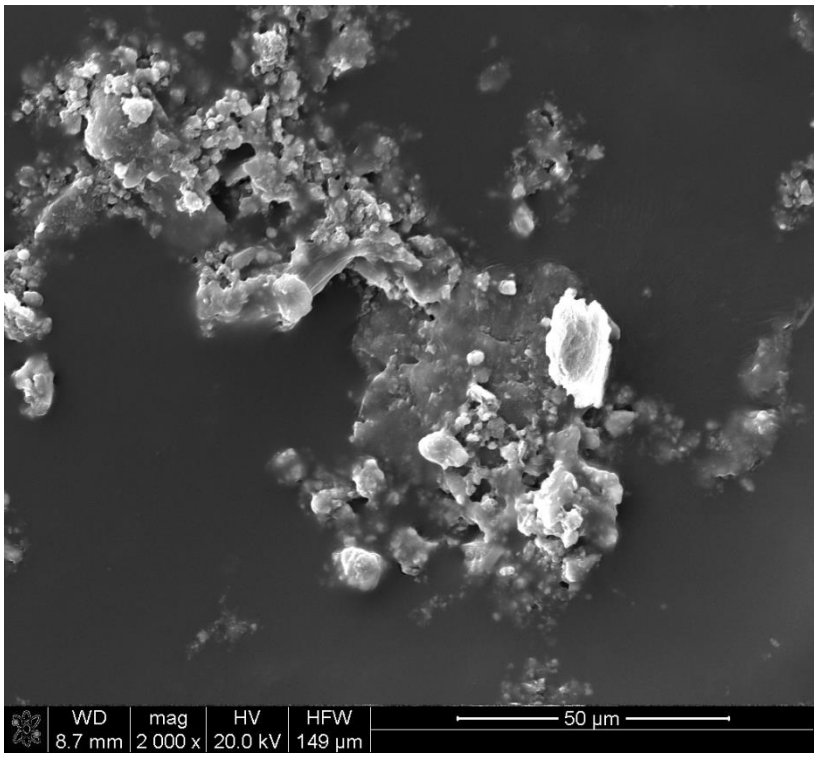

Figure 16: General appearance of ore sample 2.

All the major minerals found during the XRD examinations in both samples were identified one by one with the help of EDS unit. SEM photographs of major minerals are given in Figures 17 and 18. The EDS analyses results belonging to these images are given in Appendix B.

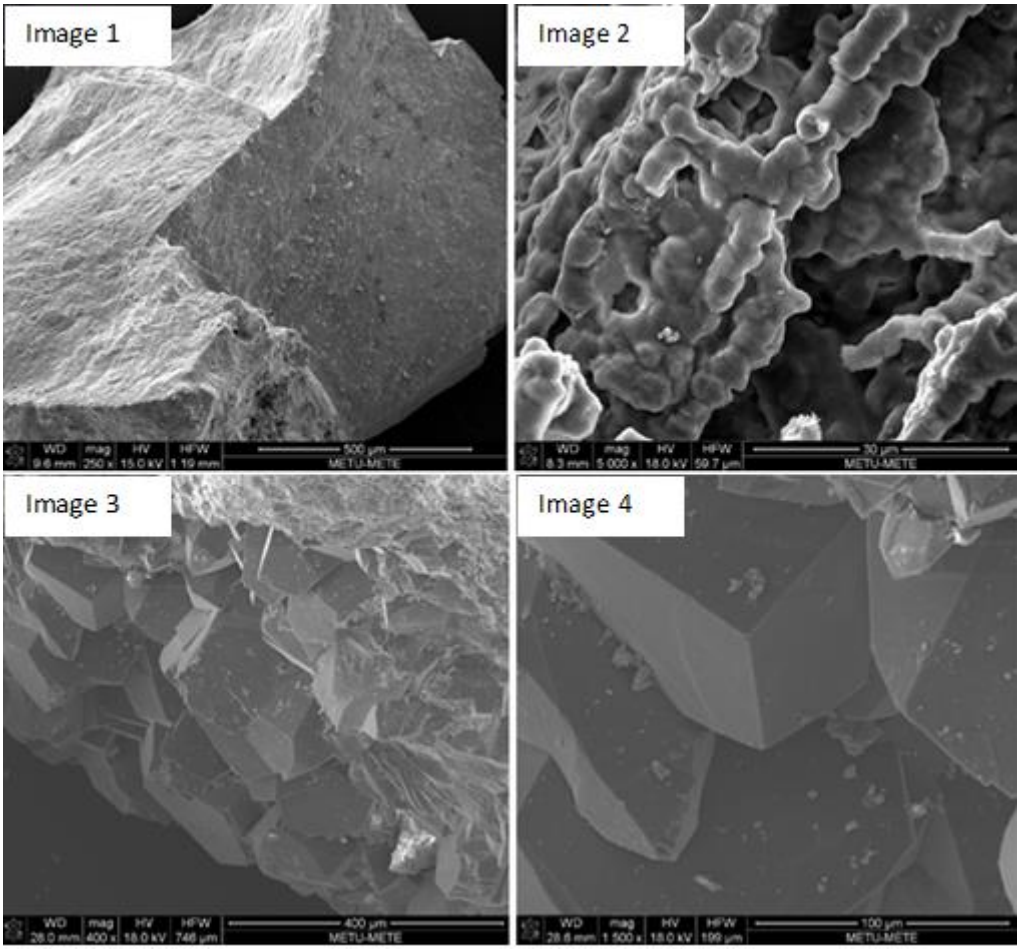

Figure 17: SEM images of selected particles of ore sample 1 (images 1-4).

In the first image, the sharp and long edges of a broken silica mineral can be seen. This type of sharp and clear cut edges is characteristic morphology of crystalline silica. The size of the particle is very large as it can be seen, since it was gathered from the original ore sample 1 and examined without any particle size reduction.

The second image belongs to a focused section on the surface of hematite with arsenic content above average. The third and fourth images belong to the same selected particle. The particle is covered with silica and at the right end side of the particle, a broken surface of goethite is present.

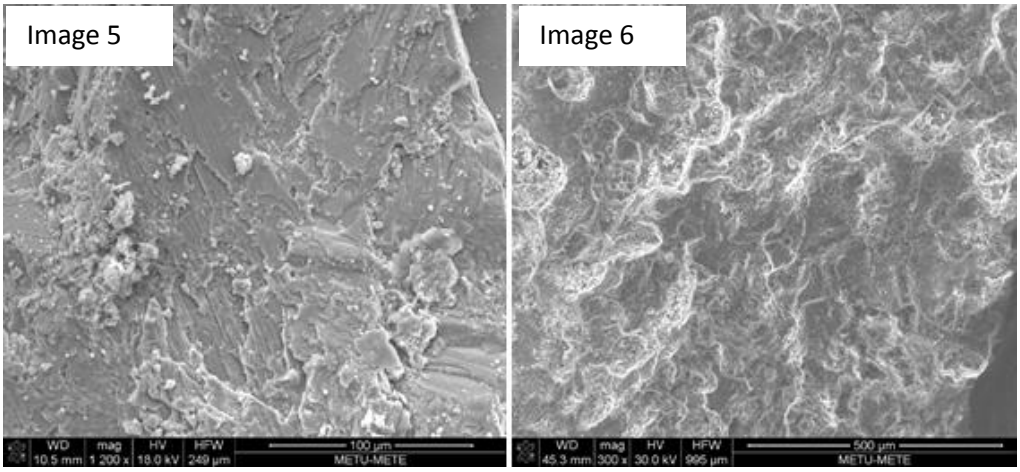

Figure 18: SEM images of selected particles of ore sample 1 (images 5 and 6).

In image 5, aluminum and chromium are present with the iron mineral. Finally in image 6, almost a pure iron mineral can be seen. The shiny marble like lines with contrast are placed among the dull and dark background show similarities with a regular iron mineral. This was also confirmed by EDS results and it is a hematite particle.

It can be seen from EDS results that the nickel, cobalt and arsenic were present in some of the examined minerals which could not be detected by the XRD study. They existed as substitutional elements in the iron mineral lattices. It was verified by SEM and XRD examinations that these lattices mainly belonged to hematite and goethite. So this meant that during the leaching of lateritic nickel ores, the unlocking of the iron lattices during acid leaching and letting the nickel and cobalt

atoms free into the aqueous solution was necessary. These target minerals showed different leaching behaviors under different temperature and pressure conditions. Their behaviors were studied and the results obtained have been presented in the results and discussion section.

3.5. Experimental Procedure

3.5.1. High Pressure Acid Leaching (HPAL) Procedure

A Parr-4532 model, 2-liter, titanium grade-4 autoclave was used for the high pressure acid leaching experiments. The autoclave was equipped with automatic heating and cooling systems and magnetically driven stirring system. The picture of the autoclave system is given in Figure 19.

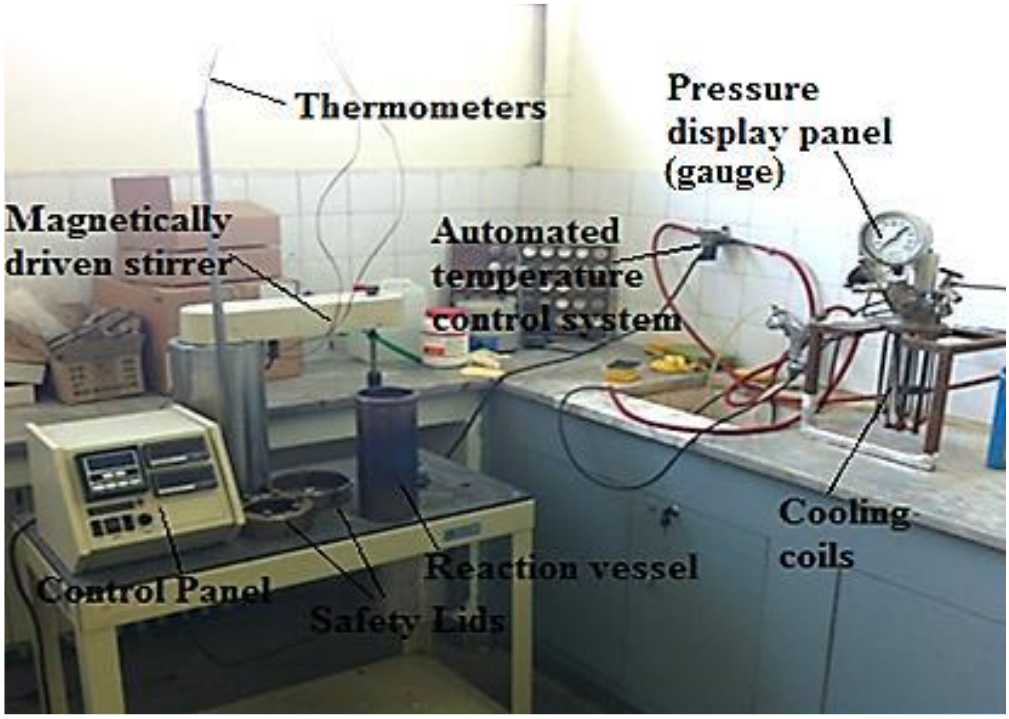

Figure 19: Titanium autoclave used in HPAL experiments (13).

The experimental procedure of the autoclave system was a little bit different from the similar cases reported in the literature. Normally, similar autoclaves have acid injection systems into the reactor container. Thus, the acid is injected directly into the container when the desired temperature and pressure are reached. Unfortunately, the current system was not available in the METU, Metallurgical and Materials Engineering hydrometallurgy laboratories.

In each pressure leaching experiment, the calculated amounts of ore, deionized water and sulfuric acid (96 wt.%) were put into the titanium container as slurry and the lid was locked up carefully to prevent any leakage and pressure loss during the experiment. After placing the container into heating unit and making the necessary connections for cooling, temperature measurement, stirring of the system and displaying screen, the heating was started. It generally took 45 minutes for the autoclave to reach 255 ^{o}C, which was designated as the reaction temperature since the industrial sized autoclave at Gördes would operate at that temperature. After the reactor reached 255 ^{o}C, the leaching process was assumed to be started at that exact point, defined as zero time for the particular experiment. After the envisioned duration was completed, the heating unit of autoclave was turned off and left for cooling for one hour. At the end of one hour cooling duration, the autoclave was carefully opened and the titanium container was weighted. Then, the slurry present in the titanium container was removed. Finally, the pregnant leaching solution and leach residue were separated via vacuum filtration by using a ceramic Buchner funnel and a vacuum pump. Whatman grade-40 filter paper was used for the separation of slurry. The leach residue was washed with deionized water which was adjusted to pH 2 with sulfuric acid addition. By adjusting the pH, the re-precipitation of metals in the pregnant leach solution (PLS) was prevented during washing operation. After measuring the PLS's density, the leach residue was dried at 105 ^{o}C overnight. The dried leach residue was dispersed into fine particles and prepared for analysis methods like,

XRD, XRF, AAS and SEM. The PLS was also sent for chemical analysis with ICP to check the ionic content of the critical elements. According to the data collected from the chemical analysis, both solid and liquid based extraction calculations became possible. Niton X-Met 820 X-ray Fluorescence (XRF) analyzer and Atomic Absorption Spectroscopy (AAS) of META Nikel Kobalt A.Ş. were used for the chemical analysis. The samples were sent to the METU Central laboratory for Inductively Coupled Plasma (ICP) analysis and Scanning Electron Microscopy (SEM) analysis were done via Nova Nanosem 430 in the Department of Metallurgy and Materials Engineering.

However, it was inevitable that the leaching process had already started as soon as all the ingredients had been put into the titanium vessel with the initiation of autoclave heating system. This may seem to be a negative aspect for the sake of the experiments but it offered an invaluable opportunity to understand the initial kinetics of leaching reactions. So, in order to investigate what happened during that time interval of heating inside the reactor, several series of experiments were conducted and this was selected as one of the important parameters of the experimental procedure. All the other parameters for the high pressure acid leaching experiments studied were;

1) Leaching duration:
    - Before reaching the reaction temperature: 15 min., 30 min., and 45 min.
    - After reaching the reaction temperature: 30 min., 60 min., and 360 min.
2) Leaching temperature:
    - 255 ^{o}C and 265 ^{o}C

3) Particle size of ore feed:

    - %100 (-0.850 mm), (-0.038 mm)

4) NaCl addition:

    - 15 g/L, 25 g/L, 35 g/L, 45 g/L, 55 g/L

The constant parameters were; solid/liquid ratio = 0.3 (excluding acid, 150 g ore and 350 cc deionized water), 100% limonitic nickel laterite ore, sulfuric acid/ore ratio = 324 kg/ton of dry ore (according to the Sherritt-Gordon acid consumption calculations).

In order to determine the free acid in the pregnant leach solution after the experiment, 0.2 molar sodium hydroxide (NaOH) solution was used. First of all, the pH meter was calibrated to pH 7.0 by a buffer solution. Then, for the titration process, 280 g/L di-potassium oxalate monohydrate ($K_2C_2O_4.H_2O$) solution was used to create a main solution to prevent some of the ions interference with the titration. For each titration, 20 cc of di-potassium oxalate monohydrate solution was diluted with 5 cc of deionized water and its pH was measured with pH meter. After noting down the measured pH, which is the target pH for the titration process, 5cc of pregnant leach solution was added to the main solution and the pH was measured again. After that point, 0.2 molar sodium hydroxide solution was started to be added slowly until reaching the target pH. The amount of used NaOH solution consumed was used for the determination of free acid content of the pregnant leach solution. The whole procedure was done in a beaker which was also magnetically stirred.

A Pt-Ag/AgCl electrode (saturated with KCl) was used for the measurement of reduction potential (ORP) and the measured values were reported according to the

Pt-Ag/AgCl reference electrode in the experimental results section. If one desires, the measured values may be converted into the Standard Hydrogen Electrode (SHE) potential values by the addition of 198 mV to the measure values.

3.5.2. Agitated Atmospheric Acid Leaching Procedure

For the agitated atmospheric acid leaching experiments, the schematically sketched set-up was used as shown in Figure 20. The experimental set-up consisted of one 250 Pyrex glass balloon, a condenser unit, contact thermometer, and a hot plate with magnetic stirring.

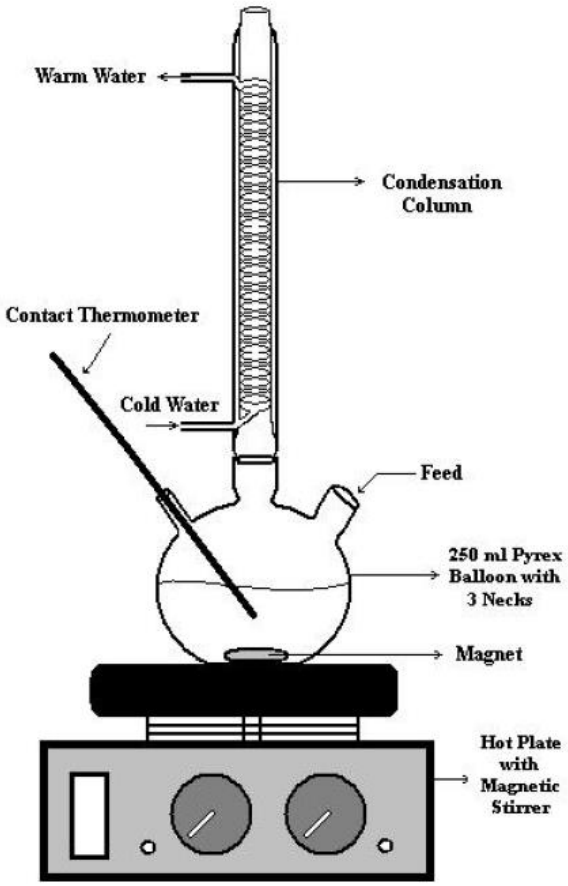

Figure 20: Sketch of agitated atmospheric acid leaching system.

First of all, predetermined amount of deionized water and calculated acid (nitric acid, sulfuric acid, hydrochloric acid) were put inside the 250 ml Pyrex glass balloon and it was placed on the hot plate. Teflon coated magnet was used for stirring purposes. After connecting the contact thermometer and condenser unit with the balloon, the heating and stirring functions were initialized. The contact thermometer was set to the respective boiling point. As soon as the mixture of deionized water and acid reached to the boiling point, the lateritic ore sample of known size and weight was added to the balloon from the feed opening. That moment was designated as the start of the experiment. During the long experiment durations, every hour both the contact thermometer and condenser were checked carefully. Upon completion of an experiment, the balloon was cooled and its pregnant leach solution was separated from the leach residue with a ceramic

Buchner funnel. Whatman grade-40 filter paper was again used for the separation of slurry. After the complete solid liquid separation, the leach residue was washed with deionized water which was adjusted to pH 2 with the type of used acid and finally dried at 105 ^{o}C and dispersed into fine powder for analysis purposes. The studied parameters in atmospheric leaching experiments were;

1) Acid Type:
    - HNO_3
    - H_2SO_4
    - HCl
2) Concentration of Acids:
    - 2N, 4N, 5N, 6N, 8N
3) Experiment Durations:
    - 12 hr, 24 hr, 48 hr
4) Particle Sizes:
    - 100% (-1.7 mm), (-0.85 mm), (-0.425 mm)

The constant parameters were; Temperature was always set at the respective boiling points, which were 105 ^{o}C for HNO_3, 98 ^{o}C for H_2SO_4 and 104 ^{o}C for HCl. The total liquid volume in each test: 75 ml, ore weight: 15 g, 100% limonitic nickel laterite ores were used.

CHAPTER 4

RESULTS AND DISCUSSION

4.1. High Pressure Acid Leaching Experiments

In the high pressure acid leaching experiments, the parameters that can be tested in order to increase the extraction efficiencies are very limited due to the industrial restrictions. However, there are some parameters that can be tested without exceeding the industrial limits. According to Whittington et al., goethite, hematite, serpentine and nontronite are the primarily nickel and cobalt containing minerals (57). Based on the literature information of many years, some basic assumptions can be made on the extraction behaviors of these primary nickel bearing minerals. One of the assumptions can be stated as, chromite and quartz are naturally acid resistant minerals and do not consume too much acid. The second assumption is that only about 5% of the stoichiometric amount of acid is consumed due to iron extracted during HPAL. The most acid consuming elements are assumed to be completely leached and hold the acid according to their abundance in the lateritic ore. Aluminum, magnesium and calcium can be stated as examples to these elements. The Sherritt-Gordon acid consumption assumption was used for the calculation of possible acid usage with a considerable amount (40 g/L) of free acid left in the pregnant leach solution to prevent the precipitation of valuable metals. The theoretical sulfuric acid consumptions of the two limonitic samples according to the Sherritt-Gordon calculation under high pressure acid leaching conditions can be seen in Tables 7 and 8.

Table 7: Theoretical sulfuric acid consumption per ton of dry Gördes lateritic ore for sample 1.

	Sample 1 Limonite	Stochiometric	**Sherritt-Gordon HPAL Conditions**	
Element	ALS (Weight percent)	Sulfuric Acid Consumption (kg/ton)	Percent Extraction	Acid Used (kg/ton)
Fe+3	29.9	787.69	5.00	39.38
Fe+2		0.00	0.00	0.00
Ni	1.08	18.03	100.00	18.03
Al	3.8	207.66	25.00	51.91
Al	3.8	92.29	75.00	69.22
Co	0.0689	1.15	100.00	1.15
Mn	0.386	6.89	100.00	6.89
Ca	0.510	12.46	100.00	12.46
Mg	0.740	29.84	100.00	29.84
Cr	0.81	15.35	5.00	0.77
As	0.855	-	0.00	-
Si	12.642	-	0.90	-
Na	0.09	3.85	45.00	0.77
Cu	0.0306	-	100.00	-
Zn	0.0251	0.38	100.00	0.38
Free Acid 40 g/L	350 cc/150 g L/S=2.33	93.20	-	93.20
Total Acid Consumption (kg/ton of dry ore)		**1269**	**-**	**324**

Table 8: Theoretical sulfuric acid consumption per ton of dry Gördes lateritic ore for sample 2.

	Sample 2 Limonite	Stochiometric	**Sherritt-Gordon HPAL Conditions**	
Element	ALS (Weight percent)	Sulfuric Acid Consumption (kg/ton)	Percent Extraction	Acid Used (kg/ton)
Fe+3	23.3	613.82	5.00	30.69
Fe+2		0.00	0.00	0.00
Ni	0.99	16.53	100.00	16.53
Al	3.7	202.19	25.00	50.55
Al	3.7	89.86	75.00	67.40
Co	0.0383	0.64	100.00	0.64
Mn	0.111	1.98	100.00	1.98
Ca	1.470	35.93	100.00	35.93
Mg	0.510	20.57	100.00	20.57
Cr	1.05	19.83	5.00	0.99
As	2.17	-	0.00	-
Si	10	-	0.90	-
Na	0.03	1.28	45.00	0.77
Cu	0.00434	-	100.00	-
Zn	0.0139	0.21	100.00	0.21
Free Acid 40 g/L	350 cc/150 g L/S=2.33	93.20	-	93.20
Total Acid Consumption (kg/ton of dry ore)		**1096**	**-**	**319**

As presented in Tables 7 and 8 for the first limonitic sample, 324 kg sulfuric acid was required per ton of dry ore for the high pressure leach experiments and it was 319 kg sulfuric acid per ton of dry ore for the second limonitic sample. Since these values are very close to each other, for the purpose of not introducing another variable parameter in the experimental studies for the comparison of the two limonitic ores 324 kg sulfuric acid per ton of dry ore was chosen as the sulfuric acid addition amount in HPAL tests. In the third column of Tables 7 and 8, the stoichiometric sulfuric acid consumptions per ton of dry ore are given. The theoretical sulfuric acid consumption of metals present in the lateritic ores studied were calculated by assuming as if all the soluble metals were present in their oxide form and 100 % of them were extracted into the pregnant leach solution.

In each initial HPAL batch test, 150 g of dry limonitic ore from each sample was taken and used as a representative nickel laterite ore. Different parameters were tested during the experimental stage and some of the parameters were kept constant during these experiments. Acid to ore ratio was one of them and it was kept constant as 324 kg/ton dry ore during all of the high pressure acid leach experiments. Solid to liquid ratio was another parameter which was kept constant as 0.3 (wt./wt.). This solid to liquid ratio was studied previously by David and it was stated that the slurries which have 42% or more solid, would result in an excessively viscous fluid that could not be pumped properly (34).

Initially, a HPAL experiment was conducted using the information of the optimum conditions gathered from the literature and previous works. According to Kaya and Gördes HPAL plant design data, the optimum temperature for the HPAL process is 255 ^{o}C for the nickel and cobalt extractions. Also 100% -850 μm particle size was chosen based upon Kaya's findings (53). The pre-determined conditions of the initial experiment can be found in Table 9.

Table 9: Optimum HPAL conditions of initial experiment.

Ore Type	Limonite – Sample 1
Leaching Temperature	255 ^{o}C
Leaching Duration	60 min.
Acid/Ore ratio	0.324 (wt./wt.)
Particle Size	-850 μm
Solid/Liquid Ratio	0.3 (wt./wt.) (excluding the acid addition)
Stirring Speed	400 rpm

Temperature is one of the most important parameter in HPAL among all others due to many reasons. One of them is the increase of water vapor pressure with respect to increasing temperature. As shown in Figure 21 beyond 150 ^{o}C, the pressure in the closed container of an autoclave increases exponentially with respect to temperature. This drastic increase in the pressure requires many conditions to be met in order to maintain its consistency. The vessel that contains it must be carefully constructed and precautions must be taken for higher pressures. This means higher capital investment for the purchase of an autoclave. When the existence of acid inside the container is considered, the strength and corrosion resistance of vessel becomes more and more important. The safety of this operation also depends on a healthy operation. If any breakdown occurs in an industrial operation, the damage will be catastrophic in terms of human lives and maintenance or even replacement of most of the equipment will be inevitable. So lower temperature operations offer better working conditions and are relatively safer. That is why obtaining the best possible nickel and cobalt extraction values at the minimum possible temperature is one of the main aims of this study.

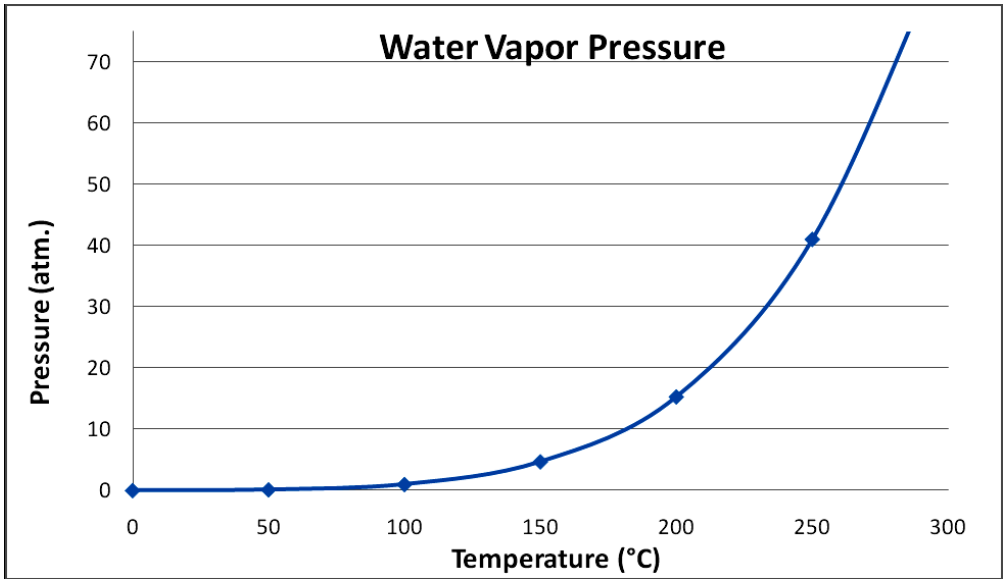

Figure 21: Variation in the vapor pressure of water with respect to temperature (53).

In order to check reliability of results, three consecutive experiments were done with ore sample 1. The nickel and cobalt extraction percentages can be seen in Table 10. The extraction percentages of HPAL experiments were calculated according to the analyses of original lateritic ores and their leach residues. So all of the leach residues of experiments were sent to chemical analysis and the solid based nickel and cobalt extraction calculations were done as it can be found in Appendix A.

Table 10: Extraction percentages of nickel and cobalt at the optimum experimental conditions for sample 1 in HPAL.

Test code: A5 (Optimum)	Ni % extraction	Co % extraction	Fe % extraction	As % extraction
Test-1	72.5	77.7	3.1	7.9
Test-2	72.1	73.5	2.3	1.2
Test-3	75.1	79.4	2.7	6.5

The complete average metal extraction values for other metals obtained under the optimum HPAL conditions are given in Table 11 for sample 1.

Table 11: Other metal extractions and ORP measurement in HPAL obtained under the optimum conditions.

HPAL experiment extractions, %	
Elements	Sample 1 (A5)
Fe	2.7
As	5.2
Al	48.1
Mg	66.9
Mn	76.6
Sc	37.7
Cu	68.7
Zn	84.3
Ca	65.4
ORP, mV	607
Free Acid, g/L	48.5

As one can see from Table 10, the obtained results are reasonably consistent. The average extraction values of these three experiments are: Ni = 73.2%, Co = 76.8%. The standard deviation for nickel extraction value is ± 1.6% and ± 3.0% for cobalt. The average extraction percentages obtained were very low when they were compared with the reported values in the literature. In most of the cases, similar experiments under the same conditions with different limonitic type ores stated extractions in 85 to 95% interval (13, 53). However, due to the mineralogical character of Gördes limonitic type of nickel laterite ore, the extraction percentages were extremely low. To increase them up to industrially

acceptable levels by adjusting the high pressure acid leaching experimental parameters was one of the aims of this study.

4.1.1. Pressure Acid Leaching of First and Second Lateritic Ore Samples

Before starting the experiments to investigate the effect of temperature and duration variation on HPAL for samples 1 and 2, the second sample was subjected to the optimum conditions previously determined and stated above, excluding the particle size. The resultant extraction percentages are given in Table 12.

Table 12: Metal extractions and ORP measurement in HPAL obtained under the optimum conditions with sample 2.

HPAL experiment extractions, %	
Elements	Sample 2 (K1)
Ni	77.8
Co	82.9
Fe	9.2
As	15.9
Al	51.3
Mg	59.7
Mn	54.8
Sc	35.4
Cu	72.5
Zn	80.2
Ca	59.3
ORP, mV	651
Free Acid, g/L	52.9

4.1.1.1. Effect of Temperature and Duration Variation on HPAL

As it was mentioned in the previous section, the HPAL temperature is important since the reaction kinetics is affected by varying temperature. It is known from the literature that increasing of the temperature might affect the valuable metal extraction percentages positively. So, it is important to obtain high nickel and cobalt extraction percentages at a reasonably low level of temperature. According to a previous study, the extraction percentage of nickel was 93% for 50 minutes of leaching duration at 240 ^{o}C. However, exactly the same percentage could be reached within 10 minutes duration at 275 ^{o}C (36). In another study, Chou et al. stated that in order to obtain fast leaching kinetics, the temperature should be close to 250 ^{o}C and increasing the temperature up to 275 ^{o}C would fasten the reaction kinetics and lower leach durations. However, increasing the temperature beyond this point to 300 ^{o}C would just lower the nickel extraction percentages. So they have generalized it and said that nickel and cobalt were leached in the first ten minutes of HPAL between 250 ^{o}C and 270 ^{o}C and thereafter, their extraction percentages were almost temperature independent (44). According to Georgiou and Papangelakis, a sharp increase in the nickel and cobalt extraction values occurred when the temperature was increased to 260 ^{o}C from 230 ^{o}C. But they found that beyond 260 ^{o}C, the rate of increase slowed down and temperature had no important influence on the nickel and cobalt extraction efficiencies (39). So the reported results in the literature about the effect of temperature on HPAL recoveries were contradictory to each other due to the differences of ore composition and mineralogy in each studied lateritic ore.

In this study, to understand the temperature effects on the nickel and cobalt extraction values, two different temperatures were experimentally tested on the ore samples 1 and 2. First test was at 255 ^{o}C and it was designated as the optimum high pressure acid leaching experimental temperature and the second one was at

the limiting temperature of 265 ºC. For the durations of experiments, again 60 minutes was selected as a standard batch-wise HPAL experimental duration and to test the limiting conditions and to understand the effect of longer leaching durations on two types of limonitic ore 360 minutes was selected. The other process parameters can be seen in Table 13. The experimental metal extractions are summarized in Table 14.

Table 13: Selected process parameters to see the effects of leaching temperature and duration upon nickel and cobalt extractions in HPAL.

Ore Name	Sample 1 and Sample 2
Leaching Temperatures	255 ºC and 265 ºC
Acid to Ore Ratio	0.324 (wt./wt.)
Leaching Durations	60 and 360 min.
Solid Concentration	30%
Particle Sizes	Sample 1: -850 μm and Sample 2: -74 μm
Stirring Speed	400 rpm

The benefit to be gained in industrial applications is clearly related with the nickel and cobalt extraction percentages. So the most important comparison must be made again on their extraction values. As reported in Table 14, the nickel and cobalt extraction percentages of HPAL experiments conducted at 255 and 265 ºC for 60 and 360 minutes by using the two different limonitic samples were quite similar. The summarized extraction values generally increased more with the increasing duration of leaching. However, with the increasing experiment temperature the nickel and cobalt extraction percentages changed very little.

Table 14: Extraction percentages of the two ore samples at two different durations with respect two different particle sizes in HPAL.

	Temperature 255 ^{o}C		Temperature 265 ^{o}C	
Minutes	Nickel Extraction %	Cobalt Extraction %	Nickel Extraction %	Cobalt Extraction %
Sample 1 – 60	73.2	76.8	76.7	80.4
Sample 1 – 360	82.6	85.8	81.2	82.1
Sample 2 – 60	77.6	83.0	78.9	84.5
Sample 2 – 360	83.2	84.7	82.0	83.5

In general, the nickel and cobalt extraction percentages were still low even after increasing of leaching temperature and duration. Most probably this was not only caused by nickel loss through secondary hematite precipitation but also occurred due to nickel loss in refractory primary hematite particles. In this current case, the extraction efficiencies were worse than Kaya's finding which was reported to be about 85% nickel extraction due to primary hematite occurrence in his leach residues (53). In theory, the simultaneously occurrence of dissolution of goethite and hematite with precipitation of ferric content as secondary hematite, might inhibit one another and retard the dissolution kinetics of minerals. In addition, it was stated that when temperature of HPAL exceeded 270 °C, unnecessary nickel losses was observed in the past since insoluble and nickel incorporated magnesium sulfate formation became favorable due to reduction in solubility of magnesium (46). In leach residue characterization part, some EDS results and SEM images will be given in order to explain the reasons for low metal extractions in HPAL.

4.1.1.2. Effect of Particle Size

The importance of particle size in high pressure acid leach experiments can be explained with the interaction amount of ore with sulfuric acid. The specific surface area of ore minerals will increase by decreasing the particle size; therefore, extra interfaces with reaction sites become available as a result. The acid attack rate will increase with increasing specific surface area, so it means that more and more host minerals will dissolve and much more nickel and cobalt will enter directly into the pregnant leach solution. On the other hand, not just nickel and cobalt, but also impurity elements like aluminum and others will be released and pollute the leach solution together with iron. The leach residue will become much finer in terms of particle size and it may cause some problems during solid-liquid separation processes. Also, grinding the lateritic nickel ore into fine particle size is more expensive and requires a high initial investment and maintenance in terms of constructing facility and machinery. So, a delicate balance should be found between the suitable particle size and the nickel and cobalt extractions.

Since the focus point of this study was to understand the low extraction percentages and to find an answer to that problem, for the particle size selection, only the optimum (60 minutes leaching duration and -850 μm particle size) and limiting conditions (360 minutes leaching duration and -38 μm particle size) were applied in high pressure acid leaching experiments. In the previous studies on similar type of limonitic ore, Kaya and Önal suggested that the optimum particle size for industrial applications was minus 850 μm (13, 53). In order to see the effect of extreme grinding on the nickel and cobalt extraction percentages, the first limonitic sample was ground to minus 38 μm. The other experimental parameters are given in Table 15.

Table 15: Parameters of the optimum and limiting condition experiment in HPAL.

Ore Name	Sample 1
Leaching Temperature	255 ^{o}C
Acid to Ore Ratio	0.324 (wt./wt.)
Leaching Durations	60 and 360 min.
Solid Concentration	30 %
Particle Sizes	-38 μm and -850 μm
Stirring Speed	400 rpm

The resultant extraction percentages of nickel and cobalt according to different particle sizes and durations are given in Table 16.

Table 16: Extraction percentages of the first sample at two different durations with respect to two different particle sizes in HPAL.

	Particle size minus 850 μm		Particle size minus 38 μm	
Minutes	Nickel Extraction %	Cobalt Extraction %	Nickel Extraction %	Cobalt Extraction %
60	73.2	76.8	82.3	85.4
360	82.6	85.8	82.4	83.5

There were clear increases in both nickel and cobalt extraction percentages with decreasing particle size at 60 minutes of duration experiments. Cobalt's general extraction values were relatively higher than those of nickel, which showed consistency with the previous works. A literature review was conducted to

understand the effect of particle size clearly. In the literature, the recommended particle size was stated to be 100% minus 0.25 or minus 0.50 mm for the best results in HPAL. Also grinding the ore more than a specific value had no visible or adverse effects on extraction values. These results of previous studies also showed similarities with the present experimental findings of 360-minute test. As seen in Table 16, the nickel and cobalt extraction percentages dropped a little with particle size reduction in longer durations of leaching. This can be explained by stating the nickel bearing minerals were already at a fine particle size and reducing them beyond a point did not affect the extractions positively. The further stages of grinding had no important effect on the leaching kinetics. Also according to Chou et al.'s study, excessive grinding might create much more new nucleation sites for aluminum and iron to precipitate with or without the presence of nickel in their structures (44).

This situation was less likely to occur for goethite due to its highly porous and extensive surface area in bulk form but the same statement could not be true for manganese minerals since they were coarser and less porous. However, there was still a portion of the cobalt that could not be extracted even at higher acidity after applying the same long durations which brought another question in mind. This seemingly untouched cobalt values could be related to secondary losses that might be entrapped with after-leaching phases such as amorphous silica or alunite or even hematite. The same situation was valid for nickel with exactly the same reason as given for cobalt. So far, the nickel could not be extracted above 83% even under the limiting conditions, which will be investigated in the following sections. A similar situation was also observed by Kaya in his thesis study and it was stated that the primary hematite was believed to be responsible for the low nickel extraction efficiencies below 85% (53).

4.1.1.3. Effect of NaCl Addition

The usage of fresh water in the industrial applications is a necessity. But in some cases, especially the plants near sea side use sea water. Or in some cases due to economic burdens of supplying fresh water to the facility, companies choose to use saline water. It is claimed that the usage of saline water in high pressure acid leaching of lateritic nickel ores may offer some benefits. In the literature, the addition of salt (sea-water) to reduce the aluminum concentration in the post digestion stages was suggested due to the formation of natroalunite, which was reported to be less soluble than the hydronium alunite. Also in the same study, the concentration of iron in solution was not affected by the addition of sea water (36). In another study, it was stated that the nickel and cobalt extractions were increased in the presence of salt (59), while a different study reported that chloride present in saline water had a positive effect on dissolution kinetics of studied ore. Also, it improved the settling and thickening characteristics of ore during HPAL process (60).

The reactions occurring during the high pressure acid leaching experiments and the residual acidity are highly affected by the water salinity. The usage of saline water in experiments favors the formation of amorphous silica with sodium jarosite, alunite and hematite. Since jarosite and alunite are the major acid consumers, which was mentioned in literature review part, saline waters enhance the acid amount needed. Vice versa, the fresh water usage decreases the formation of sodium jarosite and alunite, hence decreases the acid usage (61).

In this study, NaCl was added in order to simulate the saline water usage in HPAL experiments. Five consecutive experiments were conducted. The experimental parameters are given in Table 17 and the results obtained are plotted in Figure 22.

Table 17: Parameters of HPAL experiments with NaCl additions.

Ore Name	Sample 1
Leaching Temperature	255 ^{o}C
Acid to Ore Ratio	0.324 (wt./wt.)
Leaching Duration	60 min.
Solid Concentration	30%
Particle Size	-850 μm
Stirring Speed	400 rpm
NaCl Additions	15 g/L, 25 g/L, 35 g/L, 45 g/L, 55 g/L

The first four experiments were conducted successfully but unfortunately, the last experiment with 55 g/L NaCl addition couldn't be completed. The rupture plate of autoclave burst in the first and the second attempts to perform this experiment. This must have occurred due to highly corrosive environment of saline water under high pressure. The reaction of NaCl with sulfuric acid is given in Rxs. 4.1 and 4.2.

$$NaCl + H_2SO_4 \rightarrow NaHSO_4 + HCl \qquad \text{Rx. 4.1}$$

$$NaCl + NaHSO_4 \rightarrow Na_2SO_4 + HCl \qquad \text{Rx. 4.2}$$

The overall reaction is;

$$2NaCl + H_2SO_4 \rightarrow Na_2SO_4 + 2HCl \qquad \text{Rx. 4.3}$$

When the produced hydrochloric acid combined with sulfuric acid under high pressure, the rupture plate wasn't able to stand it even it was tried twice. The corrosive effect of even the lower amounts of NaCl addition was also observed on the used rupture plates.

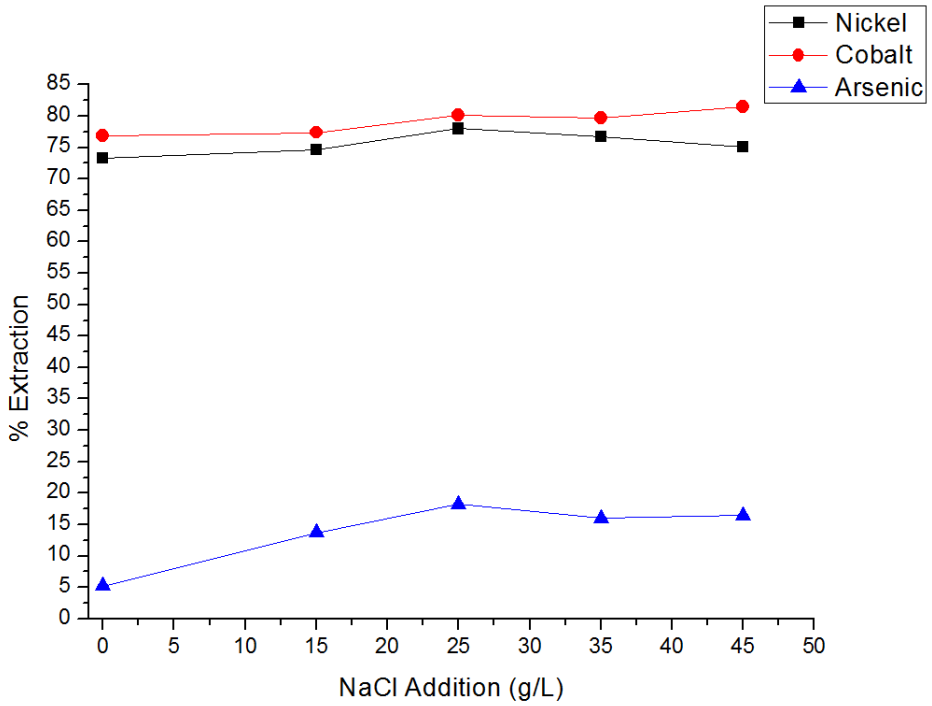

Figure 22: Extraction efficiencies of nickel, cobalt and arsenic with respect to NaCl addition in HPAL experiments.

As presented in the graphical data, the addition of NaCl in different amounts to the batch had no substantial effect on the nickel, cobalt and arsenic extractions. When it was considered from the point of arsenic extraction, it wasn't necessary to repeat the experiment with the higher arsenic bearing lateritic ore since according to Pajany et al., there were no effects of salt usage on the sorption mechanisms of arsenic to the iron oxyhydroxides (62).

In pressure acid leaching it is already known that the usage of saline water has a disadvantage that is the high amounts of acid consumption. Moreover, the initial investments of highly corrosive resistance equipment and their expensive, frequent maintenance due the usage of saline water in high pressure acid leaching applications are overwhelming. Plus, the usage of saline water causes problems in precipitation of the nickel and cobalt as intermediate products in the form of mixed nickel-cobalt hydroxide. In conclusion, NaCl addition to the HPAL experiments was not affective in increasing of the metal extractions.

4.1.1.4. Effect of Duration before/after Reaching Reaction Temperature

In METU hydrometallurgy laboratories, the batch type autoclave used in this study was initially loaded with deionized water, ore and sulfuric acid in pre-determined amounts in each experiment. After the titanium reactor was placed into the heater, the heating and stirring were started. In the optimum condition experiment, it took 45 minutes for the reactor to reach to 255 ^{o}C. After reaching that temperature, the reaction was assumed to have started. All the reaction durations were kept after that zero time, and at the end the autoclave system was allowed to be cooled for 60 minutes with water circulation through its cooling coil. But in reality, the leaching process was starting as soon as all the acid, ore and water were placed together in the titanium container. So in order to understand the leaching behavior of major minerals and to observe the effects of that elapsed time on elements ionic concentrations in the solution, two set of experiments were conducted. In the first set, the time was varied after the heating was initiated for 15, 30 and 45 minutes. After the vessel reached the designated reaction temperature of 255 ^{o}C; 30, 60 and 90 minutes elapsed in the second set of experiment. After each experiment the reactor was cooled by water circulation in the cooling coil. Following the opening of autoclave and separation of pregnant

leach solution from leach residue by filtration, the leach residue was washed with water adjusted to pH 2 with acid addition and dried at 105 ^{o}C for overnight. The dried leach residue was prepared for XRD, SEM and AAS analyses. The experiments planned for each set is given in Tables 18 and 19 below.

Table 18: Conditions of the first set of experiments before reaching the experimental temperature in HPAL.

Ore Name	Sample 1 and Sample 2		
Leaching Durations	15 min.	30 min.	45 min.
Leaching Temperatures	Max. 84 ^{o}C	Max. 181^{o}C	Reaction temp=255^{o}C
Acid to Ore Ratio	0.324 (wt./wt.)		
Solid Concentration	30 %		
Particle Sizes	-850 μm for Sample 1 and -74 μm for Sample 2		
Stirring Speed	400 rpm		

Table 19: Conditions of the second set of experiments, after reaching the experimental temperature in HPAL.

Ore Name	Sample 1 and Sample 2		
Leaching Durations	30 min.	60 min.	90 min.
Leaching Temperature	Reaction temp=255 ^{o}C		
Acid to Ore Ratio	0.324 (wt./wt.)		
Solid Concentration	30%		
Particle Sizes	-850 μm for Sample 1 and -74 μm for Sample 2		
Stirring Speed	400 rpm		

The experimental results of nickel and cobalt extractions and the comparison of important elements with respect to ore type and reaction durations are given in Figures 23 to 26:

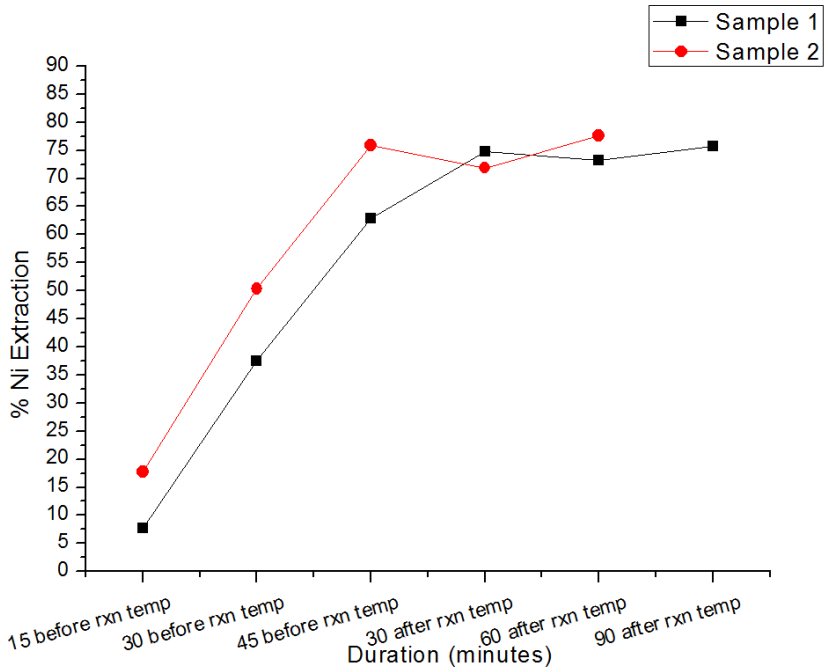

Figure 23: Nickel extraction percentages of two samples with respect to different durations before and after reaching the reaction temperature (255 ^{o}C).

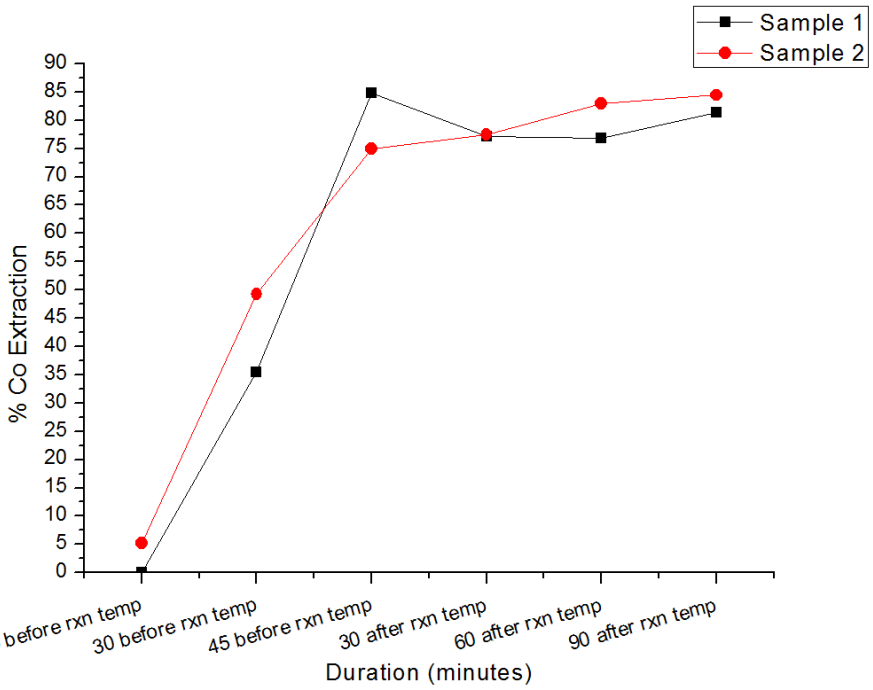

Figure 24: Cobalt extraction percentages of two samples with respect to different durations before and after reaching the reaction temperature (255 ^{o}C).

As shown in the mentioned figures, the nickel and cobalt extraction values increased with the increasing leaching duration which was expected. The difference between the extraction percentages of different type of ores may be due to the small mineralogical differences. However, the theory that the arsenic content of the ore (mostly in the goethite and hematite crystals) might be inhibiting the leaching kinetics, appeared to be not true.

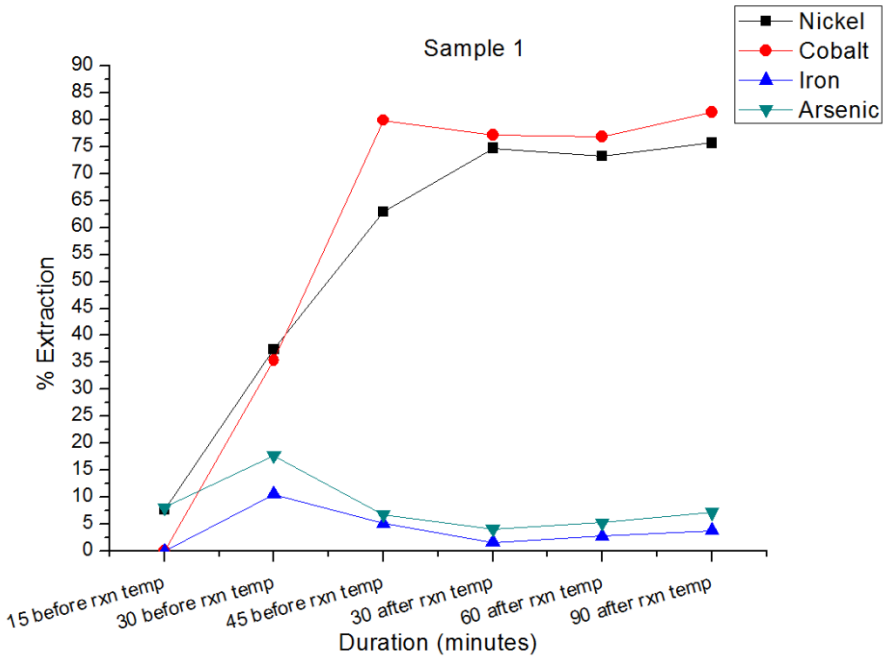

Figure 25: Comparison of nickel, cobalt, iron and arsenic extractions over time obtained from HPAL of sample 1.

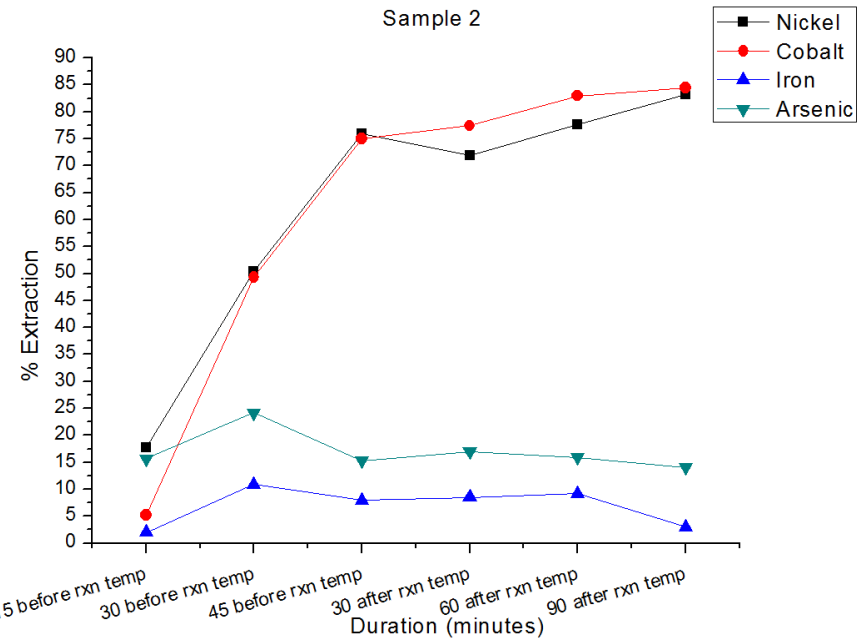

Figure 26: Comparison of nickel, cobalt, iron and arsenic extractions over time obtained from HPAL of sample 2.

When we compare the leaching behavior of nickel and cobalt together for the different type of ores, everything seemed to be as expected; since the increasing rate of ionic concentration of nickel and cobalt in pregnant leach solution was observed at early durations of leaching, leading to decreasing dissolution rate at longer durations. On the other hand, iron and arsenic had different dissolution paths than nickel and cobalt but showed consistency with each other. As it can be seen, they both dissolved and precipitated even before the start of experiment at the assumed zero time. The relation between arsenic and iron has been studied and shown before due to environmental reasons to purify the water from arsenic by the adsorption of arsenic by synthetic or natural iron oxide additions. According to Partey et al., the sorption mechanisms of arsenic on goethite and hematite in lateritic ores had a spontaneous nature (63).

In another study, it was stated that arsenic bonds strongly with the metal oxides of Fe and Mn depending on pH and redox potential by adsorption mechanism. At natural water pH value, hematite was able to adsorb more than 80% of arsenic and showed a behavior of increase in this percentage with decreasing pH values (62). This explains the current situation of simultaneous precipitation of arsenic and iron in HPAL. In both Figures 25 and 26, the same behavior was observed. So we can say that, in the precipitated hematite (secondary hematite) arsenic could be found within its structure. When the leach residue was examined with SEM and analyzed with EDS, this was partially proven. In one of the leach residues formed after reaching 255 ^{o}C in 90 minutes, some amount of nickel was found with arsenic present in its EDS. Also some images given in Figures 27 and 28 showed an indication of precipitation of secondary hematite upon the primary hematite with undissolved nickel content. EDS of these images had no arsenic content. The EDS that belonged to the image in Figure 27 also showed the secondary hematite precipitation on the primary hematite during leaching or cooling and thus inhibited the dissolution reaction.

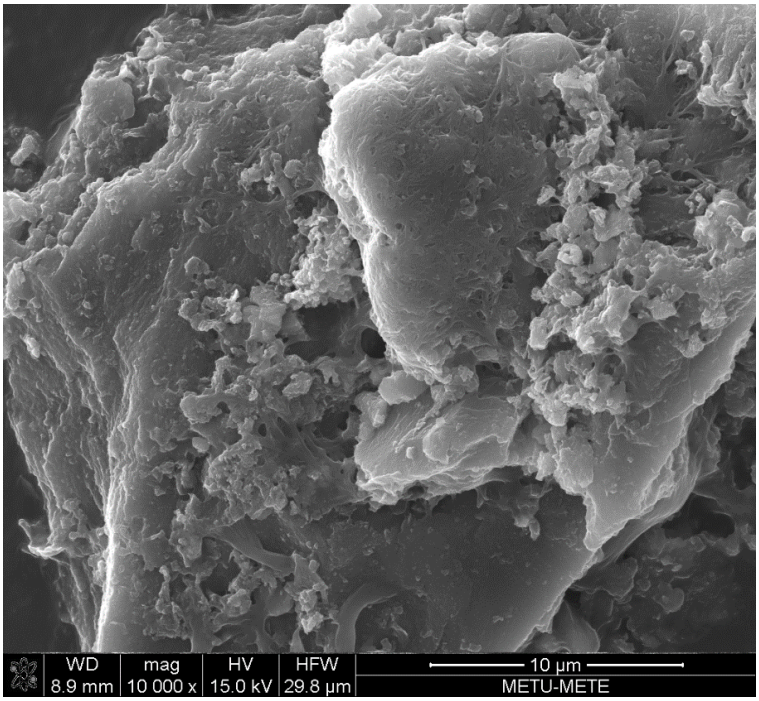

Figure 27: SEM images of secondary hematite particles deposited on primary hematite in the leach residue.

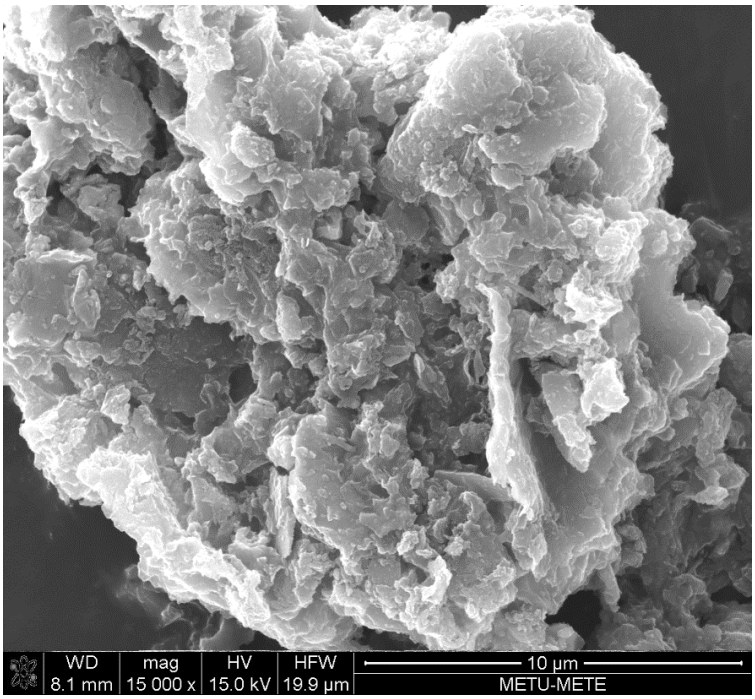

Figure 28: SEM images of secondary hematite with primary hematite in the leach residue.

4.2. Agitated Atmospheric Leaching Experiments

In this part, the results of agitated atmospheric leaching experiments have been presented. It was mentioned in earlier sections that the atmospheric acid leaching has both positive and negative aspects when it is compared with high pressure acid leaching. In order to understand reasons for the low extraction percentages of nickel and cobalt in HPAL experiments, the same ore samples were subjected to atmospheric leaching with different parameters like; various acid types at different concentrations, different durations of leaching and particle sizes. All the optimum parameter determining experiments were conducted by using ore sample 1, since only ore sample 1 had arrived in a condition that could be used in different particle sizes. After the determination of the experimental parameters for ore sample 1, all the optimum conditions obtained were tested on ore sample 2 in order to compare the different ore samples. The resultant extraction percentages of nickel and cobalt for both ore samples are given in this section.

4.2.1. Effect of Acid Type and its Concentration

In order to determine the effects of different type of acids on the metal extraction values of limonitic ores, different sets of experiments were conducted at different acid concentrations. Nitric acid (HNO_3), sulfuric acid (H_2SO_4) and hydrochloric acid (HCl) were used in consecutive order in the atmospheric leach experiments. The related concentrations of these three types of acid and other experimental parameters are given in Table 20.

Table 20: Conditions of atmospheric leaching experiments to compare acid types and to determine the best concentrations.

Ore Name	Sample 1		
Leaching Duration	48 h		
Leaching Temperature	Boiling Point		
Solid/Liquid Ratio	0.2 (wt./vol.)		
Acid Types	HNO_3	H_2SO_4	HCl
Acid Concentrations	4 N, 6 N, 8 N	2 N, 4 N, 5 N	2 N, 4 N, 5 N
Particle Size	-850 μm		
Stirring Speed	500 rpm		

The best acid concentrations reported were 6 N for H_2SO_4, and 5 N for both H_2SO_4 and HCl based on literature review. All the experiments were conducted at the boiling temperatures. The graphical presentations of nickel and cobalt extractions are given in Figures 29 and 30. In the following Figures 31, 32 and 33 the extractions of Ni, Co, Fe and As for the three different acids are presented. The leach residues were processed according to procedure given in Chapter 3 and characterized with XRF and AAS to obtain the necessary data for extraction calculations. Nickel, cobalt, iron and arsenic extraction values were calculated from the chemical analyses.

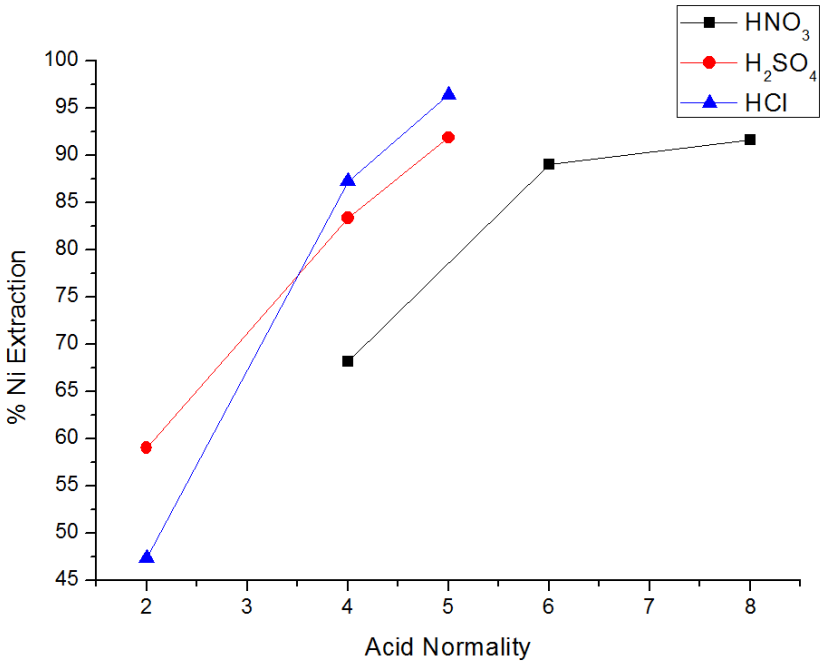

Figure 29: Nickel extraction percentages with respect to three acid types at three different concentrations.

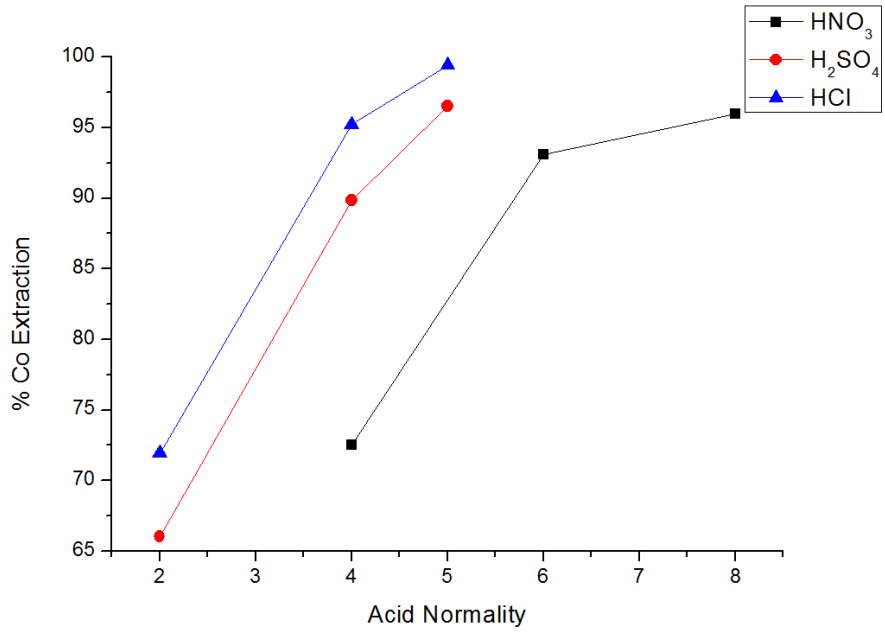

Figure 30: Cobalt extraction percentages with respect to three acid types at three different concentrations.

As presented in Figures 29 and 30, the nickel and cobalt extractions showed increasing tendencies with the increasing acid concentrations regardless of the acid type used as it was expected. The highest extraction values were obtained for nickel and cobalt by using all of the acid types at their highest concentrations. At the same concentration (4 N), the comparison of each acid in terms of nickel and cobalt extraction percentages is possible. From the graphs, it is noticed that the highest extraction values could be achieved with HCl acid. Sulfuric acid seemed to be the second strongest acid at the same concentration after hydrochloric acid. Finally, nitric acid was the weakest one among these three acids. But it was possible to obtain similar nickel and cobalt extraction values with higher concentrations of nitric acid.

It is also clear from the figures that the very high extraction percentages could be reached with atmospheric acid leaching by using ore sample 1. Although acid consumption was much higher than HPAL, the nickel and cobalt could be leached almost 100% with hydrochloric acid and 90 to 95 % with sulfuric and nitric acids.

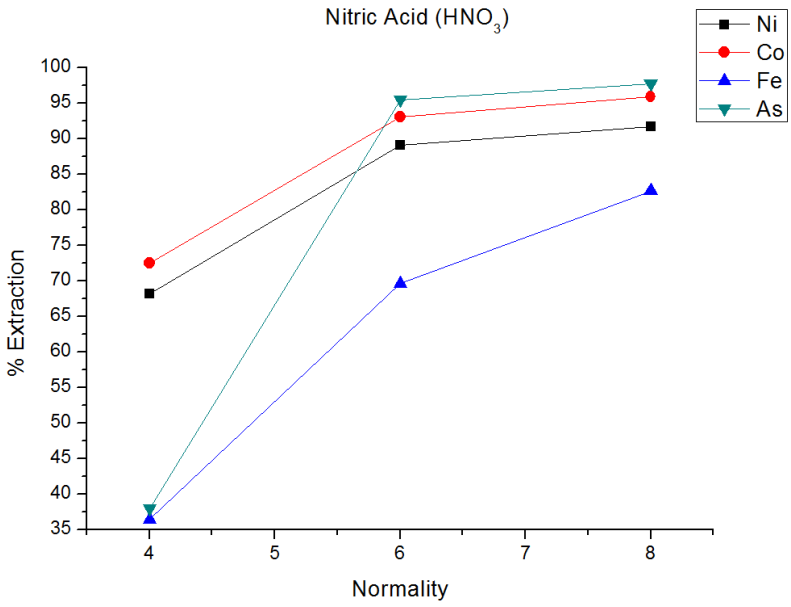

Figure 31: Extraction percentages of nickel, cobalt, iron and arsenic in atmospheric leaching experiments conducted with nitric acid at 4 N, 6 N, and 8 N concentrations.

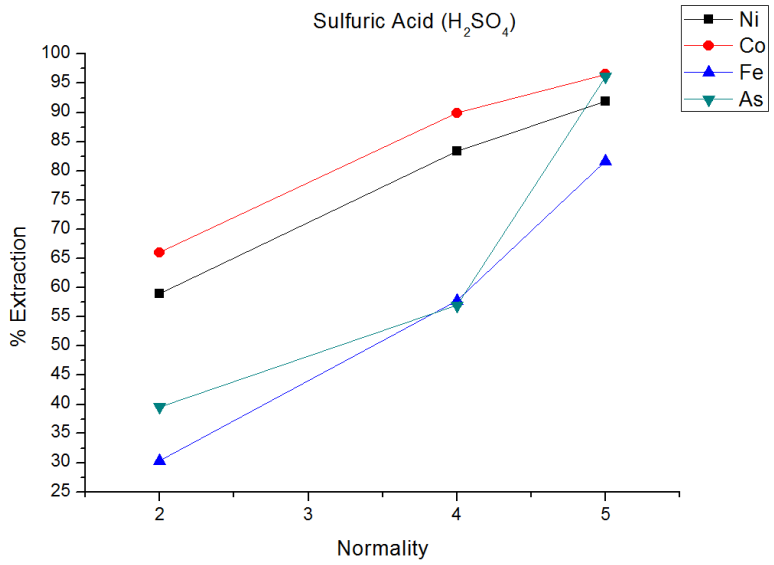

Figure 32: Extraction percentages of nickel, cobalt, iron and arsenic in atmospheric leaching experiments conducted with sulfuric acid at 2 N, 4 N, and 5 N concentrations.

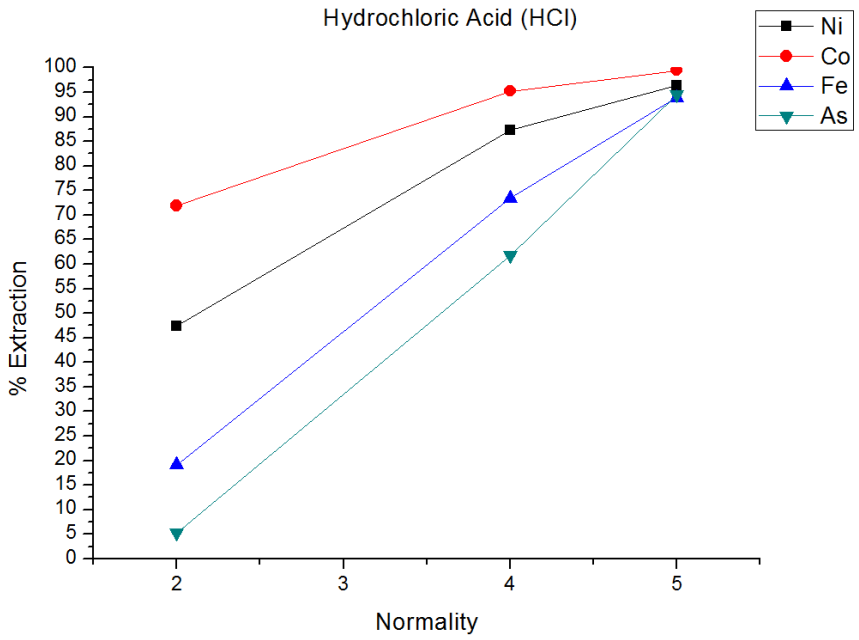

Figure 33: Extraction percentages of nickel, cobalt, iron and arsenic in atmospheric leaching experiments conducted with hydrochloric acid at 2 N, 4 N, and 5 N concentrations.

In the experiments conducted with different acids, the nickel and cobalt had similar dissolution rates with each other since they were mainly locked in the same goethite and hematite minerals. So it was understandable that with the increasing acid concentration, the nickel and cobalt were freed of their host crystal structure more and more until they were almost completely leached. As it was stated in the literature review and sample characterization part that most of the nickel and cobalt bearing goethite and hematite minerals were existing in the ore under a certain particle size which could be leached in very short durations at low acid concentrations. But for complete leaching, which means the complete dissolution of iron minerals regardless of particle size, it takes time and higher acid concentrations for more acid-ore interactions. As shown in Figures 31, 32 and 33, at the lowest acid concentrations, the nickel and cobalt had higher extraction percentages than iron. But with the increasing acid concentration, the

iron caught up with them. In all acid types after the nickel and cobalt have reached a certain extraction percentages, the dissolution rates slowed down. In the case of arsenic, it had a similar dissolution behavior to that of iron. In HPAL experiments, the dissolution and precipitation of arsenic alongside with iron was already observed. This was already a known relationship of arsenic with iron from literature review part. In the present case, arsenic was also another substitution element like nickel and cobalt in the crystal structure of iron minerals. In all these three graphical data, the arsenic and iron were noticed to be dissolved and reached to higher percentages unlike high pressure acid leaching experiments. The precipitation of iron did not occur in atmospheric leaching experiments since high temperature and pressure in autoclave environment causes the precipitation and thus supposedly results in nickel and cobalt losses along with them into leach residue. Since the precipitation of iron did not occur in atmospheric acid leaching, the acid consumption became extremely high when it was compared with HPAL experiments.

The duration of these initial experiments were 48 h long. This might appear too long for some acid types since they reach their upper limits of extraction in a shorter time. The duration of atmospheric leaching experiments was the next sub topic to be studied.

In summary the strength of acids could be put in an order from the strongest to the weakest like; hydrochloric, sulfuric and nitric acid. The optimum concentration of the acids were determined as; 5 N for both hydrochloric and sulfuric acids, 6 N for nitric acid. These concentrations were chosen because there was no great extraction percentage difference between the next strongest concentrations of each acid. It wouldn't be wise to increase concentrations any further since this would increase the acid consumptions from an industrial perspective.

4.2.2. Effect of Leaching Duration

In this part, the effects of leaching duration on the extraction percentages of nickel and cobalt in atmospheric leaching were studied. The pre-determined conditions were; acid concentration for each acid type, solid to liquid ratio, leaching temperature, particle size, stirring speed and ore type. The studied durations were 12, 24 and 48 h. These experimental durations were chosen according to similar studies in the literature and were based on the previous set of experiments. Because, in the previous set of experiments all the experimental durations were fixed at 48 h, which is relatively long for industrial applications in terms of feasibility and the nickel and cobalt extraction percentages were as high as it could get, so studying lower durations would be wiser. The parameters of this set of experiments are given in Table 21.

Table 21: Conditions of atmospheric leaching experiments to determine the optimum leaching durations.

Ore Name	Sample 1		
Leaching Durations	12, 24 and 48 h		
Leaching Temperature	Boiling Point		
Solid/Liquid Ratio	0.2 (wt./vol.)		
Acid Types	HNO_3	H_2SO_4	HCl
Acid Concentrations	6 N	5 N	5 N
Particle Size	-850 μm		
Stirring Speed	500 rpm		

In Figures 34 and 35, the extraction percentages of nickel and cobalt increased with increasing experimental durations with different types of acids. This was expected because the longer the acid-ore surface interactions lasts, the more dissolution occurs. By increasing the experimental durations, the dissolution

kinetics gave more time for acid to penetrate into the ore particles and dissolve the metals from host minerals.

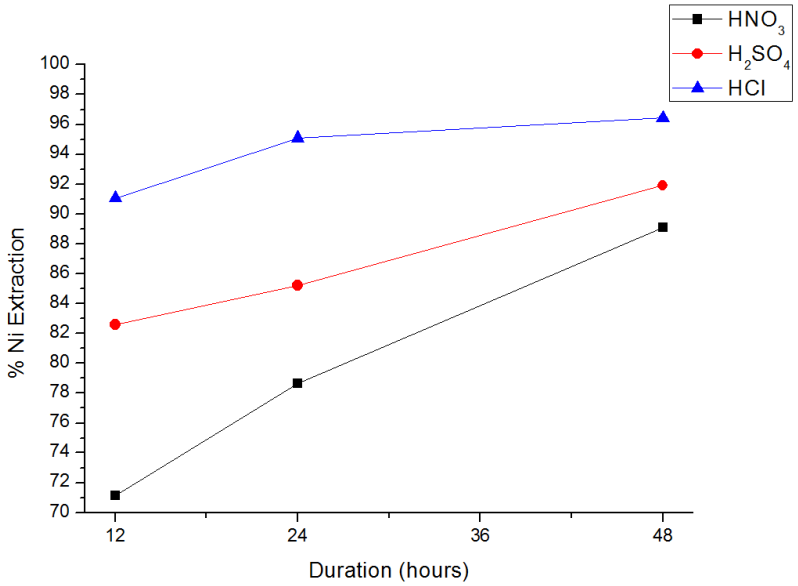

Figure 34: Nickel extraction percentages with respect to three acid types at three different experimental durations.

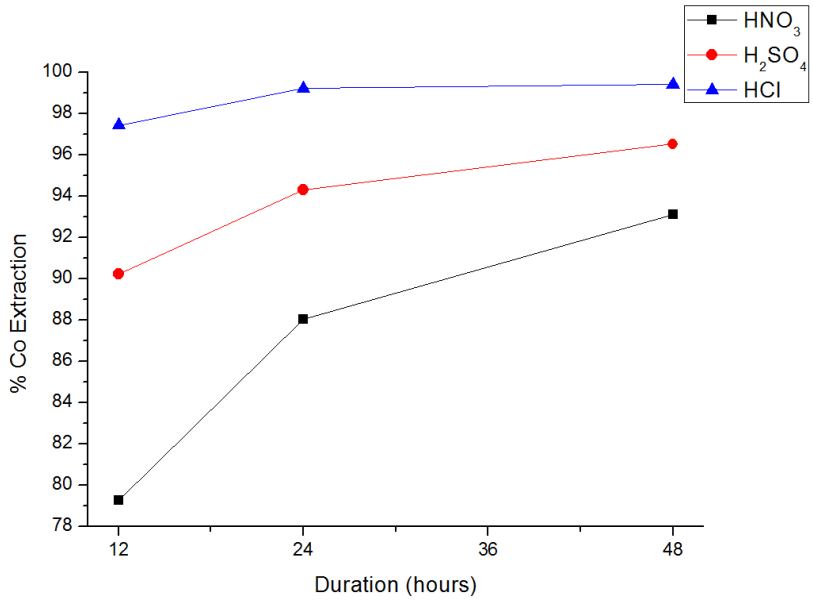

Figure 35: Cobalt extraction percentages with respect to three acid types at three different experimental durations.

In Figures 34 and 35, it can be seen that after 12 h of leaching, the nickel and cobalt extraction values were relatively low. By increasing the duration to 24 h, the same values increased a little bit, but for the nitric and sulfuric acid's case, the best extractions were obtained at 48 h. For hydrochloric acid, there was only a little difference between the extraction values of 24 and 48 h. So the optimum durations were selected for nitric and sulfuric acid as 48 and 24 h for hydrochloric acid respectively.

In Figures 36, 37 and 38, the elemental dissolution rates with respect to duration of leaching for different acids are given. The reason for the optimum conditions stated above can be more easily seen in these figures. In the first 24 h, most of the nickel and cobalt had already been leached and during the next 24 h the dissolution rate decreased substantially. Also arsenic showed the same sort of similar behavior to nickel and cobalt with the increasing experimental durations and the ionic content of arsenic in the PLS increased alongside with that of iron. This was also occurring due to increased duration of acid-ore interaction which resulted in better unlocking of hematite and goethite lattices. The extraction values of iron didn't reach to very high percentages like Ni, Co and As. The undissolved iron might be present in silica or chromite particles with the presence of some nickel and cobalt elements.

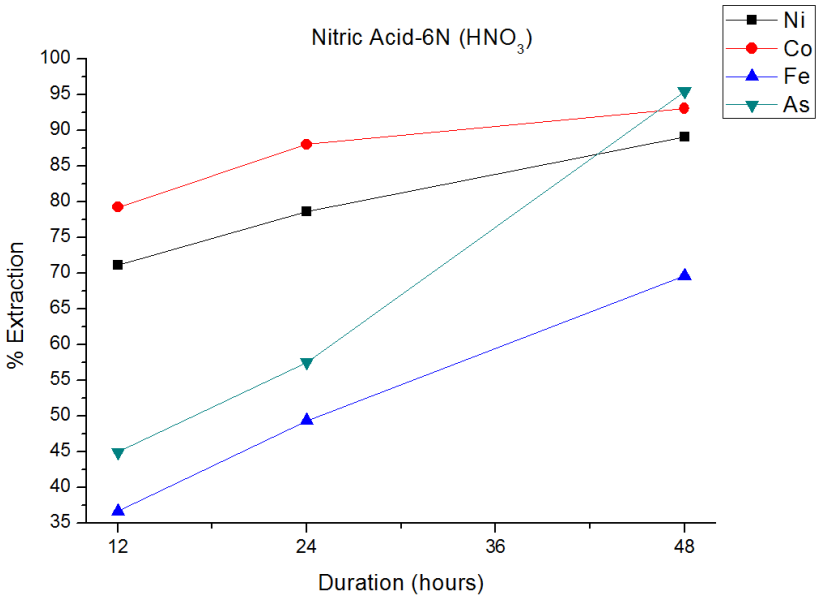

Figure 36: Extraction percentages of nickel, cobalt, iron and arsenic from atmospheric leaching experiments conducted with nitric acid for 12, 24 and 48 h long.

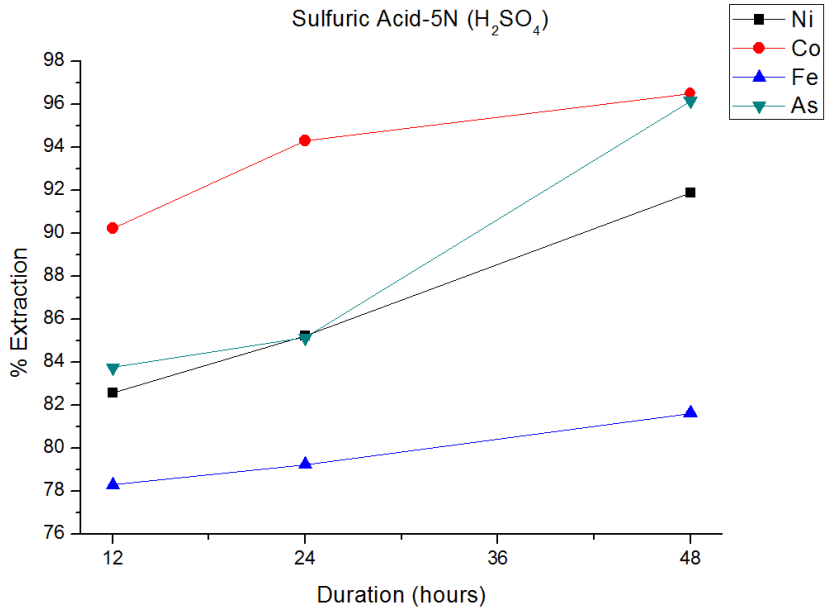

Figure 37: Extraction percentages of nickel, cobalt, iron and arsenic from atmospheric leaching experiments conducted with sulfuric acid for 12, 24 and 48 h long.

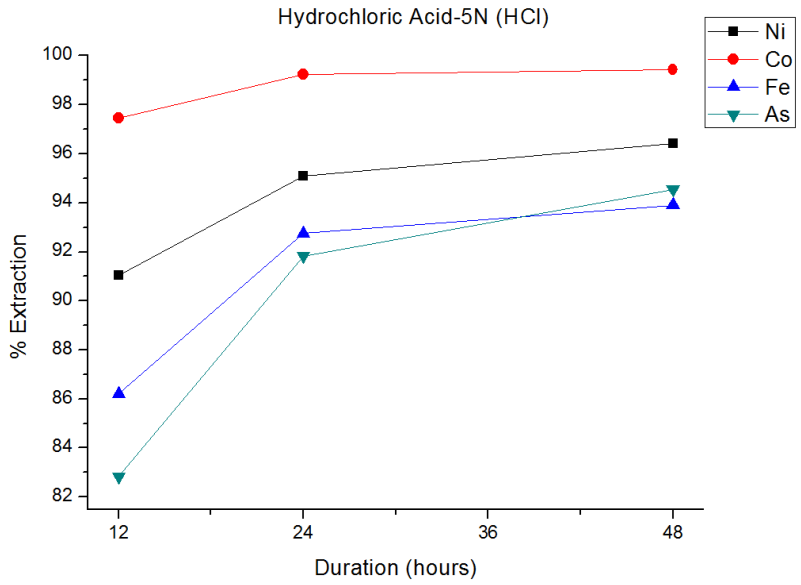

Figure 38: Extraction percentages of nickel, cobalt, iron and arsenic from atmospheric leaching experiments conducted with hydrochloric acid for 12, 24 and 48 h long.

4.2.3. Effect of Particle Size

Particle size is one of the important parameters of atmospheric acid leaching experiments. The consecutive set of experiments was carried out to understand the effect particle size on extraction efficiencies of nickel and cobalt by using ore sample 1. Up to this point, the optimum concentrations and durations of experiments were determined for each acid type. A new set of experiment was conducted with these determined optimum conditions to find out the effect of particle size. The conditions for this set of experiment are given in Table 22.

Table 22: Conditions of atmospheric leaching experiments to investigate the particle size effect.

Ore Name	Sample 1		
Leaching Temperature	Boiling Point		
Solid/Liquid Ratio	0.2 (wt./vol.)		
Acid Types	HNO_3	H_2SO_4	HCl
Acid Concentrations	6 N	5 N	5 N
Leaching Durations	48 h	48 h	24 h
Particle Sizes	-1700 μm, -850 μm and -425 μm		
Stirring Speed	500 rpm		

In the graphical data presented in Figures 39 and 40, the nickel and cobalt extraction percentages with respect to nitric, sulfuric and hydrochloric acids at three different particle sizes are given. It was expected that with the decreasing particle size of ore sample, the metal extraction efficiencies would be increased. However, according to the results obtained, the extraction percentages of nickel and cobalt by using different particle sizes were very close to each other for all acid types. The possible reason could be presence of the strongly acidic environment and strong agitation that might have decreased the particle size during the leaching operation. Also, in the lateritic ore sample 1 ground to minus 850 μm, more than 50% of the particles were minus 38 μm as given in Table 5.

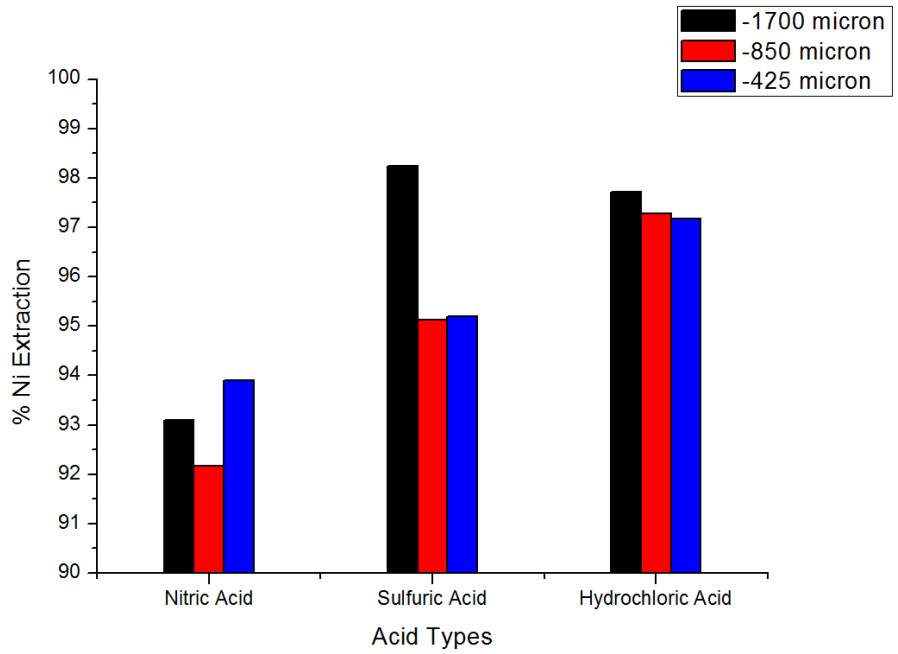

Figure 39: Effect of particle size difference in atmospheric leaching experiments on nickel extraction efficiency in terms of different acid types.

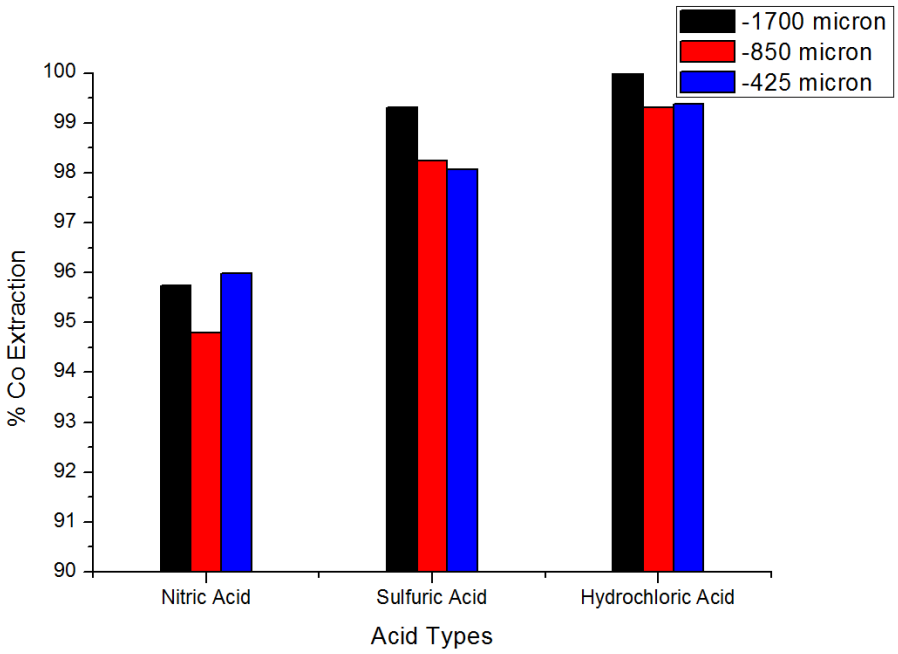

Figure 40: Effect of particle size difference in atmospheric leaching experiments on cobalt extraction efficiency in terms of different acid types.

In conclusion, for the ore samples under study grinding to minus 1700 μm particle size was selected for all types of acid. This is also beneficial for industrial applications in possible atmospheric leaching plants, because decreasing the particle size requires supporting facilities which have great initial and maintenance costs. Also, decreasing the particle size may cause problems in the solid/liquid separation stage, since finer particle sized ores could clog the pipeline and result in higher cost maintenances and have possible risk to shut down the whole operation. So in terms of feasibility, the coarser particle sizes are much more suitable for atmospheric leaching since they offer almost the same nickel and cobalt extraction efficiencies compared to finer particle sizes.

4.2.4. Comparison of Ore Samples 1 and 2 under the Optimum Conditions

In the previous parts, the experiments were conducted in order to find out the optimum conditions for atmospheric leaching of ore sample 1. In Table 23, all of the experimental conditions are stated for testing the two different ore samples.

Table 23: Conditions of experiments to compare the different ore samples.

Ore Names	Sample 1 and Sample 2		
Leaching Temperature	Boiling Point		
Solid/Liquid Ratio	0.2 (wt./vol.)		
Acid Types	HNO_3	H_2SO_4	HCl
Acid Concentrations	6 N	5 N	5 N
Leaching Durations	48 h	48 h	24 h
Particle Size	-74 μm		
Stirring Speed	500 rpm		

To compare the ore samples with each other, a new set of experiments was conducted at the optimum conditions except the particle size. The chosen particle size for this set of experiments was minus 74 µm, because of the arrival of entire ore sample 2 at minus 74 µm. In order to provide a healthy comparison and since there were almost no extraction efficiency differences in terms of nickel and cobalt between coarse and fine particle size ores, so minus 74 µm was selected as the particle size to be studied. The selected portion of sample 1 was reduced down to the necessary particle size to be used in the experiments. The results are presented in graphical form in Figures 41, 42, 43 and 44 as bar diagrams with respect to Ni, Co, Fe and As extraction values for the different acid types.

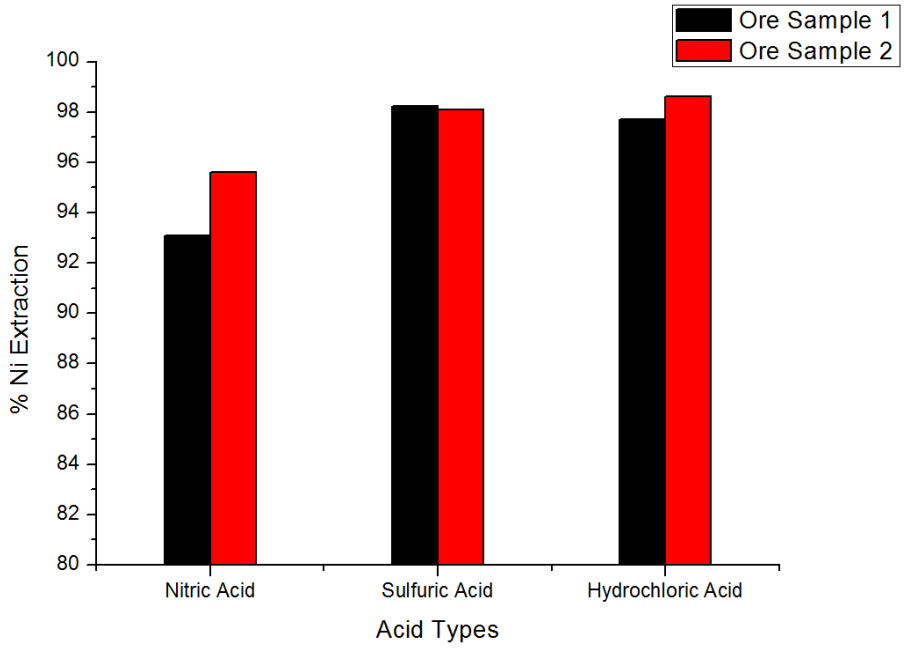

Figure 41: Comparison of ore samples 1 and 2 with respect to nickel extraction efficiencies for different acid types in atmospheric leaching experiments.

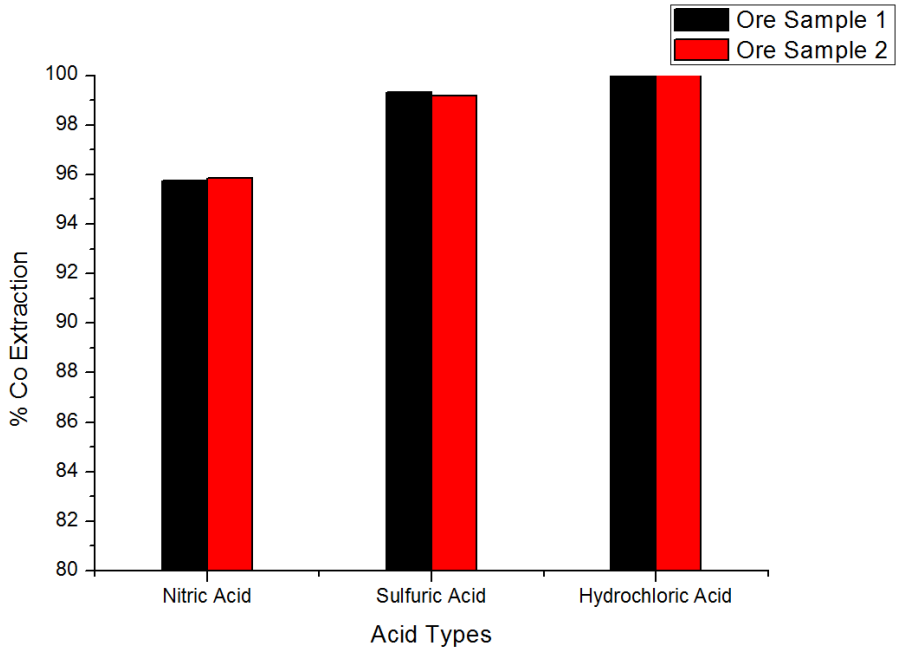

Figure 42: Comparison of ore samples 1 and 2 with respect to cobalt extraction efficiencies for different acid types in atmospheric leaching experiments.

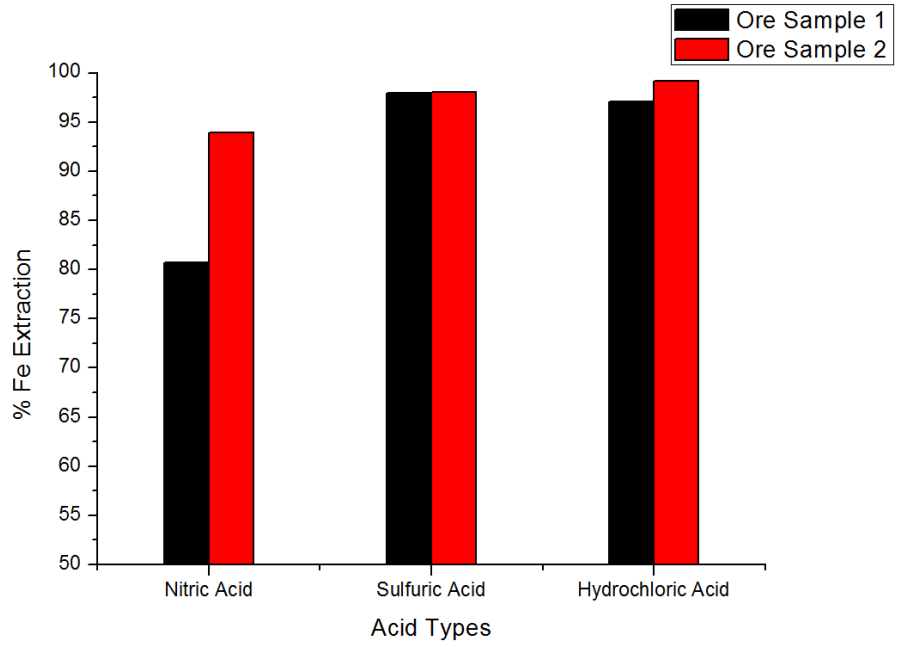

Figure 43: Comparison of ore samples 1 and 2 with respect to iron extraction efficiencies for different acid types in atmospheric leaching experiments.

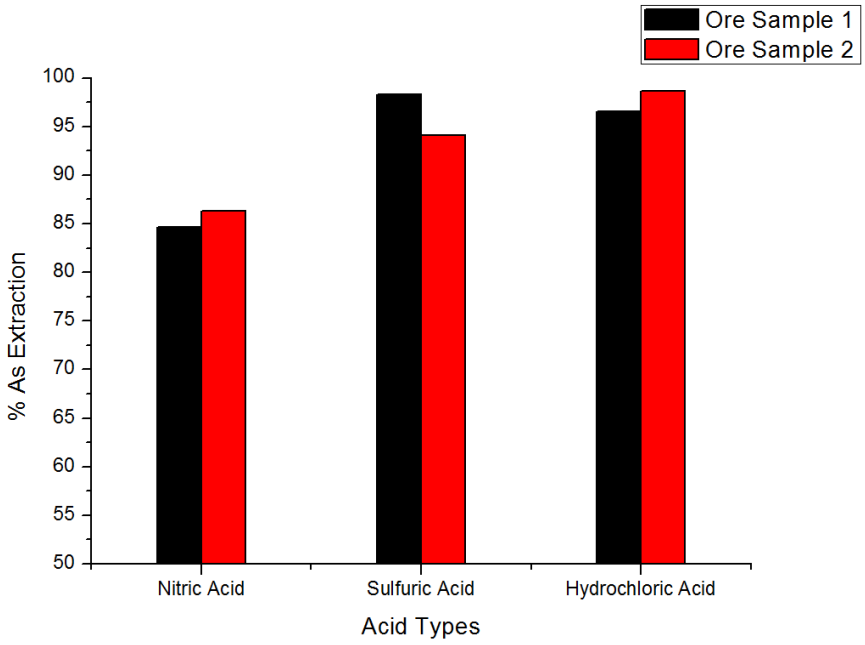

Figure 44: Comparison of ore samples 1 and 2 with respect to arsenic extraction efficiencies for different acid types in atmospheric leaching experiments.

According to the graphical interpretation of resultant data, the extraction efficiencies were almost identical with each other. There were no substantial differences between ore samples in terms of nickel and cobalt extraction values with respect to different types of acid. So, in terms of mineralogy, the high arsenic containing ore sample 2 showed no difference with less arsenic containing ore sample 1. In fact this result was expected, since there was no precipitation of metals occurring like in HPAL experiments. Arsenic was not expected to inhibit the dissolution kinetics of nickel, cobalt and iron in any way so the theory put forward was confirmed. It was also clear that iron was leached in greater percentages from both ore types by using different types of acid as compared to HPAL.

When the results of metal extraction efficiencies for sample 2 were considered, the effect of different acid types was found to be as expected. Nitric acid granted the lowest nickel and cobalt extraction percentages and these values increased with the use of sulfuric acid and hydrochloric acid, respectively when the red bars were compared in a consecutive manner. But the reason for the difference being quite low between acid types was because the experiments were planned with the optimum conditions in order to obtain the best possible extraction values individually.

4.3. Leach Residue Characterization of the Optimum Condition Experiments

The characterization stage of the leach residues of both HPAL and atmospheric experiments have great importance in terms of understanding the low extraction values by revealing the nickel and cobalt losses with leach residue. This problem was also encountered by Kaya, using the same limonitic sample from the same open pit mine in Gördes/Turkey. In his study, the primary hematite was stated to be responsible for the low extractions by not being leached entirely (53).

Two different kinds of ore samples were used in the experimental stage to understand the effect of arsenic on the leaching kinetics by means of the resultant nickel and cobalt losses. But it was seen that the presence of high arsenic content in the limonitic laterite ore did not affect greatly the nickel and cobalt extraction efficiencies in HPAL experiments. In atmospheric leaching experiments, there were no problematic issues encountered with the nickel and cobalt dissolution percentages. The only issue with the atmospheric experiments was the economic feasibility of both upstream processes and downstream processes due to high acid consumption alongside with the need of high amount of neutralizing agent due to high residual acid content.

XRD and SEM analyses were done to investigate the reasons for the low extraction efficiencies of nickel and cobalt (< 80%) of HPAL experiments. In these studies what was inhibiting the dissolution mechanisms during dissolution-precipitation in high temperature and pressure environment was investigated. As it was discussed in the earlier sections, the precipitation of hematite (secondary hematite) over the undissolved hematite (primary hematite) or goethite by nucleating on its surface due to low surface energy and covering it partially and/or entirely, thus preventing its contact with acidic media, could be one of the reasons of low nickel and cobalt extraction efficiencies. As a second reason, the arsenic's inhibiting effect on dissolution of hematite, thus preventing nickel and cobalt to become free from iron crystal structures during dissolution was considered. But this option was eliminated due to the previous obtained experimental results which clearly showed that the both ore samples with different arsenic contents gave similar nickel extraction efficiencies under the same experimental conditions. Also XRD patterns of leach residues obtained under the optimum condition of atmospheric leaching experiments with two different kinds of ore were investigated. The SEM imaging and EDS analyses were also done to characterize their leach residues.

4.3.1. XRD Characterizations

4.3.1.1. XRD Investigation of HPAL Residues

XRD patterns of HPAL leach residue obtained under the optimum conditions of leaching and HPAL leach residue formed under the limiting conditions of leaching are given in Figures 45 and 47. These XRD data belong to the experiments in which sample 1 was used. Also, the HPAL experiments conducted with sample 2 under both the optimum conditions and limiting conditions of

leaching are given in Figures 46 and 48. One can see from these figures that all of the goethite mineral that were present in the original samples 1 and 2's XRD patterns had completely disappeared from the leach residues. In Figures 45 and 46, the HPAL experiments under optimum conditions with both sample can be compared with the original ores' XRD patterns. So as a result, all of the nickel and cobalt in the crystal structure of goethite mineral were completely transferred into the solution. But this also meant that iron in goethite was also completely leached and its ionic content increased in the pregnant leach solution. This dissolution was one of the major iron sources which had transferred into the PLS that would precipitate simultaneously as secondary hematite during the experiment. Also serpentine was the other mineral that existed in the original ores' XRD patterns but it had completely vanished during the HPAL experiments. However, the situation was different with the hematite mineral. It was expected that the leaching of primary hematite could create problems in HPAL, which could be responsible for the losses of nickel and cobalt in leach residue. Since a great quantity of lost nickel was still encapsulated in the iron crystal structure. It was either in the original primary hematite structure or in the precipitated hematite structure. It was impossible to differentiate this by XRD examinations.

Alunite was another newly formed phase present in the leach residues. Alunite's presence in the leach residues indicated that it was formed during HPAL due to the precipitation of aluminum since the original ores had some amounts present.

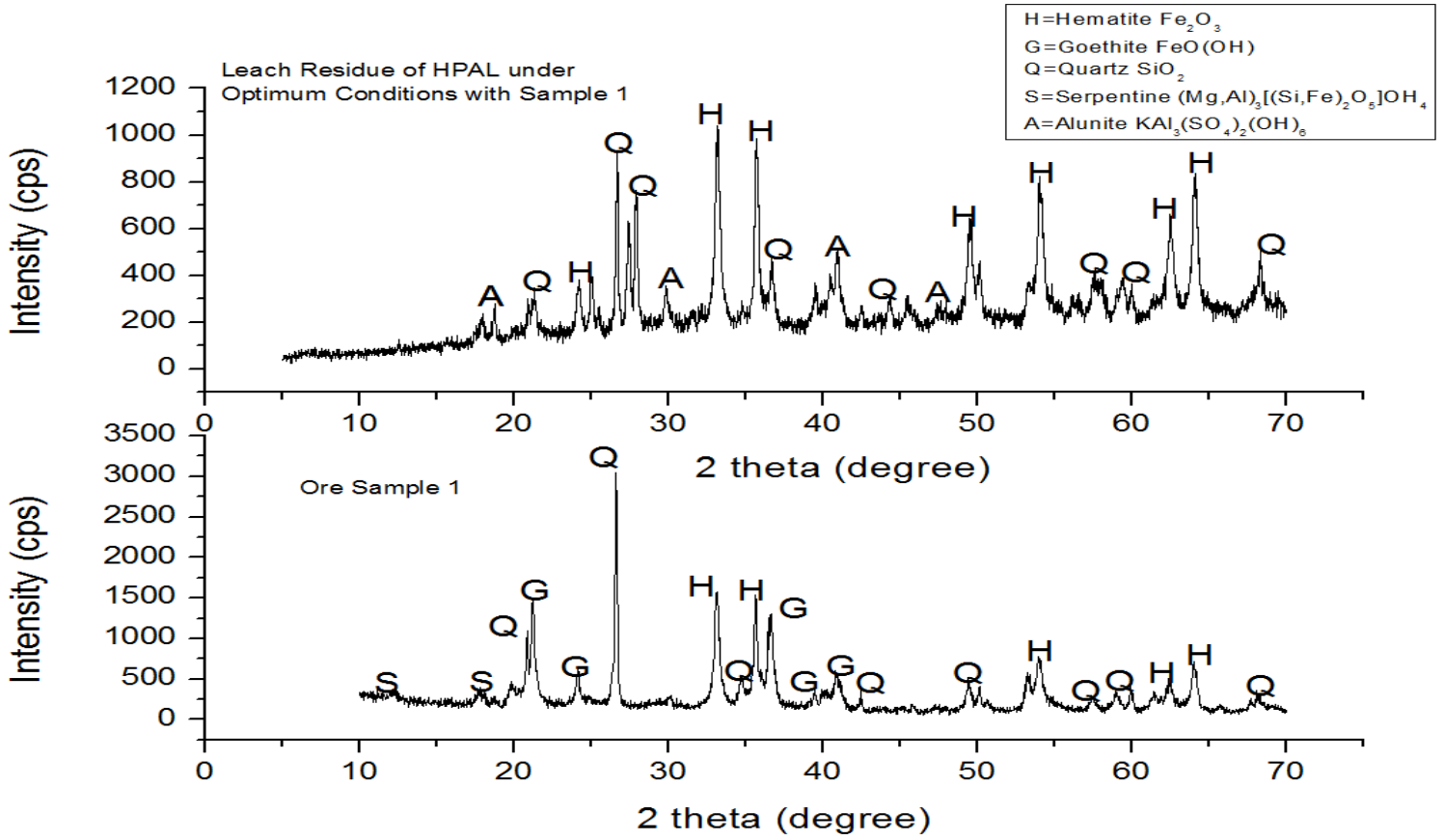

Figure 45: Comparison of leach residue XRD patterns of HPAL experiment (A5) under optimum conditions and its original ore sample 1.

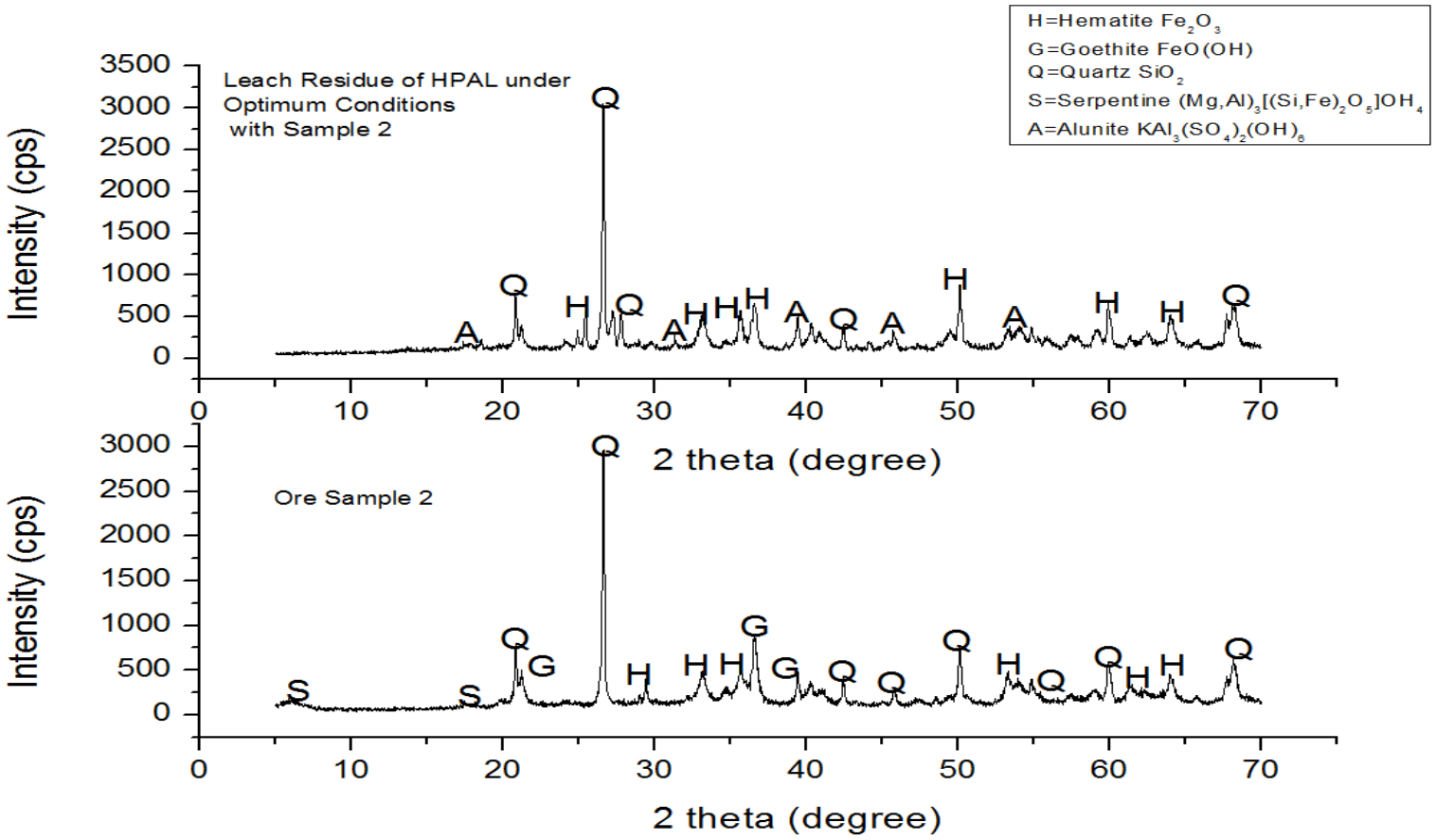

Figure 46: Comparison of leach residue XRD patterns of HPAL experiment (K1) under optimum conditions and its original ore sample 2.

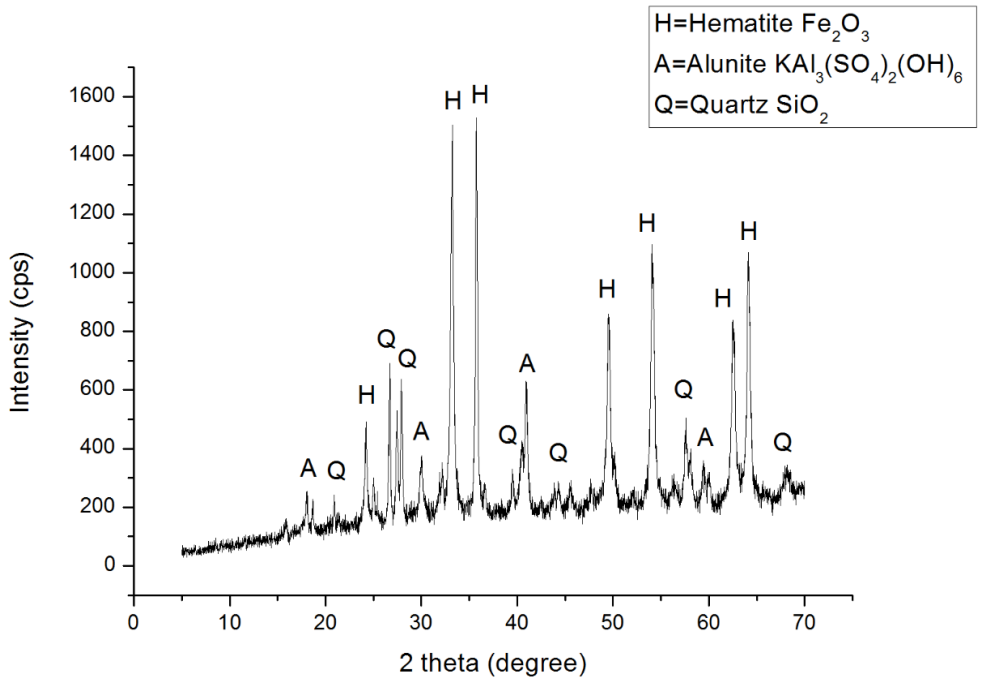

Figure 47: Leach residue XRD pattern of HPAL experiment coded as "D3" conducted with ore sample 1 under the limiting conditions.

Results given in the Figures 47, hematite dominated the patterns by itself with sharp peaks but on the other hand in Figure 48 which was conducted with sample 2, was dominated by quartz. This was mostly because of quartz transform into gel-like silica in the high agitation and acidic media without dissolving in D3 and not in K7. Major quartz peaks were significantly decreased in their intensities by dissolving and increasing the silicon concentration in the PLS. Also gel-like silica is amorphous and invisible in XRD patterns. But the remaining crystalline silica preserved its place weakly in the leach residues with respect to hematite particles. However, amorphous silica was mentioned in several articles and held responsible for nickel and cobalt losses inside the leach residues. Again this can only be investigated by SEM imaging and checked with EDS analyses.

Other than the major phases that could be detected by XRD examinations, according to the previous works of Önal, there could be undetected minor phases like chromite, etc. These phases will also be looked for in the SEM examinations. Chromium can also be present in the leach residues in a form other than chromite such as substitutional element in primary hematite crystal and inside the alunite structure as a replacement for OH^- ions.

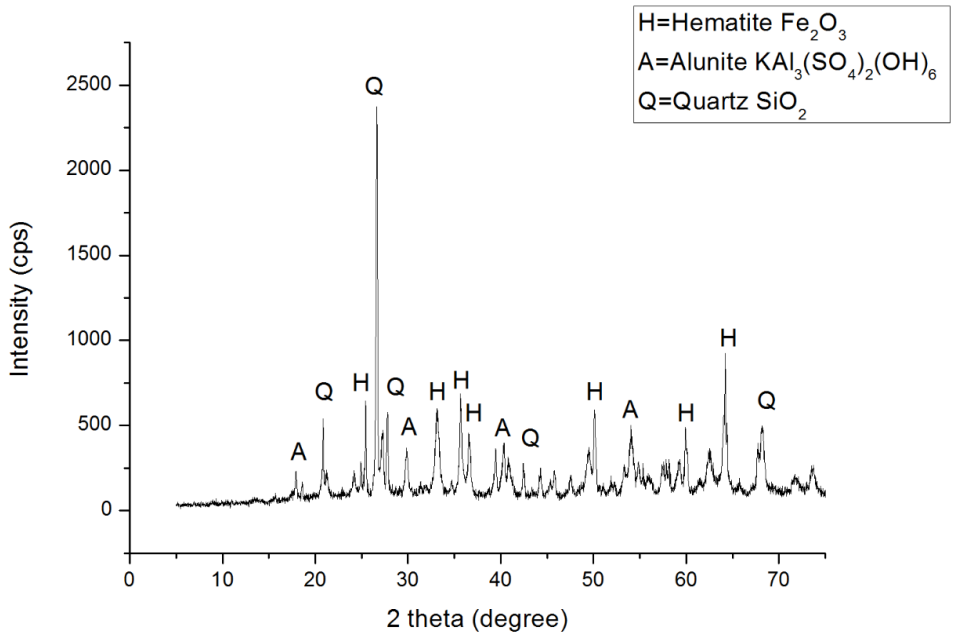

Figure 48: Leach residue XRD pattern of HPAL experiment coded as "K7" conducted with ore sample 2 under the limiting conditions.

In the XRD patterns of experiments with ore sample 2, the main quartz peak held its position while decreasing in intensity. The intensity difference could even be observed between Figures 46 and 48 which were obtained under the optimum condition and limiting condition of HPAL experiments, respectively. The existence of hematite was similar with sample 1's XRD patterns. Again there was

no clear evidence of arsenic's inhibiting effect on the dissolution of iron crystals by comparing the XRD patterns. The only visible difference was in the intensity of the major quartz peaks.

In conclusion, it was not possible to clarify the nickel and cobalt losses either by the primary hematite or secondary hematite from the XRD data. Distinguishing primary and secondary hematite according to the particle size was not easy since secondary hematite would dominate the leach residue by forming clusters and covering the primary hematite. But XRD findings could help us to evaluate the SEM results in a better way to understand what was inhibiting the dissolution kinetics. Also the formation of amorphous silica could be one of the reasons for nickel losses which were mentioned in literature.

4.3.1.2. XRD Investigation of Atmospheric Leach Residues

The first three XRD patterns in Figures 49, 50 and 51 belong to the leach residues of atmospheric leaching experiments conducted with sample 1 under the optimum conditions with different acid types. Similarly, Figures 52, 53 and 54 belong to sample 2. When the first three patterns were compared with the original ore sample 1's XRD pattern, it could be seen that the serpentine, which was a minor mineral, had completely vanished during atmospheric leaching experiment. Goethite peaks kept their positions in the leach residues but with greatly reduced intensities and smaller goethite peaks had completely disappeared. As one of the major nickel and cobalt host minerals in the ore, this almost complete disappearance of goethite was a positive finding. However, undissolved goethite peaks also showed that goethite mineral could be present without nickel and cobalt in its structure, since nickel and cobalt extraction efficiencies were really

high (> 90%). The same situation was also possible for hematite. Again the major hematite peaks did not completely disappear but stayed in the leach residue with lowered intensities and this showed that although hematite crystal was one the major nickel and cobalt host minerals, it could also exist without the presence of nickel and cobalt.

The extraction efficiencies which were presented in the previous parts showed that iron was also leached at great quantities during atmospheric acid leaching. This was expected since there was no precipitation of ionic iron in the form of hematite like in the HPAL experiments due to lack of high temperature and pressure conditions. Since iron was dissolved between 65-80 % of its total content, the rest of iron existed as undissolved hematite and goethite, which were found in the XRD patterns. The quartz peaks held their intensity mostly within the leach residues.

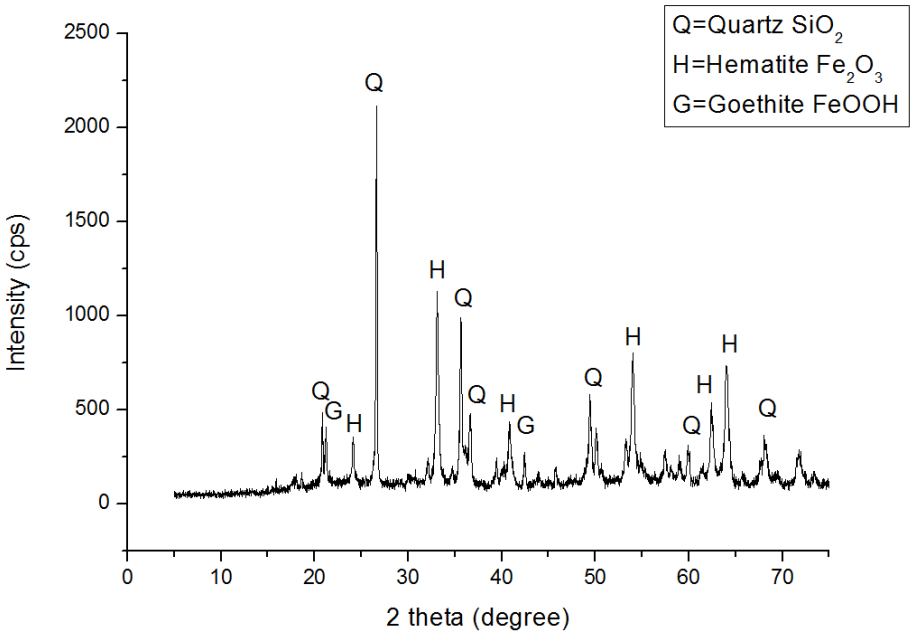

Figure 49: Leach residue XRD pattern of atmospheric leaching experiment conducted with sample 1 using nitric acid under the optimum conditions.

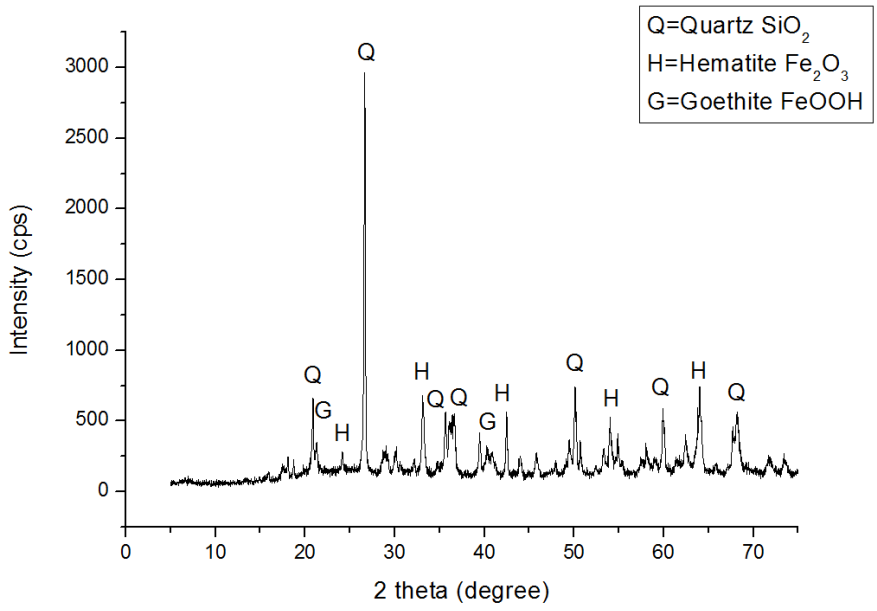

Figure 50: Leach residue XRD pattern of atmospheric leaching experiment conducted with sample 1 using sulfuric acid under the optimum conditions.

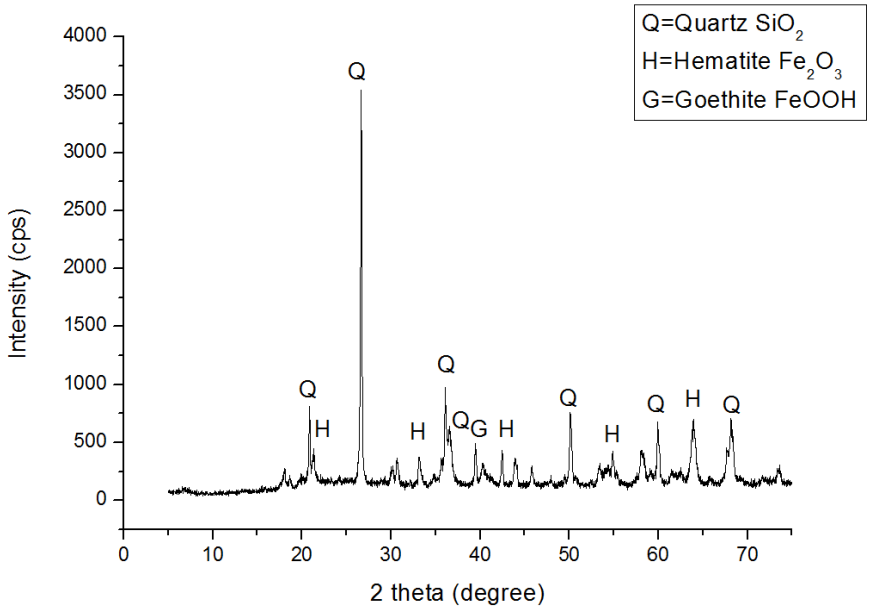

Figure 51: Leach residue XRD pattern of atmospheric experiment conducted with sample 1 using hydrochloric acid under the optimum conditions.

There were also clear changes in XRD patterns of the experiments with different acid types. It is already known and presented in previous sections that the strongest acid among the three of them is hydrochloric acid. The second is sulfuric acid and the weakest is nitric acid. This distinction was reflected in the XRD patterns by the intensities of undissolved goethite and hematite peaks. Their peak intensities were getting lower and lower with respect to increasing strength of acids. This was also supported by the extraction efficiencies since the highest of them belonged to hydrochloric acid. These peak intensities were also changed by the weight of the leach residue. Quartz like undissolved particles stayed still in the leach residue while the total amount of initial ore was reduced and this affected the distinct peaks of minerals in the XRD patterns.

Again there were no obvious differences in XRD patterns between different types of ore with low and high arsenic contents. When the same acid's XRD patterns were compared both had undissolved goethite and hematite. The quartz peaks

present in the leach residues were almost untouched. Moreover, there were no findings in the leach residues that could be related to the varying arsenic content.

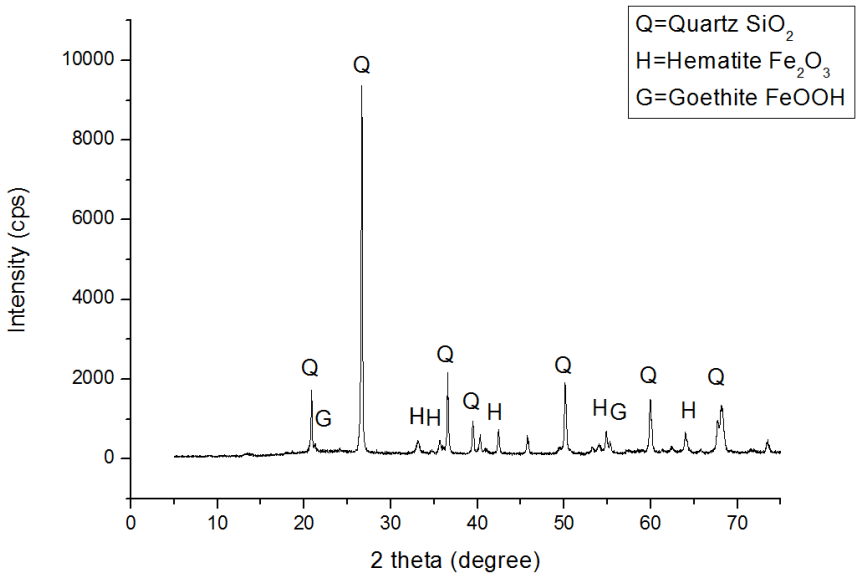

Figure 52: Leach residue XRD pattern of atmospheric leaching experiment conducted with sample 2 using nitric acid under the optimum conditions.

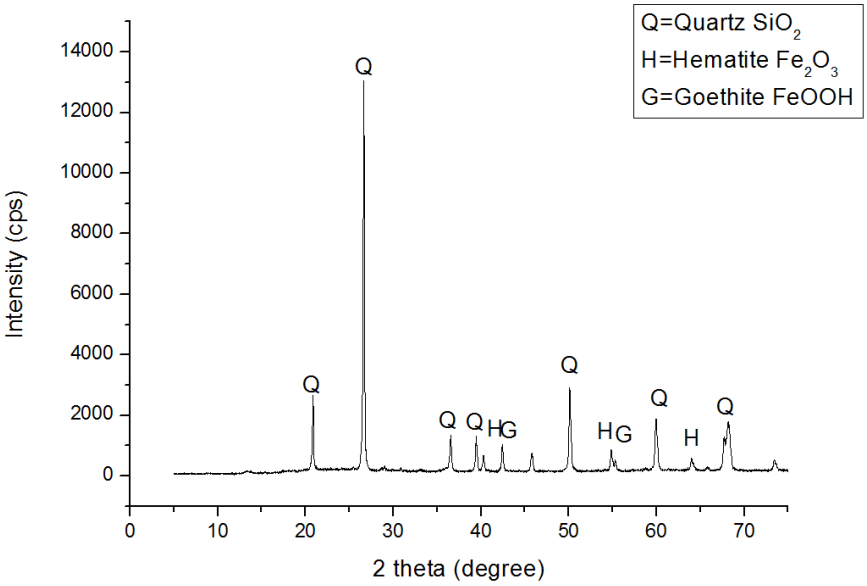

Figure 53: Leach residue XRD pattern of atmospheric leaching experiment conducted with sample 2 using sulfuric acid under the optimum conditions.

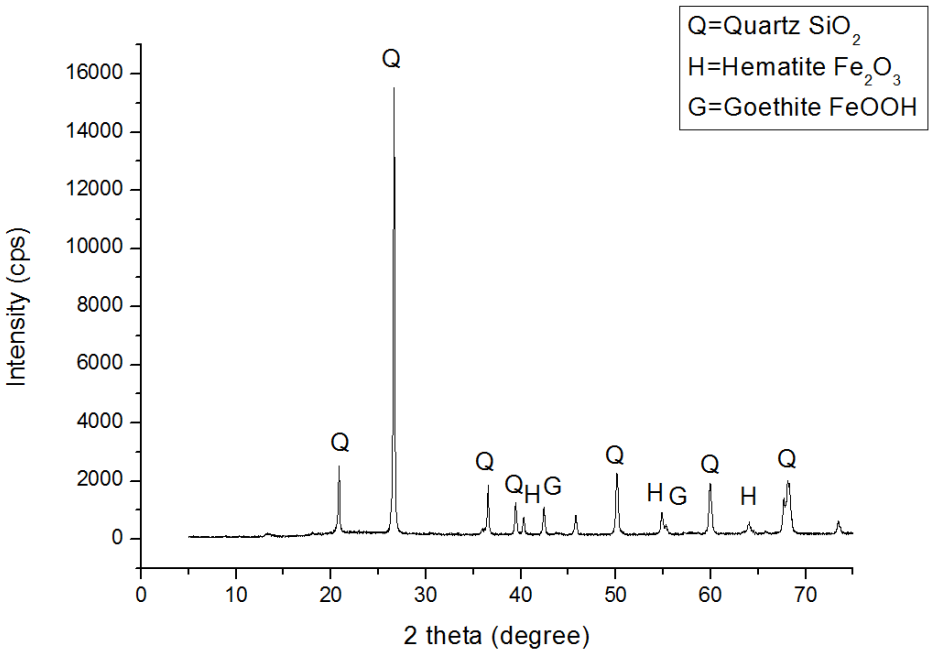

Figure 54: Leach residue XRD pattern of atmospheric leaching experiment conducted with sample 2 using hydrochloric acid under the optimum conditions.

4.3.2. SEM Characterizations

4.3.2.1. SEM Characterization of HPAL Residues

In the SEM examination of HPAL leach residues, the morphology and chemical structure of minerals were investigated based on the XRD examination findings. There were three main phases present in the XRD patterns; silica, hematite and alunite. However, amorphous silica, chromite and many others were also expected to be present in the leach residues. Identification and investigation of these phases would enlighten the nickel and cobalt losses with the leach residues. Especially the investigation of the presence of primary and secondary hematite and their dissolution-precipitation morphology were very important in confirming the theory of secondary hematite's inhibiting effect of the dissolution of primary hematite by precipitating on it.

In Figure 55, the general appearances of sample 1's leach residue can be seen. The numbered particles with red color are respectively: 1) silica, 2) alunite, 3) chromite, 4) hematite, 5) alunite, silica and hematite. The other parts are mostly the mixture of hematite, silica and alunite. The EDS of these red numbered particles can be found in Appendix B.

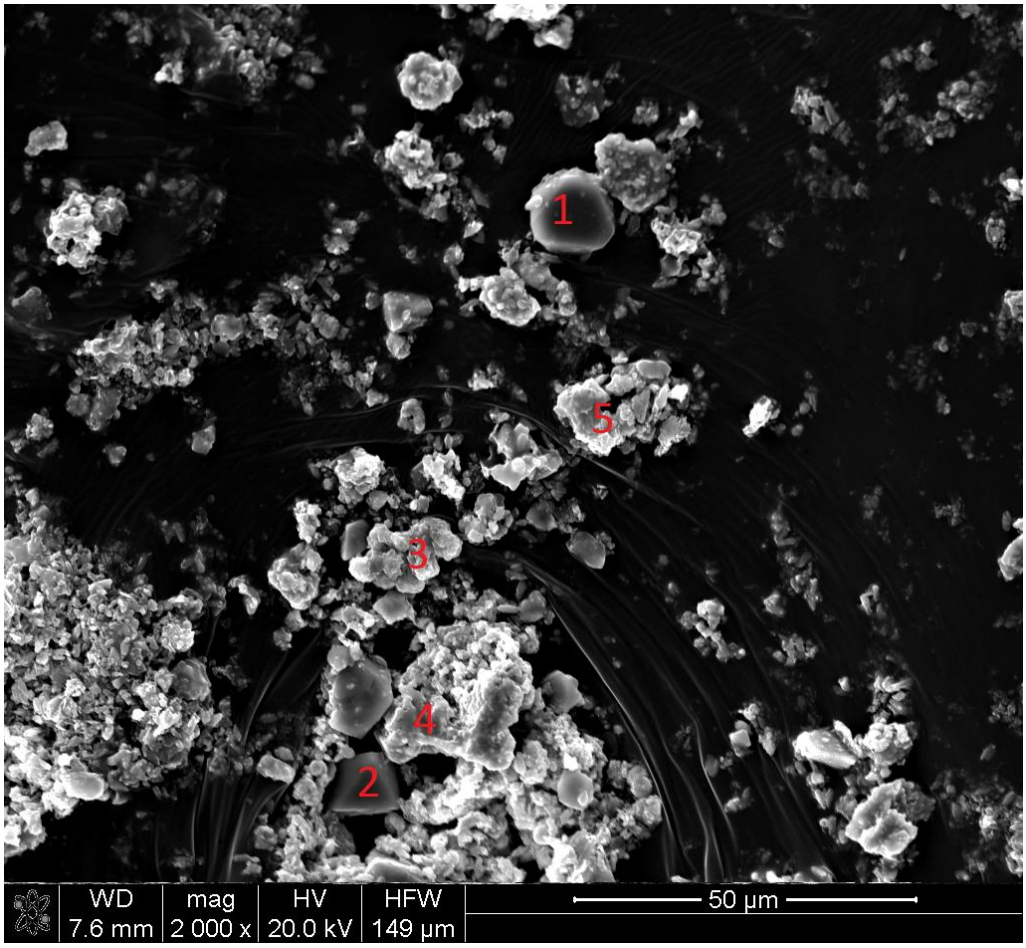

Figure 55: General view of sample 1's HPAL leach residue obtained under the optimum conditions of leaching.

In the examination of general view, each of the major phases which were identified in XRD were found and checked with EDS analyses. Chromite and pyrite as minor minerals were also found that could not be detected by XRD. Amorphous silica, primary and secondary hematite particles, crystalline silica and isolated nickel sulfate's SEM images are given in Figure 56. From this figure, the SEM images of; 1) Amorphous silica with alunite, 2) Pyrite, 3) Secondary hematite, 4) Nucleated secondary hematite on primary hematite, 5) Chromite, 6) Secondary hematite bits on primary hematite can be seen. The EDS results of all the images are given in Appendix B.

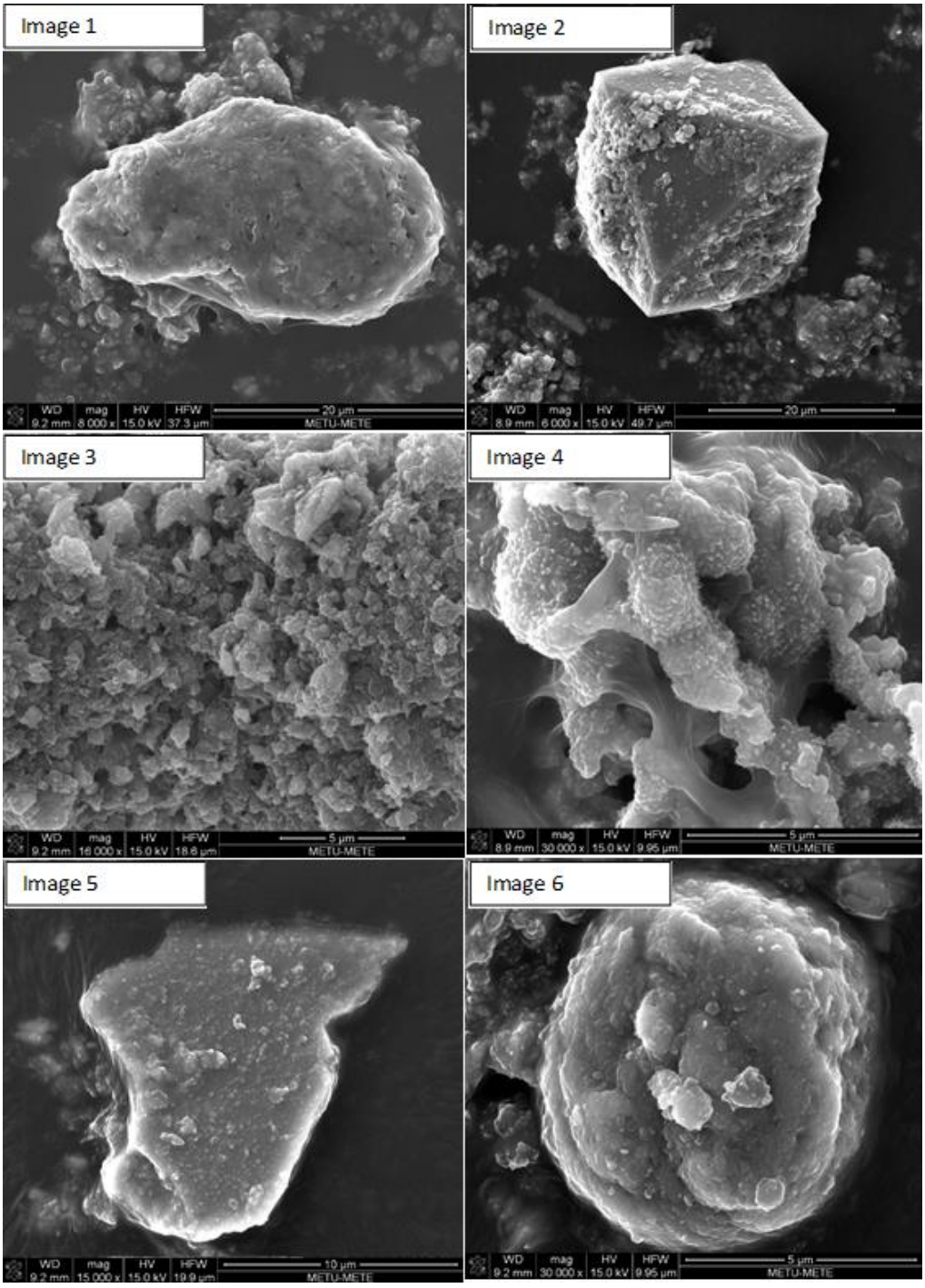

Figure 56: Several SEM images of HPAL leach residue obtained for sample 1 under the optimum conditions of leaching.

In image 1, nickel was found to be present inside a mixture of amorphous silica and alunite. This was in contradiction with the findings of Önal, since in his study it was stated that nickel could not be found in gelatinous silica (13). Another study conducted by Lou et al. showed that high acidic environments can prevent the nickel's adsorption by amorphous silica. But with the possibility of recovery of free acid, the acidic environment would be reduced of its power and this adsorption could occur (10). Images 3, 4 and 6 show the secondary hematite occurrence in the leach residue and in images 4 and 6, these secondary hematite particles are present on primary hematite. The EDS of these particles showed that the mentioned particles were totally composed of hematite. The observation of relatively smaller clusters of nucleated hematite particles on the top of the relatively large primary hematite particles, partially confirmed the expectations. However, the complete coverage of the primary hematite could not be observed in any of the cases, since these leach residues were washed after separating them from pregnant leach solution and after that they were dried overnight and dispersed into fine particles to prepare them for SEM usage. This process itself could damage the samples partially and prevent us from observing the right image that was desired. But this doesn't mean the collapse of our theory since the observation of secondary hematite on primary hematite was found in the leach residues of both samples 1. The SEM images of similar particles in HPAL leach residues of sample 1 were also found in sample 2's HPAL leach residues. One can observe the following particles in Figure 57 for sample 2 as respectively numbered images; 1) Primary hematite, 2) Secondary hematite precipitation, 3) Crystalline silica, 4) Pyrite, 5) Alunite, 6) Mixture of hematite, silica, alunite and chromite.

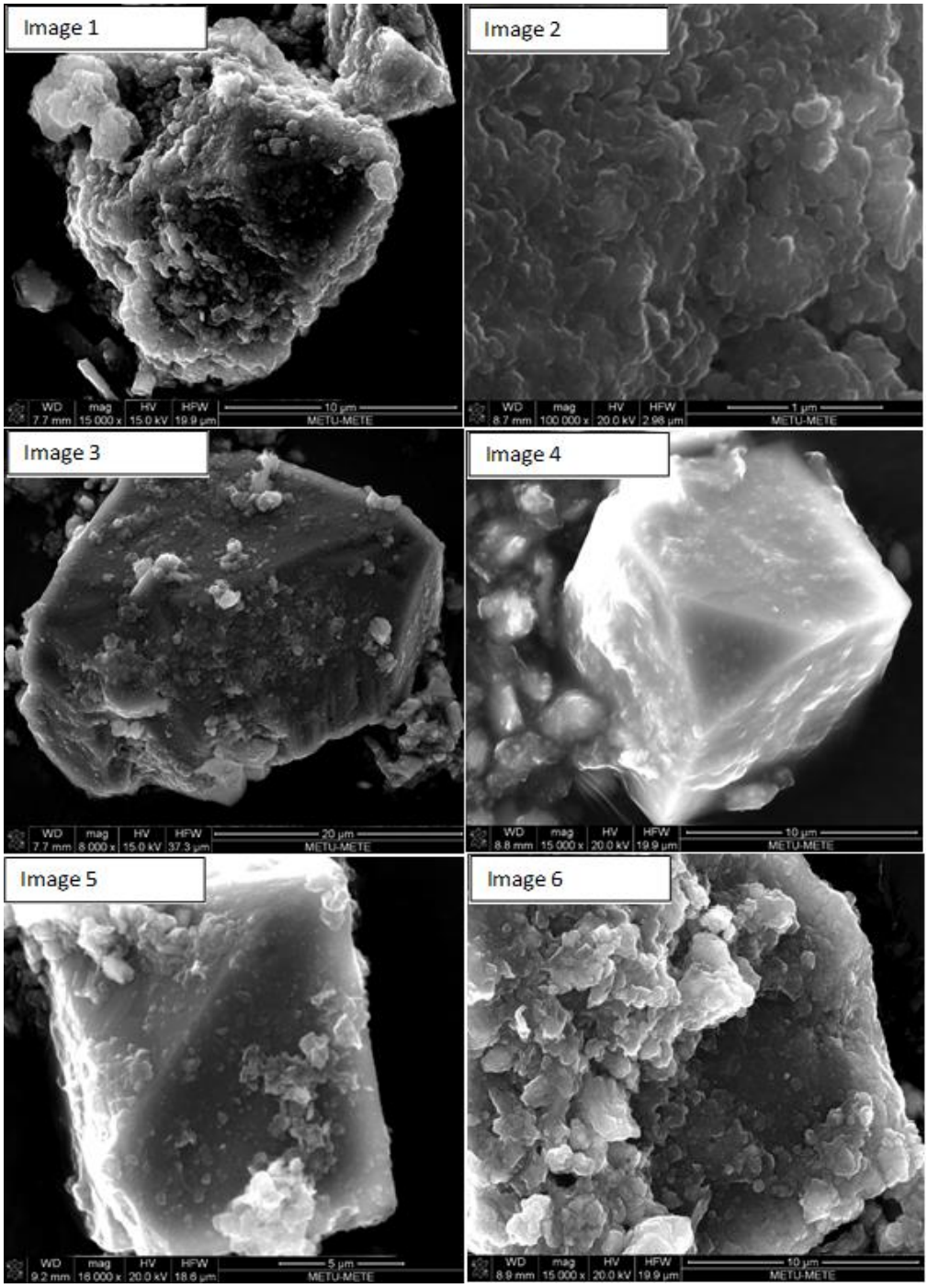

Figure 57: Several SEM images of HPAL leach residues for sample 2 obtained under the optimum conditions of leaching.

As presented in images 1 and 2 in Figure 57, the precipitates were made up of clusters of highly agglomerated particles. All of these images were analyzed with EDS and almost none of them were found to be as pure substances except crystalline silica. Alunite was also found in many places as expected, since the presence of it was shown in XRD investigations. Its morphology was like sharp, cut-like edges with resemblance to smaller plaques. Pyrite again was found in sample 2's leach residue like the first sample. However, after many hours of SEM search of more pyrite and similar perfect-cube with cut edges could not be detected. The reason for the absence of pyrite in the XRD of leach residues should be due to its presence in small amounts in the original ores.

It is known from the literature that, hematite is not associated with amorphous silica during its dissolution and precipitation. This phenomenon can be observed in images since silica was always found to be pure with or without having its crystal structure and the precipitated hematite was only found with its own structure which could easily be identified by the contrast of its images.

Nickel was found in hematite particles with or without the presence of arsenic. The existence of arsenic seemed to have no effect on its extraction efficiencies. In the leach residue of high arsenic bearing ore sample 2, it was proven with many different EDS analyses that hematite was found with or without nickel and with or without the presence of arsenic. From the images and EDS results, no conclusions could be drawn since all possible combinations of types of hematite were observed. Since the calculation of the amount of each type in the entire leach residue was not possible.

4.3.2.2. SEM Characterization of Atmospheric Leach Residues

From the investigations of XRD patterns of leach residues of atmospheric leaching experiments quartz, hematite as major minerals and goethite as a minor mineral were found. Since there was no precipitation of ions in atmospheric leaching, the secondary hematite occurrence was not expected to be found in leach residues. However, since it was confirmed from both XRD results and iron's concentration in the pregnant leach solution and leach residue, the undissolved iron minerals were expected to be found in the SEM images and EDS results. Aluminum also didn't precipitate and form alunite like in HPAL experiments as seen in images 1 and 2 in Figure 58.

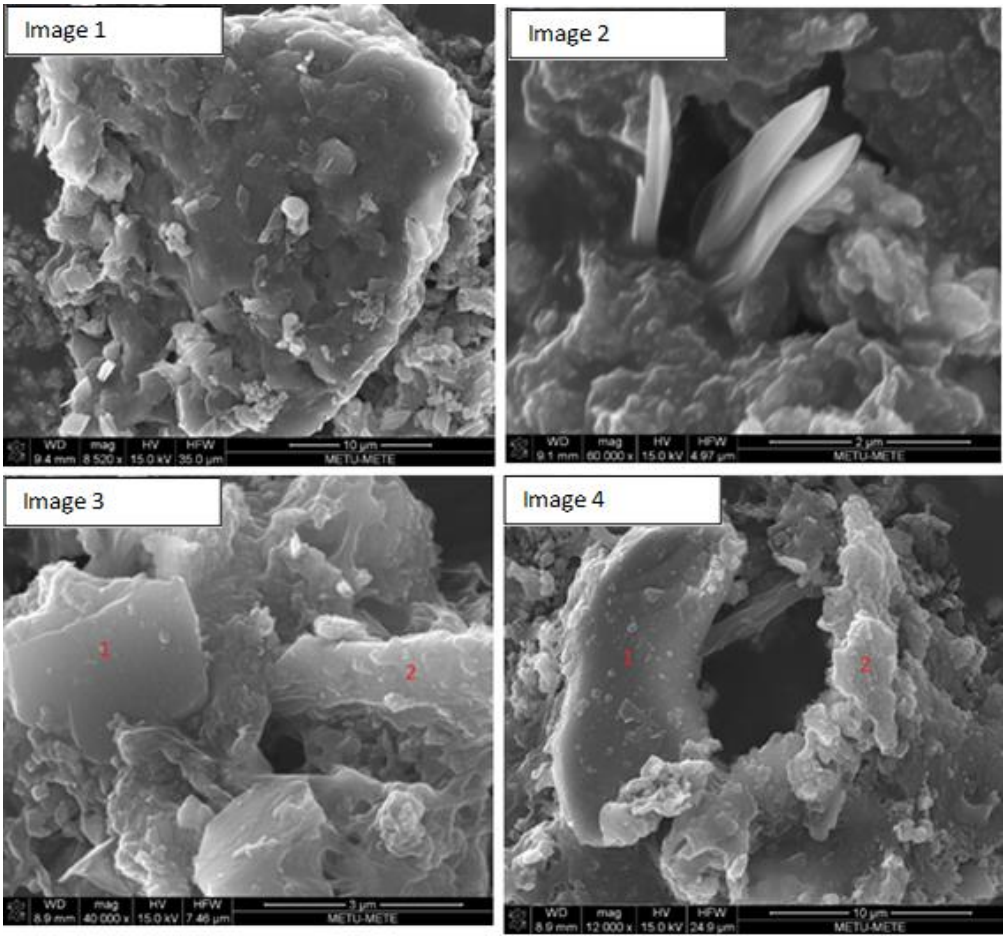

Figure 58: Several SEM images of atmospheric leach residues obtained under the optimum conditions of leaching.

Number 1 and number 2 particles in image 3, belong to silica and chromite particles, respectively. Same are the numbered particles 1 and 2 in image 4 which belong to silica and hematite with arsenic content. The EDS results of the images in Figures 56, 57 and 58 are given in Appendix B.

In conclusion, although there was no clear effect of different ore samples in terms of extraction efficiencies of atmospheric acid leaching, SEM imaging and EDS analyses were conducted to be sure. Both ore samples which were acid leached with three different kinds of acid under the determined optimum conditions gave almost the same results. Neither nickel nor cobalt was found in the leach residues.

This finding indicated the presence of hematite and goethite crystals without nickel content existing in the limonitic ore samples. Chromite found in the leach residues was the same as in HPAL residue although it didn't show up in the XRD results. All the minerals in the XRD patterns that were detected in SEM imaging verified with EDS analyses which can be found in Appendix B.

CHAPTER 5

CONCLUSIONS

The aim of this study was to compare the high pressure acid leaching and agitated atmospheric acid leaching by using two refractory lateritic nickel ore samples which were obtained from Manisa/Gördes open pit mine located in western part of Turkey. To investigate the possible reasons of low extraction values of nickel and cobalt in HPAL under the optimum conditions based on previous studies on the similar ores, was one of the main objectives. The second main objective was to determine the best possible experimental conditions to obtain the maximum extraction efficiencies of nickel and cobalt. So throughout the experimental examinations, various process parameters were tested with the intention of getting the best extraction percentages and finding out explanations of low extraction values of refractory nickel ore. The results obtained from this study are summarized below:

- Chemical characterization of Gördes ore samples showed that the ore sample 1 had 1.08% nickel and 0.069% cobalt together with 29.90% iron, 0.85% arsenic, 3.80% aluminum, 0.74% magnesium, 1.09% chromium and 27.09% SiO_2. On the other hand, the sample 2 had 0.98% nickel and 0.038% cobalt together with 23.3% iron, 2.2% arsenic, 3.7% aluminum, 0.51% magnesium, 1.05% chromium and 34.60% SiO_2.

- Particle size analysis of sample 1 showed that 50% of this ore sample was below 38 μm. The second lateritic sample which was high in arsenic content was supplied at minus 74 micron particle size.
- XRD and DTA-TGA examinations of the original run-of-mine ores revealed that the major minerals present were goethite, quartz, hematite and minor mineral was serpentine. SEM-EDS examinations have shown that the nickel was found within mainly in the crystal structures of goethite and hematite.
- Theoretical sulfuric acid consumption calculations based on the chemical ore compositions indicated that 324 kg/ton of dry ore for HPAL experiments was needed.
- The optimum conditions for HPAL experiments were 255 ^{o}C leaching temperature, 1 h leaching duration, 0.324 acid to ore ratio, 100% -850 μm particle size, 0.3 solid to liquid ratio and 400 rpm stirring speed with no additions.
- At these optimum conditions, the average extraction efficiencies were; 73.2% Ni, 76.8% Co, 2.7% Fe, and 5.2% As for HPAL of sample 1. They were found to be 77.8% Ni, 82.9% Co, 9.2% Fe, and 15.9% As for HPAL of sample 2. The increase in the mentioned extraction values for both samples were limited as HPAL temperature was increased to 265 ^{o}C and the leaching duration was extended to 360 minutes in the limiting condition experiments. Further grinding of the samples to finer sizes did not also raise the extraction values above 90%.
- The optimum conditions for atmospheric agitated acid leaching were; minus 1.7 mm particle size, at the boiling points, leaching durations 48 h for nitric and sulfuric acids whereas 24 h for hydrochloric acid, 5 N acid concentration for sulfuric and hydrochloric acids whereas 6 N for nitric acid, 0.2 solid to liquid ratio and 500 rpm stirring speed.
- At these optimum conditions, the extraction efficiencies for nitric, sulfuric and hydrochloric acids by using samples 1 and 2 are given in Table 24.

From the table it can be seen that the hydrochloric acid was the strongest and the nitric acid was the weakest acid among these three acids in the extraction of nickel and cobalt from lateritic ores.

Table 24: Extraction efficiencies of agitated atmospheric acid leaching experiments.

	Sample 1			Sample 2		
Acid Type / Elements	Nitric Acid	Sulfuric Acid	Hydrochloric Acid	Nitric Acid	Sulfuric Acid	Hydrochloric Acid
% Ni	93.1	98.2	97.7	95.6	98.1	98.6
% Co	95.7	99.3	100.0	95.8	99.2	100.0
% Fe	80.7	98.0	97.1	93.9	98.1	99.2
% As	84.6	98.3	96.6	86.3	94.1	98.6

- In the XRD examinations of the HPAL leach residues; hematite, alunite and quartz were found as the major phases. In atmospheric agitated leaching experiments goethite, quartz and hematite were the major phases. There were no difference in XRD patterns of both HPAL and atmospheric leaching experiments of different type of ores.
- According to the SEM investigations, all of the major phases were found as images and confirmed by EDS analyses which were found in both HPAL and atmospheric leach residues. Moreover, hematite and goethite were found with/without arsenic content in the leach residues. In some of those EDS analyses, lost nickel was found. Also others minerals or phases like chromite, amorphous silica, alunite and pyrite were detected.
- The theory of arsenic's inhibiting effect on the dissolution and precipitation kinetics of iron minerals in autoclave which might have caused the loss of nickel and cobalt was refuted completely.

- The precipitations of iron on to undissolved iron minerals during dissolution-precipitation in HPAL experiments and inhibit it by coating and preventing their contact with the leach solution was partially confirmed. In SEM images, the primary hematite was found partially coated with secondary hematite particles which had precipitated during HPAL.

Recommendations for Future Studies

The HPAL experiments were conducted with batch type autoclave which had no acid injection system and no sampling system during the experiments. It would have been much better to inject acid when the reactor reached its desired temperature. Also, taking samples without interfering with the experiment would be much better in terms of time and energy. Moreover with the use of this kind of equipment, the obtained data would be more representative of the real HPAL operation.

HPAL experiments could also be conducted within a synchrotron facility to observe the behavioral kinetics of minerals in-situ. Thus, the theories would become much easy to test and understanding the low nickel and cobalt extraction percentages in HPAL would be easy to reveal.

REFERENCES

1. R.G. McDonald, B.I. Whittington, Atmospheric Acid Leaching of Nickel Laterites Review Part I. Sulphuric Acid Technologies, Hydrometallurgy, 91: p. 33-55, Karawara, Perth , 2007.

2. Mineweb, [Online] Moneyweb Holdings Limited. http://www.mineweb.com/mineweb/content/en/mineweb-base-metals?oid=198149&sn=Detail. [Cited: 04.01.2014].

3. London Metal Exchange, Nickel. [Online] http://www.lme.com/en-gb/metals/non-ferrous/nickel/,[Cited: 04.01.2014].

4. J.H. Caterford, Mineralogical Aspects of the Extractive Metallurgy of Nickeliferous Laterites. North Queensland, Australia : in The Aus. I.M.M. Conference, 1978.

5. B. I. Whittington, D. Muir, Pressure Acid Leaching of Nickel Laterites: A Review, Mineral Processing and Extractive Metallurgy Review, 2000.

6. British Geological Survey, Definition, Mineralogy and Deposits. 2008.

7. D. G. E. Kerfoot. Ullmann's Encyclopedia of Industrial Chemistry, Wiley Interscience, pp. 1–63, 2005.

8. W. Ahmad, Nickel Laterites. 2008.

9. G.M.Mudd, Ore Geology Reviews, 38,9-26, 2010.

10. U.S. Geological Survey, U.S. Department of the Interior. Mineral Commodity Summaries, 2013.

11. A.D. Dalvi, W.G. Bacon, R.C. Osbourne, The Past and the Future of Nickel Laterites, Ontario, Canada, 2004.

12. K. Liu, Q. Chen, H. Hu, Z. Yin, B. Wu, Hydrometallurgy, Vols. 104, 32–38, 2010.

13. M.A.R. Önal, Pressure Acid Leaching of Çaldağ Lateritic Nickel Ore, M.Sc. Thesis in Metallurgical and Materials Engineering. Ankara : Middle East Technical University, 2013.

14. D. Dimaki, S. Agatzini, Nickel and Cobalt Recovery from Low-grade Nickel Oxide Ores by the Technique of Heap Leaching using Dilute Sulphuric Acid at Ambient Temperature. 1001555 Greek Patent, 1991.

15. S. Agatzini-Leonardoua, P.E. Tsakiridis, Hydrometallurgical Process for the Separation and Recovery of Nickel from Sulphate Heap Leach Liquor of Nickeliferrous Laterite Ores, Minerals Engineering, pp. 1181-1192, Vol. 22, 2009.

16. Wikipedia. [Online] http://en.wikipedia.org/wiki/Heap_leaching, [Cited: 05 25, 2014].

17. B.Willis, ALTA 2012, Nickel/Cobalt & Copper, pp. 45-76, 2012.

18. J. Reid, S. Barnett. Australia : ALTA 2002 Nickel/Cobalt 8 Melbourne, 2002.

19. S. Chander, Atmospheric Pressure Leaching of Nickeliferous Laterites in Acidic Media, Transactions of the Indian Institute of Metals, Vols. 35, No:4,pp 366-371, 1982.

20. G.B. Harris, T.J. Magee, V.I. Lakshmanan, R. Sridhar, The Jaguar Nickel Inc. Sechol Nickel Project Atmospheric Chloride Leach Process, International Laterite Nickel Symposium, TMS, pp. 219-241, 2004.

21. P. Tzeferis, S. Agatzini, E.T. Nerantzis, Mineral Leaching of Non-Sulfide Nickel Ores Using Hetertrophic Micro-Organism, Letters in Applied Microbiology, Vols. 18, pp. 209-213, 1994.

22. C.I. Apostolidis, P.A. Ditssin, The Kinetics of Sulphuric Acid Leaching of Nickel and Magnesium from Reduction Roasted Serpentine, Hydrometallurgy, pp.181-196, Vol. 3, 1978.

23. J.H. Canterford, Leaching of Some Australian Nickeliferous Laterites with Sulfuric Acid at Atmospheric Pressure. Australia : Proc. Australas. Inst. Min. Metal, Vols. 265, pp. 19-26, 1978.

24. L.B. Sukla, S.C. Panda, P.K. Jena, Recovery of Cobalt, Nickel and Copper from Converter Slag Through Roasting with Ammonium Sulphate and Sulfuric Acid, Hydrometallurgy, pp. 153-165, Vol. 16, 1986.

25. N. Panagiiotopoulos, S. Agatzini, A. Kontopoulos, Extraction of Nickel and Cobalt from Serpentinic Type Laterites by Atmospheric Pressure Sulfuric Acid Leaching, New Orleans : TSM-AIME Annual Meeting, 1986.

26. N. Panagiotopoulos, A. Kontopoulos, Atmospheric Pressure Sulfuric Acid Leaching of Low-Grade Hematitic Laterites, Extractive Metallurgy of Nickel & Cobalt, pp. 447-459, 1988.

27. W. Curlook, Direct Atmosphere Leaching of Saprolitic Nickel Laterites with Sulfuric Acid, International Laterite Nickel Symposium, TMS, 2004.

28. H. Lui, J.D. Gillaspie, C.A. Lewis, D.A. Neudorf, S. Barnett, Atmospheric Leaching of Laterites with Iron Precipitation as Goethite, International Laterite Nickel Symposium, Atmospheric Leaching, TMS, 2004.

29. E. Büyükakıncı, Extraction of Nickel and Cobalt from Lateritic Ores, M.Sc. Thesis in Metallurgical and Materials Engineering. Ankara : Middle East Technical University, 2008.

30. Y.A. Topkaya, C.H. Köse, Column leaching of Nontronitic Laterite and Recovery of Nickel and Cobalt from Pregnant Leach Solution, Ontario, Canada : Annual Hydrometallurgy Meeting, 2009.

31. F. McCarthy, G. Brock. The Direct Nickel Process Continued Progress on the Pathway to Commercialisation, ALTA, 2012.

32. A. Taylor, M.L. Jansen, Nickel/Cobalt 2000 Proceedings, Perth, Australia : ALTA, 2000.

33. R.R.R. Moskalyk, A.M. Alfantazi, Minerals Engineering, Vols. 15, 593-605, 2005.

34. D. David. Metallurgical Plant Design and Operating Strategies, pp. 223-232, Perth, Western Australia, 2008.

35. T. Norgate, S. Jahanshahi, Minerals Engineering, Vols. 24, 698-707, 2011.

36. E. Krause, B.C. Blakey, V.G. Papangelakis. ALTA 1998 Nickel/Cobalt Pressure Leaching and Hydrometallurgy Forum ALTA Metallurgical Services, Melbourne, Australia, 1998.

37. M. Baghalha, V.G. Papangelakis, Metallurgical and Materials Transactions B, Vol. 29B, 1998.

38. D.H. Rubisov, J.M. Krowinkel V.G. Papangelakis, Hydrometallurgy, Vols. 58, 1-11, 2000.

39. D. Georgiou, V.G. Papangelakis, Hydrometallurgy, Vols. 49, 23-46, 1998.

40. D. Georgiou, V.G. Papangelakis, Minerals Engineering, Vols. 17, 461-463, 2004.

41. V. G. Papangelakis, D. Georgiou, D. H. Rubisov. Montreal, Canada : Second International Symposium on Iron Control in Hydrometallurgy, pp. 263–273, 1996.

42. J.H. Loveday, Minerals Engineering, Vols. 21, 533–538, 2008.

43. E. Mendelovici, S. Yariv, R. Villalba, Aluminum-bearing Goethite in Venezuelen Laterites, Clays and Clay Minerals, Vols. 27(5), pp. 367-372, 1979.

44. E.C.C. Chou, P.B. Qeuneau, R.S. Rickard, Metallurgical Transactions B, Vols. 8B, 547-553, 1976.

45. S.I. Sobol, Revista Technologica, Vol. 7, 1969.

46. F.T.D. Silva, Minerals Engineering, Vols. 5, 1061-1067, 1992.

47. D. Marshall, M. Buarzaiga, TMS International Laterite Nickel Symposium, pp. 307-316, 2004.

48. A. Manceau, A.I. Gorshkov, V.A. Dritis, American Mineralogist, Vols. 77, 1144-1157, 1992.

49. J. Roqué-Rosell, J.F.W. Mosselmans, J.A.Proenza, M.Labrador, S. Gali, K.D. Atkinson, P.D. Quinn, Chemical Geology, Vols. 275, 9-18, 2010.

50. N. Hazen, E. Chou, Development of Process Design Criteria for HPAL Nickel Laterite Projects.. Melbourne : ALTA Metalurgical Services, 1997.

51. B. Harris, G. White. Perth, Western Australia : ALTA 2011 Nickel/Cobalt & Copper, pp. 1-13, 2011.

52. D.J. Cordier, Scandium, 1997.

53. Ş. Kaya, High Pressure Leaching of Turkish Laterites, M.Sc. Thesis in Metallurgical and Materials Engineering. Ankara : Middle East Technical University, 2011.

54. F. A. Lopez, M.C. Ramirez, J.A. Lopez-Delgado, A. Pons, F.J. Alguacil. Journal of Thermal Analysis, Vols. 94, 517-522, 2008.

55. M. Landers, R.J. Gilkes, M.A. Wells, Clays and Clay Minerals, Vols. 57, 751-770, 2009.

56. A. Basile, J. Hughes, A.J. McFarlane, S.K. Bhargava, Minerals Engineering, Vols. 23, 407-412, 2010.

57. B.I. Whittington, J.A. Johnson, L.P. Quan, R.G. McDonald, D. Muir, Pressure Acid Leaching of Arid-region Nickel Laterite Ore, Part II. Effect of Ore Type. Hydrometallurgy, 70: p. 47-62, 2003.

58. D. Blight, I.G. Muir, The Syerston Polymetallic Project. Melbourne : ALTA Metalurgical Services, 1996.

59. J. H. Kayle, Pressure Acid Leaching of Australian Nickel/Cobalt Laterites. Nickel'96 Mineral to Market, Vols. pp. 245-250, 1996.

60. B.I Whittington, R.G. McDonald, J.A. Johnson, D. Muir, Pressure Acid Leaching of Arid-region Nickel Laterite Ore Part I: Effect of Water Quality, Bently, Australia, 2003.

61. Y. Mamindy-Pajany, C. Hurel, N. Marmier, M. Romeo, Arsenic Adsorption on to Hematite and Goethite, Nice, France : Comptes Rendus Chimie, 2008.

62. F. Partey, D. Norman, S. Ndur, R. Nartey, Arsenic Sorption onto Laterite Iron Concretions: Temperature Effect, Tarkwa, Ghana : Journal of Colloid and Interface Science, 2008.

63. W. Luo, Q. Feng, L. Ou, G. Zhang, Y. Lu, Hydrometallurgy, Vols. 96, 171–175, 2009.

64. R.R. Moskalyk, A.M. Alfantazi, Nickel Laterite Processing and Electrowinning Practice, Minerals Engineering, pp. 593-605, 2002.

65. D.D. MacDonald, P. Butler, The Thermodynamics of Aluminum-Water Systems at Elevated Temperatures, Corrosion Science, Vols. 13(4), pp. 259-274, 1972.

66. International Nickel Study Group. [Online] 2014. http://www.insg.org/prodnickel.aspx. [Cited: 11.02.2014].

APPENDIX A

EXAMPLE OF METAL EXTRACTION CALCULATIONS

The chemical analysis of original limonite sample and leach residues obtained at the end of leaching were performed according to the AAS analysis results of the leach residue done by META Nikel Kobalt A.Ş. The extractions of nickel and cobalt were found according to equation given below:

$$\% \text{ Extraction of M} = \left[1 - \frac{Residual\ Weight\ (g) x\ \%\ M\ in\ Residue}{Ore\ Weight\ in\ Batch\ (g) x\ \%\ M\ in\ Ore\ Feed}\right] x\ 100$$

Example of metal extraction calculations for the nickel and cobalt are given in below according to Table 25. The data in Table 25 belongs to HPAL experiment "A5" which was conducted under optimum conditions with sample 1.

Table 25: Experimental data for the optimum HPAL conditions for solid based extraction calculations.

Experimental Data	Nickel	Cobalt
% Metal in Leach Residue	0.324	0.015
Leach Residue Weight (g)	148.23	148.23
Ore Weight (g)	150	150
% Metal in Ore Feed	1.196	0.064

% Extraction of Ni = $\left[1 - \frac{148.23\ g\ x\ 0.324}{150\ g\ x\ 1.196}\right] x\ 100 = 73.2\ \%$

% Extraction of Co = $\left[1 - \frac{148.23\ g\ x\ 0.015}{150\ g\ x\ 0.064}\right] x\ 100 = 76.8\ \%$

APPENDIX B

EDS RESULTS OF GIVEN SEM IMAGES

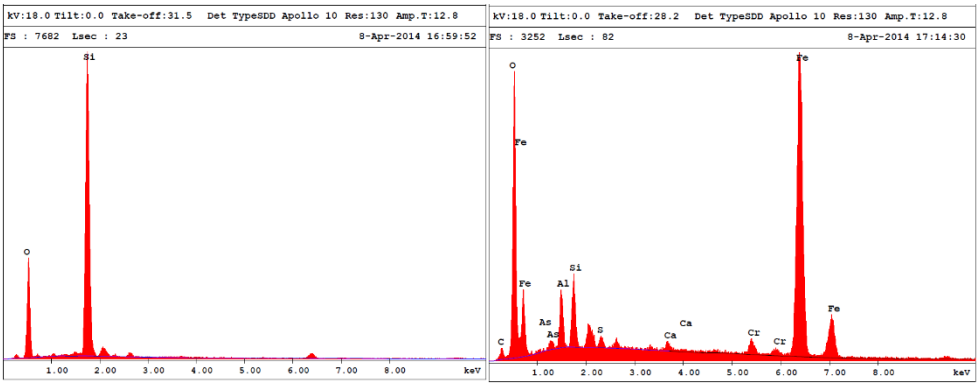

Figure 59: EDS results of images 1 and 2 in Figure 17 (pure crystalline silica and hematite with arsenic).

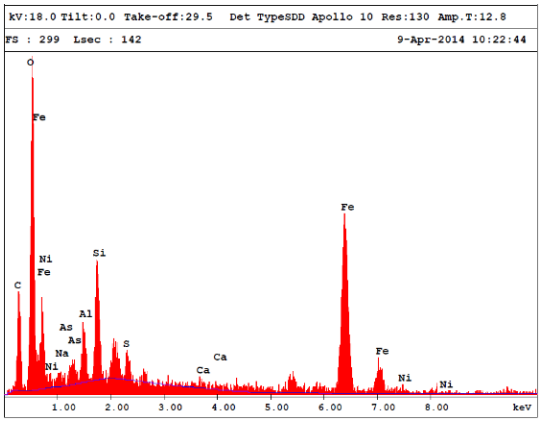

Figure 60: EDS result of image 3 in Figure 17 and Image 5 in Figure 18 (goethite with arsenic).

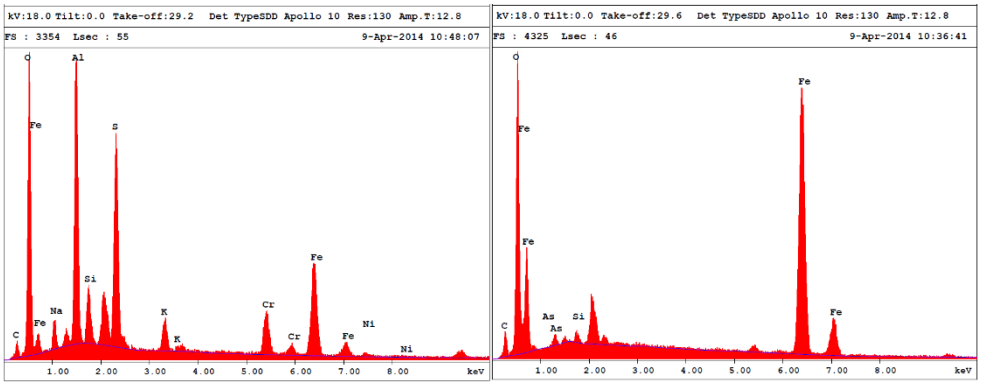

Figure 61: EDS results of images 5 and 6 in Figure 18 (alumina mixed with various compounds and pure iron mineral with arsenic content).

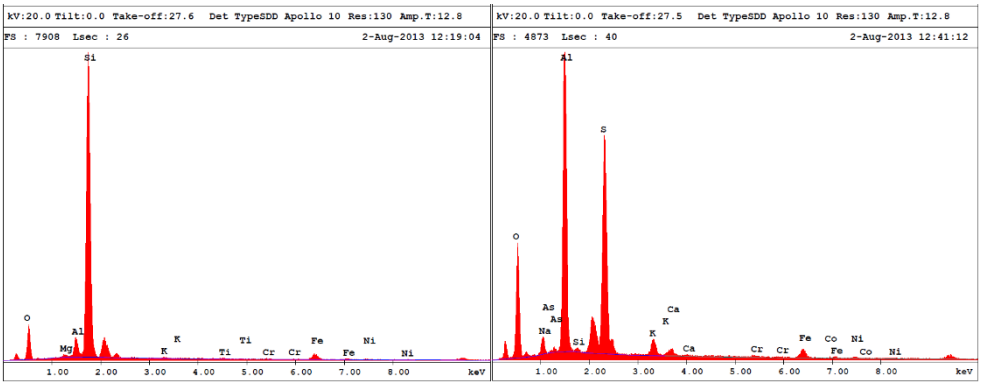

Figure 62: EDS results of images 1 and 2 in Figure 59 (silica and alunite).

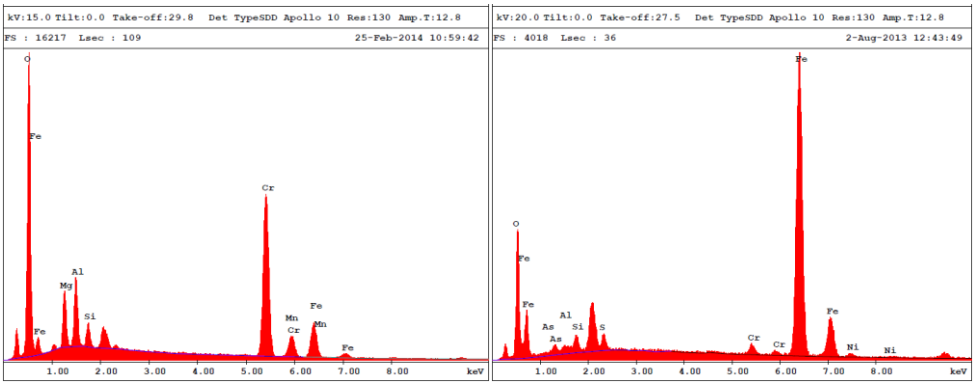

Figure 63: EDS results of images 3 and 4 in Figure 59 (chromite and hematite).

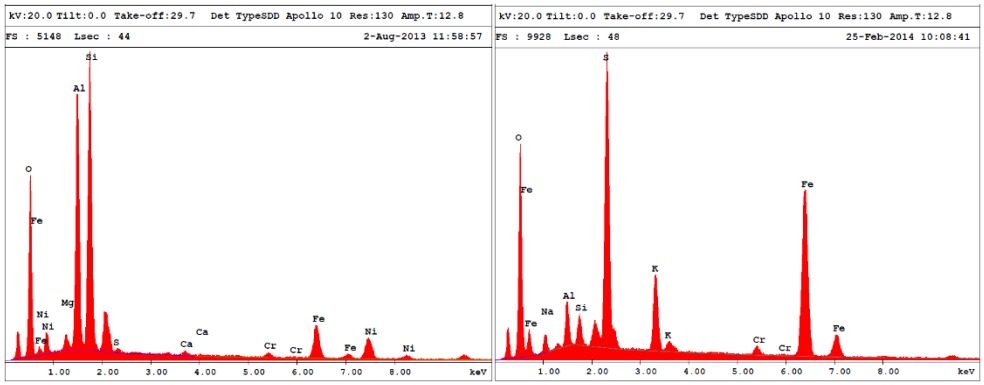

Figure 64: EDS results of images 1 and 2 in Figure 60 (silica and alunite with nickel content and pyrite).

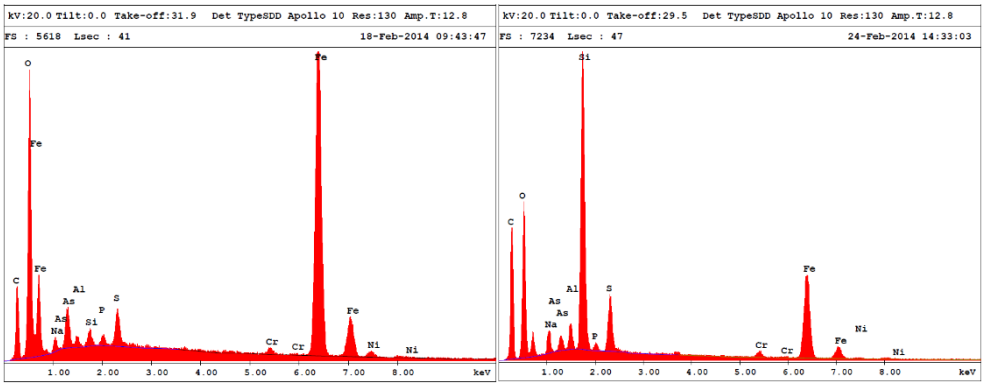

Figure 65: EDS results of images 1 and 2 in Figure 61 (primary hematite and secondary hematite).

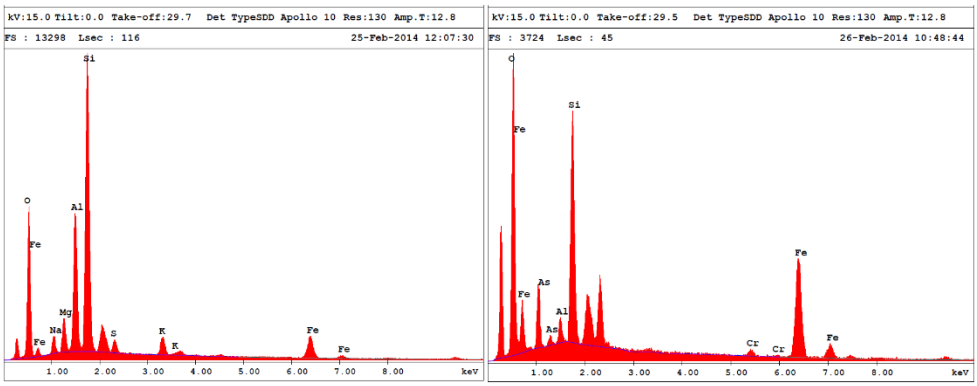

Figure 66: EDS results of images 1 and number 2 in image 4 in Figure 62 (alunite and hematite with arsenic content).